# Computational Analysis of Hemodynamic Parameters in the Management of Cerebrovascular Diseases (Intracranial Aneurysms and Moyamoya Disease)

Kaavya Karunanithi

A thesis of The Faculty of Medicine and Health Sciences, Macquarie University, submitted in fulfilment of the requirements for the degree of Doctor of Philosophy.

December 2015

Supervisor:

Itsu Sen (Yi Qian) PhD

Co-supervisors:

Alberto Avolio PhD

William Yang PhD

MACQUARIE University
SYDNEY·AUSTRALIA

# Declaration of originality

I hereby declare that the work presented in this thesis has not been submitted for a higher degree to any other university or institution. To the best of my knowledge this submission contains no material previously published or written by another person, except where due reference is stated otherwise. Any contribution made to the research by others is explicitly acknowledged. Ethics Committee approvals for all patient data collected were obtained from Macquarie University (Number: 5201100750).

Kaavya Karunanithi

Faculty of Medicine and Health Sciences

Macquarie University

04/12/2015

# Table of Contents

# Acknowledgements

I would like to express my deepest gratitude to my advisor Prof Yi Qian for his continued support and expert guidance for the entire duration of my PhD. I also would like to thank other members of my dissertation committee; Prof Alberto Avolio, my co-advisor for his unending enthusiasm and words of encouragement in trying times, Dr William Yang at CSIRO, Melbourne, for helping me gain some hands-on experience with Particle Image Velocimetry and Dr Chang-Joon Lee, who has been my mentor in learning CFD principles and techniques. I am also, thankful to Macquarie University for the scholarship funding received.

I would like to thank all my friends and colleagues at the Australian School of Advanced Medicine, Macquarie University; Dr David Verrelli and Dr. Fengping Zhu, for enhancing my thesis with their valuable suggestions and insights; Olivia, for being my after-hours-at-work companion; Jude, my partner in crime and Daneh, my go-to counsellor. I feel fortunate to have my beautiful family in Sydney, especially Shiva who has been my cheerleader in this arduous yet rewarding journey

I am thankful to the Almighty and my parents; Prof Karunanithi Anaimuthu & Mrs Ratnamala Karunanithi, for without either of them I never would have seen my PhD through. They have stood by me all my life for which I shall be eternally grateful.

To conclude, no good things happen without caffeine and therefore I am obliged to thank Kaldi, the Abyssinian goat herder and coffee discoverer[1], for his contribution to the advancement of Science


[1] Ncausa.org,. 'National Coffee Association USA > About Coffee > History Of Coffee'. N.p., 2015. Web. 19 Nov. 2015.

# Publications

## Journal publications

1. **Karunanithi, K**., Lee, C. J., Chong, W., & Qian, Y. (2015). The influence of flow diverter's angle of curvature across the aneurysm neck on its hemodynamics. Proceedings of the Institution of Mechanical Engineers, Part H: Journal of Engineering in Medicine, 229(8), 560-569.
2. **Karunanithi, K**., Han, C., Lee, C.-J., Shi, W., Duan, L., & Qian, Y. (2015). Identification of a hemodynamic parameter for assessing treatment outcome of EDAS in Moyamoya disease. Journal of Biomechanics, 48(2), 304-309.
3. Zhu, F.P., **Karunanithi, K**., (co-authored) Qian, Y., Mao, Y., Xu, B., Gu, Y., Morgan, M. (2015) Assessing surgical treatment outcome following superficial temporal artery to middle cerebral artery bypass based on computational haemodynamic analysis. Journal of Biomechanics, 48(15), 4053-4058
4. **Karunanithi, K**., Zhu, F.P., Mao, Y., Qian, Y., Characterization of Pressure Drop Index (PDI) in MMD patients treated with combined direct & indirect revascularization surgery, Journal of Medical Engineering and Physics-Accepted
5. Zhang, W., Qian, Y., Lin, J., Lv, P., **Karunanithi, K**., & Zeng, M. (2014). Hemodynamic analysis of renal artery stenosis using computational fluid dynamics technology based on unenhanced steady-state free precession magnetic resonance angiography: preliminary results. [Evaluation Studies]. Int J Cardiovasc Imaging, 30(2), 367-375.

## Conference proceedings

1. **Karunanithi, K**., C.-J. L., Yu Zhang and Yi Qian. (2012). Risk Stratification of Cerebral Aneurysms using CFD-A Review. Paper presented at the 9th

International Conference on CFD in the Minerals and Process Industries, Melbourne, Australia

2. **Karunanithi, K**., C. J. L., Winston Chong, Qian, Y. (2013, 16-18th December). Effect of angle of curvature of flow diverter on the hemodynamics of cerebral aneurysms-A CFD study. Paper presented at the 3rd International Conference on Computational and Mathematical Biomedical Engineering, HongKong PRC.
3. **Karunanithi, K**., Z., Zhu, F.P., Qian, Y., Mao, Ying. (2015, 25-29th August). Computational Analysis of Hemodynamic Parameters of MMD Patients Treated with STA-MCA Bypass. Paper presented at the 37th International IEEE Conference of Engineering and Medicine in Biology Society, Milano, Italy.

# Declaration of contributions

## Chapter 3

The influence of flow diverter's angle of curvature across the aneurysm neck on its hemodynamics

Authors:

Karunanithi, Kaavya-Study design, Data collection and Analysis, Manuscript Draft
Lee, C.J, Chong, W, and Qian, Y-Academic advisory and manuscript correction

## Chapter 4

Identification of a hemodynamic parameter for assessing treatment outcome of EDAS in Moyamoya disease

Authors:
Karunanithi, K-Study design, data analysis and manuscript draft (co-author)
Han, C-Study design, data collection and manuscript revision (co-author)
C.-J., Shi, W., Duan, L., & Qian, Y-Academic advisory and manuscript correction

## Chapter 5

Assessing surgical treatment outcome following superficial temporal artery to middle cerebral artery bypass based on computational haemodynamic analysis.

Authors:
Zhu, F-Study design, data analysis and manuscript draft (co-author)
Karunanithi, K-study design, data analysis and manuscript revision (co-author)
Qian, Y., Mao, Y., Xu, B., Gu, Y., Morgan, M -Academic advisory and manuscript correction

## Chapter 6

Characterization of Pressure Drop Index (PDI) in MMD patients treated with combined direct & indirect revascularization surgery

Authors:
Karunanithi, K -Study design, data analysis and manuscript draft (co-author)
Zhu, F.P-study design, data collection and manuscript revision (co-author)
Qian, Y., Mao, Y., Xu, B., Gu, Y., Morgan, M -Academic advisory and manuscript correction

# List of Figures

# List of Tables

# List of Abbreviations

# Abstract

The vasculature that supplies blood to the brain is tightly regulated and any abnormalities in its structure; aneurysms and Moyamoya disease (MMD) cause a multitude of complications including but not limited to Sub-arachnoid hemorrhage (SAH), transient ischemic attacks (TIA), stenosis etc. The blood flow dynamics of these vascular disorders plays a critical role in the origin and development of the disease. Computational Fluid Dynamic (CFD) techniques help us understand the underlying mechanism that promotes disease prognosis. In this study we aim to computationally analyze the hemodynamic parameters that will help assess the treatment outcome of cerebrovascular diseases such as intracranial aneurysms and MMD.

In our initial study we attempted to understand the relationship between the free segment of Flow Diverter (FD)'s angle and the Metal Coverage Rate (MCR) across the aneurysm neck and its influence on flow reduction and Energy Loss (EL). Our results from two patient specific aneurysms; A (Aspect Ratio=3.1) and B (Aspect Ratio=2.9) with three FD configurations each (0°, 10° and 25°), suggested that an optimal MCR in the range of 50-60% across the aneurysm neck brings about maximum flow reduction inside the aneurysm facilitating its occlusion. It also yielded higher percentage reduction in Energy Loss when compared to the no-stent case indicating a lower risk of rupture compared to other stent configurations.

The second part of the dissertation deals with the application of CFD principles to understand the hemodynamics of scarcely known Moyamoya disease, which is caused due to progressive occlusion of the Internal Carotid Arteries (ICA). A total of 34 adult MMD patients; 8-treated bilaterally with indirect EDAS revascularization, 26-treated unilaterally with combined direct STA-MCA bypass and indirect EDMS revascularization (18-incomplete Circle of Willis, 8-complete Circle of Willis), were computationally analyzed to identify a novel hemodynamic parameter, Pressure Drop Index (PDI) which correlated with Matsushima's angiographic

grading (A-Significant improvement; B-Limited Improvement; C-No Improvement) across all patients. We also sought to evaluate the characteristic remodeling of ICA post-surgery in the 18 patients (incomplete CoW) who have undergone combined revascularization surgery to illustrate how vascular tortuosity and Wall Shear stress (WSS) affect treatment outcome. Negligible changes in WSS and a decrease in vascular tortuosity was found in patients classified A accompanied with a decrease in surgical ICA diameter. Patients from group C had an increase in wall shear stress values with severe stenotic regions developing in surgical ICA.

The results of our studies have established that parameters such as Metal Coverage Rate and Pressure Drop Index play a vital role in influencing the progression of cerebrovascular disorders. Work towards quantifying the statistical significance of the parameters of interest is currently underway. This will help us establish CFD as a non-invasive, complementary diagnostic tool to aide clinicians in the treatment planning and management of intracranial aneurysms and MMD.

# Chapter 1

# *Cerebrovascular Diseases: An Introduction*

## 1.1 Cerebral Circulation

Cerebral autonomic regulation refers to the ability of brain to maintain a constant cerebral blood flow (CBF) to the brain despite differences in perfusion pressure. The brain's myogenic mechanism utilizes approximately $1/5^{th}$ of the total resting oxygen in the body. (1) In a resting physiological state, where the blood pressure is within the normotensive range of 60-160 mm of Hg, the volume of blood flow to the brain has been established as approximately 50ml/100 g of brain tissue. (2) Blood pressure refers to the pressure exerted by the flow of blood on the walls of the vessels. In the systemic circulation, aside from the circadian pressure oscillations, there is an alternating fluctuation in blood pressure due to systolic and diastolic loops. Hence accurate regulation of oxygen delivery is crucial for its sustenance.

The blood pressure is measured in mm of Hg and it follows an alternating pattern of systolic increase and diastolic reduction. The smooth muscle cells found in the walls of the blood vessels play a key role in the muscular constriction and vasodilation which is required to regulate the blood flow during systolic increase and diastolic reduction in pressure correspondingly. (3) The autonomic regulation of CBF is significantly well developed in comparison to other vascular beds as the large arterial diameters of the brain responds to changes in blood pressure by rendering appropriate vascular resistance to maintain the local micro vascular pressure. (4)

### 1.1.1 Circle of Willis (CoW)

Circle of Willis (circulus arteriosus cerebri) refers to the anastomotic network of blood vessels situated at the interpeduncular fossa of the base of the brain. A typical Circle of Willis is a closed circuit network of symmetrical vessels that consists of principal arteries supplying blood to both cerebral hemispheres. Alpers et al., 1959 reported that the textbook configuration of a closed CoW was found only in 52.3% of cases.(5, 6) Variations in its structure: classified according to Ozaki's classifications, were found to correspond with

various cerebrovascular diseases such as intracranial aneurysms, infarcts and Moyamoya disease. (7) As seen from Figure 1.1, the CoW consists of the left and right Internal Carotid Arteries (ICA), A1 segments of left and right Anterior Cerebral Arteries (ACA), an Anterior Communicating artery (ACOM), left and right Posterior Communicating arteries (PCOM), P1 segments of right and left Posterior Cerebral Arteries (PCA) and a single Basilar Artery (BA) which is formed by the intracranial fusion of two vertebral arteries (8)

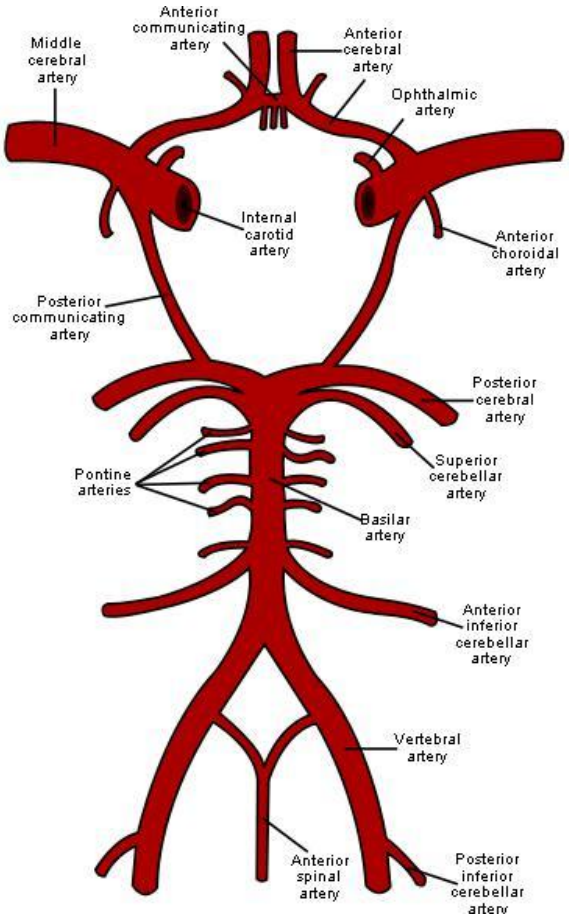


Figure 1-1: Schematic representation of Circle of Willis (circulus arteriosus cerebri) and its associated blood vessels

## 1.2 Intracranial Aneurysms

Cerebral aneurysm is a localized dilation of the blood vessel. It is a cerebrovascular condition where the blood vessel becomes enlarged to form a balloon like structure due to weakness of

the arterial wall. Aneurysm initiation is caused by loss or wearing of smooth muscles (media) and elastic fibers (adventitia) making the intimal aneurysm walls stiff. They most commonly occur at the branching points of major arteries in the CoW.

According to National Institute of Neurological Disorders and Stroke at the National Institute of Health (NIH), aneurysms are frequently classified into various categories based on the morphology and location. Based on their shape they are commonly classified into

- Saccular- otherwise known as a berry aneurysm, this is the most widely occurring aneurysm with a rounded, pouch-like shape connected to the parent artery via a neck,
- Fusiform-also known as an atherosclerotic aneurysm formed due to excessive stretching of media for a prolonged period of time and
- Dissecting-Dissecting aneurysms or Arterial Dissections are nontraumatic in origin and are formed due to cystic medial necrosis or a tear intimally or subintimally. If the dissection occurs intimally, it results in lumen constriction and sometimes the intramural hematoma may extend into the subadventitial plane to form a sac like outpouch. [Figure 2]

Depending on the aneurysm height, they are broadly classified as Small (2mm-7mm), Medium (7mm-12mm), Large (13mm-24mm) and Giant aneurysms (>25mm). (9)A number of clinical studies have reported that the most frequent locations of aneurysm formation includes the ICA and its associated branches followed by Middle Cerebral Artery (MCA) bifurcation and ACA.(10)

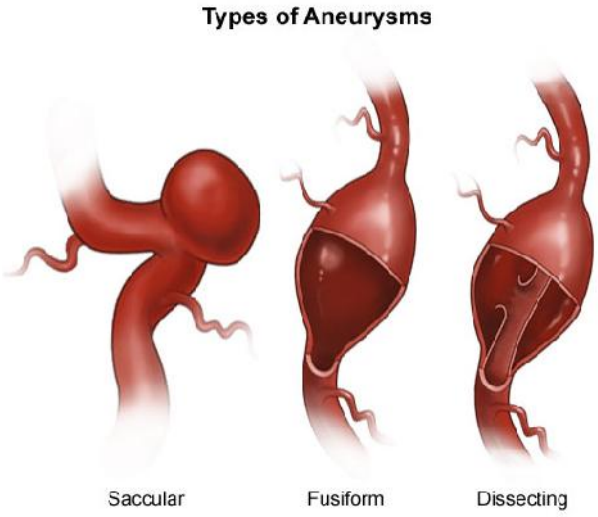


Figure 1-2 Morphological classification of Aneurysm

### 1.2.1 Pathogenesis and Epidemiology

***Epidemiology***

Saccular aneurysms or berry aneurysm, as opposed to fusiform or dissecting aneurysms, are widespread contributing for almost 90% of reported aneurysms. (11) In a systemic review conducted by Vlak MH et al., a prevalence rate of 3.2% (Mean age = 50 years) is reported for a study design consisting of 83 study populations from 21 countries. The percentage of incidence is significantly higher for individuals older than 30 years of age, with higher rates of occurrence in ICA bifurcation, ACom-ACA junction, trifurcation of MCA and other anterior circulating sites.(12, 13) If occurring in young people, the aneurysms are more commonly found in the posterior circulation with sites such as basilar artery bifurcation and junction of vertebral artery. (14)Women are also reported to have a 3:1 incidence rate (adults) and a 2:1 ratio of incidence rate (children) of Unruptured Intracranial Aneurysms (UIA) in comparison to their male counterparts.(15, 16) These acquired lesions are responsible for 80-85% of non-traumatic Subarachnoid Hemorrhages (SAH) (17). A 22% prevalence rate for multiple aneurysms has been confirmed by various studies.(18)

## *Etiology & Pathogenesis*

### Genetic Factors

The effect of aneurysm morphology and hemodynamics play a critical role in aneurysm development and rupture. A conclusive etiology of intracranial aneurysm has not been proven. Yet there have been multiple studies aimed at investigating the causative risk factors that contribute to aneurysm development and rupture in individuals. A detailed study of arterial biomechanics have established that rupture occurs due to loss of collagen at a rate higher than collagen synthesis thereby causing the wall stress to exceed that of the wall strength.(19, 20)

Heritable connective tissue anomalies like autosomal polycystic kidney disease, Ehlers-Danlos syndrome, Marfan's syndrome, Noonan's syndrome and pseudoxanthoma elasticum have been reported to cause neurovascular manifestations such as intracranial aneurysms and cervical artery dissections due to endothelial wall weakening. (21, 22). This association of neurovascular diseases with heritable connective tissue disorders may work to through light to understand the pathogenesis of ICA. The correlation between congenital anomalies of the cerebral artery and intracranial aneurysms is further supported by a study conducted by Nakajima, K et al. Their study reported 8 cases of aneurysm occurrence from 26 patients with cerebrovascular anomalies with an incidence rate of 30.8%. They report a significant link between defect of tunica media vasorum and intracranial aneurysm development. (23)

Familial prevalence of intracranial aneurysms has been extensively investigated since 1954.(24) A study of the existing literature revealed a familial aneurysm occurrence rate in the range of 2.5 -30% depending on the varying factors such as age, first/second degree familial aneurysm, genetic diversity etc., of the sample population studied(25-27). Additionally there have been findings which state that the risk of rupture for familial aneurysms is four times higher than the risk of general population. (28, 29) Genome wide

linkage studies of familial aneurysms have indicated several polymorphisms of genes such as endothelial nitric oxide synthase gene, interleukin-6, and elastase and cyclin-dependent kinase inhibitor 2B to have a significant correlation with intracranial aneurysms. (21, 30) Knowledge of inherent genetic risk factors will lead to development of a robust diagnostic tool for identifying patients at a higher risk for aneurysm development.

Apart from the genetic factors, variations or modifications of Circle of Willis was found to pose a higher risk for sporadic aneurysm incidence.(31) A study done by Kayembe et al., has reported significantly higher incidence of aneurysm initiation in patients having asymmetrical ACA and asymmetrical PComA.(7)

Arterial wall weakening due to inherited aberrations of collagen or elastase gene have been now proved to cause intracranial aneurysms. We also know that there exist preferential sites: namely the large cerebral arteries, with highest incidence of intracranial aneurysms. The high circulation propensity at these sites is believed to contribute to the aneurysm origin and rupture.(32)

### Environmental Factors

In addition to innate risk factors, other acquired factors related to lifestyle such as cigarette smoking and alcohol consumption have been linked to greater incidence of aneurysm occurrence. Numerous studies indicate a significantly higher risk of rupture and SAH (3.7-13.1%) for current cigarette smokers compared to the control group.(33-35) Moderate to heavy consumption of alcohol had an odd ratio of 2.2 associated to SAH. They have been found to have a higher percentage risk of rupture (0.4-5.1%) when compared to individuals who have not had alcohol.(36) Despite the low number of reported SAH cases with reported cocaine intake, the influence of cocaine on aneurysmal rupture has been detailed in several studies. The elevated blood pressure introduced by cocaine abuse leads to endothelial

weakening thereby contributing to aneurysmal development and rupture.(37, 38) The elevated blood pressure linked hypertension has been a significant risk factor for aneurysm genesis and rupture.(39, 40) Infectious intracranial aneurysms report for 2-3% of all intracranial aneurysms. They can be classified as mycotic infected or bacterial infected aneurysms.(41) Lastly, cases of aneurysm development from trauma, although rare, have also been clinically noted.(42)

### 1.2.2 Clinical presentation and Diagnosis

#### *Clinical Presentation*

Most aneurysms are asymptomatic until they rupture. Aneurysm rupture leads to bleeding in the sub arachnoid space leading to a Sub Arachnoid Hemorrhage (SAH).

**Symptomatic ICA**

- **Subarachnoid Hemorrhage**

Intracranial aneurysm rupture leading to a SAH is the first point of diagnosis for many patients. Sub arachnoid hemorrhage can sometimes lead to intra-ventricular and intra-cerebral hemorrhage. In 20% of the reported cases, the patient initially presented with an acute onset of headache called as sentinel headache, usually days or even weeks before the actual rupture. This is due to the preliminary leakage of blood at the rupture site.(43) This "*warning leak*" is commonly misdiagnosed as migraine or sinus conditions. In other patients, the onset of headache due to rupture is often sudden and progresses within a few minutes. The headache is accompanied with bouts of nausea and vomiting.(44) The leakage then mixes with cerebrospinal fluid (CSF) and patients may experience intense lower back or neck pain as this bloody CSF travels downward. Motor deficit may or may not occur and based on the grading of SAH which is done using various methods such as GCS grading system, Hunt and Hess (1968) grading system and the World Federation of Neurological Surgeons grading system

(WFNS). The WFNS is the gold standard and is classified based on the Glasgow Coma Score.(45)

- **Cerebral Ischemia**

Cerebral ischemia refers to deprivation of blood flow to arteries which may result in an ischemic stroke/transient ischemic attack (IS/TIA). In patients with reported SAH from aneurysm rupture, delayed cerebral ischemia from vasospasm is the leading cause of death and disability. (46) In patients with unruptured thrombosed intracranial aneurysms embolization and subsequent recanalization of thrombus leads to blockage of arteries downstream which results in a IS/TIA(47).

- **Mass Effect**

Large/giant unruptured aneurysms may sometimes push on the brain parenchyma, cranial nerves result in neurological symptoms leading to a "*mass effect*". The most commonly reported symptom is a headache and a third nerve palsy.(48) Based on the aneurysm location other neurological deficits such as seizures, cranial neuropathies, and mild visual focus deficits etc., .may are present. Timely diagnosis of "mass effect" is essential as unruptured intracranial aneurysms exhibiting mass effect is reported to have a higher risk of impending rupture (~6%).(49, 50)

### Asymptomatic ICA

Most tiny-small aneurysms do not rupture nor do they cause ischemic and neurological deficits. This can be deducted from the comparison between reported aneurysm incidence rate (~2 %) and the reported cases of SAH (0.6-1.3%).(10, 51) These unruptured asymptomatic intracranial aneurysms (UAIA) are often found in large scale autopsy and angiographic studies to have the minimal rupture risk rates.(52, 53) Extensive screening programs for patients at risk for aneurysm development (familial linkage and polycystic kidney disease)

have identified numerous patients with tiny-small aneurysms that present no clinical symptoms. These aneurysms are conservatively managed sans surgical treatment.(49, 54) The course of progression of UAIA is not clearly understood and hence there currently exists no standard course of management. A prospective randomized controlled trial called "Endovascular Aneurysm Management Trial" is underway and is expected to complete in 2021. (55)

## *Diagnosis*

### Sub Arachnoid Hemorrhage

The direst presentation of an aneurysm rupture is a sub arachnoid hemorrhage. Earlier the reported mortality rates from SAH were in the range of 40-50%. With the advanced in diagnostic imaging methods, this has now fallen to 24%.(56, 57)

### *Computed Tomography (CT) and CSF Analysis*

A non-contrast CT scan is often the first diagnostic test in identifying an acute SAH with sensitivities ranging from 98-100% in the first 12 hours of SAH. It decreases to 93% in between 12-24 hours and therein falling to 57-85% after the first 24 hours (58-60). If an SAH is missed by CT a lumbar puncture for CSF analysis is the next logical step in diagnosing. The hemorrhage results in blood leaking into CSF which further travels posterior towards the spinal. A spinal tap containing bloody CSF (xanthochromia) is a definite indicator of SAH.(61)

A Magnetic Resonance Imaging (MRI) scan is of no significance in detecting acute SAH. Yet Ogawa T et al., observed a high detection rate of 90-100% by using moderately T2 weighted imaging method in MRI for diagnosing sub-acute and chronic SAH.(62)

## Intracranial Aneurysms

80-90% of non-traumatic SAH have an aneurysmal origin(63). SAH as a result of aneurysm rupture can have a fatal effect on the individual. Angiography is the go-to method for diagnosis of intracranial aneurysms.

### *Angiography*

The gold standard in diagnosis of intracranial aneurysms has been the Digital Subtraction Angiography (DSA). DSA is a contrast based interventional technique used for imaging blood vessels amongst the bony and soft tissue environment. DSA follows the principle of conventional angiography wherein the contrast medium is filled intra-arterially and a digital image is obtained with the contrast specified arteries against a blank background. Advanced imaging techniques such as 3D rotational angiography have led to the improvement in resolution making the detection of aneurysms <3mm, a possibility.(64) However, it is still considered highly invasive and risky with a reported 1% complication rate.(65) Considering the cost-benefits ratio, when performed by a highly skilled interventional neuroradiologist, the complication rates can be brought down to 0.3% with the best chance in accurate detection of intracranial aneurysms.

To tackle the issue of DSA's invasive nature, two lesser invasive imaging modalities have been garnering attention in recent times. Magnetic Resonance Angiography (MRA) has been used in detection of intracranial aneurysms since 1990. Latest research has led to the development of techniques such as 3D time of flight (TOF) and contrast enhanced MRA. (66)In spite of having a relatively high specificity and sensitivity, MRA has limitations with patient mobility. A patient suffering with SAH will be unable to remain stationary during the procedure. As a result of lack of static and turbulent flow, spin artifacts and simulated aneurysms are quite common in MRA images. (67)Numerous investigators have looked into Multi Detector CT Angiography (MDCTA) as a viable replacement for the invasive DSA in

recent times.(68, 69) With the help of modern technology, inventions such as 3D Digital Subtraction CTA have even proved to have higher specificity than DSA. (70)Contrast injected 3D CT scan is preferred by surgeons as they are quite dynamic and robust in terms of aneurysm axis plane location. CTA works best for aneurysms larger than 3mm in diameter with reported specificity rates of 96-98% in comparison to DSA.(71) However, the radiation dosage issues and lack of spatial resolution of CTA in detection of aneurysms <3 mm in diameter & in carotid artery lesions have been put forth against its use as a standalone diagnostic imaging technique for aneurysm detection. (72)

### 1.2.3 Treatment of Intracranial aneurysms

The recommended course of treatment for incidental intracranial aneurysms remains a controversial topic of debate. Conservative management-observation, endovascular techniques (EVT) and surgical clipping are the three options for a patient diagnosed with intracranial aneurysm. It is suggested that an appropriate course of treatment should be decided upon only after weighing benefits of intervention against the risk involved.

Observation is advised by multiple prediction studies such as i) the International Study of Unruptured Intracranial Aneurysms (ISUIA), ii) PHASES score for prediction of risk of rupture iii) Small Unruptured Aneurysm Verification (SUAVe) and iv) Unruptured Cerebral Aneurysm Study of Japan (UCAS), only under the following conditions: patients older than 64 years of age with no prior history of SAH and no familial occurrence of aneurysm and possessing aneurysms <7mm in size with no symptoms present. Observation is also advised for patients with small aneurysms in the anterior circulation. (15, 73) It includes serial monitoring of patients for sudden onset of symptoms and continuing non-invasive CTA and

MRA for checking aneurysm morphology

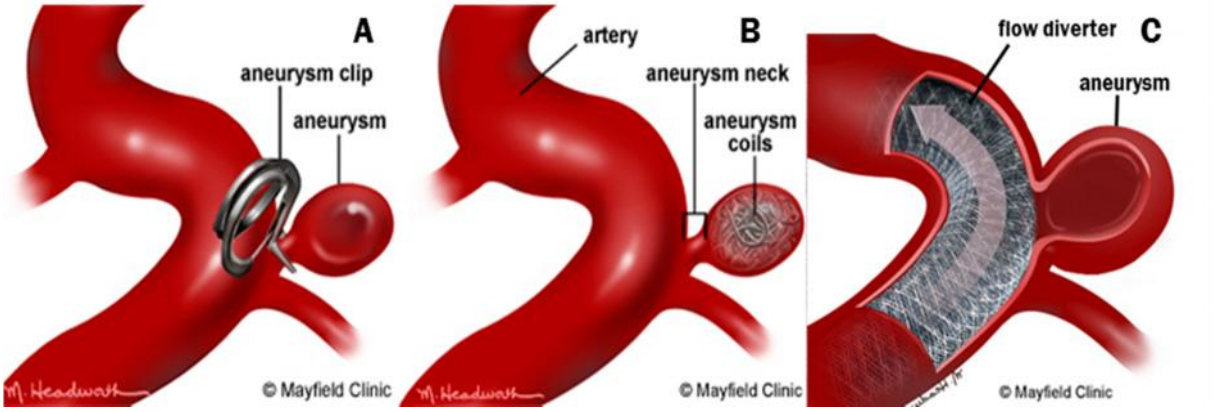


Figure 1-3: Schematic illustration of A: Microvascular aneurysm clipping B: Coil embolization and C: Flow Diversion treatment

### *Microvascular Clipping*

Microvascular Clipping is the oldest surgical technique for aneurysm treatment. Following craniotomy, a surgical clip-made of titanium, is placed at the aneurysm neck thus cutting it off from the parent vessel. [Figure 1.3 A]The treatment has a superior efficiency rate and the one year risk of rupture following the procedure is as low as 0.9%. The mortality rates for surgical clipping are low (~3%). However, the highly invasive nature of the procedure is a prime disadvantage as older patients do not recover well from the trauma of microvascular clipping. This has led to a high mortality and morbidity rate of 2.6-3.8 % and 10.9-12.1 % respectively following treatment.(74)

### *Endovascular technique*

Endovascular technique (EVT) includes introduction of a guided micro catheter to deploy specialized tools: coils and flow diverting stents, inside the aneurysm for achieving occlusion. Until the turn of the century, the only method for endovascular treatment of aneurysms was coil embolization. Coil embolization was first described by Guido Guglielmi.in 1991. He introduced detachable coils through a micro catheter guided by electric current into the

aneurysm [Figure 1.3 B]. The aneurysm lumen was filled with coils until it was cut off from circulation. This promoted thrombosis inside the aneurysm and helped its occlusion.(75, 76) To prevent thromboembolic complications, especially in wide necked aneurysms, comprehensive techniques such as balloon assisted coiling or stent assisted coiling are practiced.(77) A systemic review of 30 studies revealed a combined mortality and morbidity rate of 0.6% and 7% respectively for 1397 aneurysms treated with coil embolization. (78)

Flow diverting stents such as SILK (Balt Extrusion, Montmorency, France), Pipeline Embolization Device (ev3/Covidien, Irvine, California) and SURPASS (Stryker Neurovascular, Fremont, CA) are closed mesh stents designed and developed to treat large unruptured saccular or fusiform intracranial aneurysms [Figure 1.3 C]. They are placed lining the intima of parent vessel wall to alter hemodynamics thereby enabling endoluminal reconstruction and aneurysm obliteration. In contrast to the coil embolization technique, flow diversion technique is gradual with occlusion happening anywhere between 6-12 months after treatment. This is due to the natural reconstruction of endothelial layer over the stent and gradual shrinking of the aneurysm due to blood flow deprivation. Flow diversion although new, has already shown promising results in reducing the rebleeding rates. The largest retrospective multicenter study for assessing flow diverter efficiency was carried out for PED and it determined the 30 day mortality and morbidity rate to be 2.5% and 5.5% respectively.

Ischemic strokes due to thromboembolism, arterial dissections, spontaneous intraparenchymal hemorrhage, thromboembolic complications, rebleeding or SAH and occlusion of perforators and side branches are possible post-operative complications following EVT.(79) Current research focuses on investigating the hemodynamics of intracranial aneurysms in order to understand the mechanism of endovascular reconstruction and mitigate the risks involved.

## 1.3 Moyamoya Disease

Moyamoya disease (MMD) was originally thought to be a primary hypoplastic condition of the internal carotid arteries. It has since then been redefined as a secondary condition and has been defined as the development of collateral vasculature due to stenosis or occlusion of the internal carotid arteries. The name “Moyamoya” in Japanese is analogous to “puff of smoke”. This is due to the smoky or hazy visualization of the collateral vasculature in angiograms.

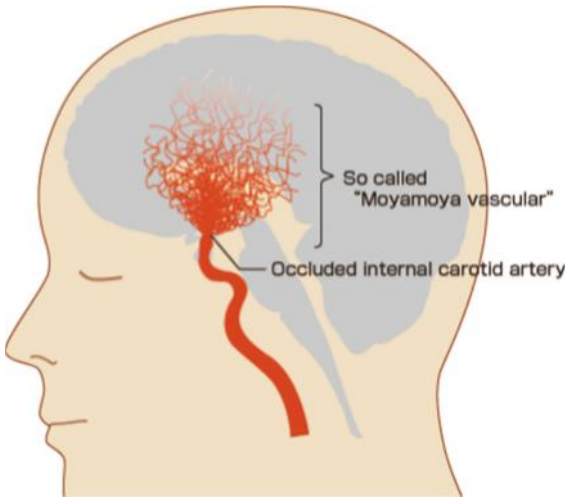


Figure 1-4 Schematic illustration of the occluded ICA with development of Moyamoya collaterals

### 1.3.1 Pathogenesis and Epidemiology

***Epidemiology***

Moyamoya disease is predominantly of Asian origin. The reported incidence rate is highest for Japan, China and Korea. Japan reported an incidence rate of 3.16 per 100,000 people in 1994. This has since increased to 6.03 per 100,000 people. In comparison to Japan, the reported incidence rates in Europe were 0.3 per 100,000 people, 2.2 per 100,000 for African Americans, 0.5 per 100,000 people among Hispanics and US recorded lower occurrences of 0.086 per 100,000 people. The onset of Moyamoya disease spikes particularly in two sets of age groups: pediatric (5-10 years old) have recorded the highest spike followed by a

secondary spike at adult (40-50 years old) stage. As with intracranial aneurysms, females are more susceptible to MMD in comparison to their male counterparts. The reported female to male ratio in MMD is 1.8:1.(80)

## *Etiology and Pathophysiology*

### Etiology

#### *Genetic factors*

The etiology of MMD is poorly understood. Genetic factors are believed to play a critical role in its pathogenesis since the reported rates of familial incidence is significantly high. In Japan approximately 10% of cases reported have a first degree relative diagnosed with MMD. In United States, the number is not too far and is reported as 6%. p.R4859K and p.R4810K polymorphisms on RNF 213 gene has been revealed to play a key role in MMD pathogenesis.(81) Apart from this, mutations in the following gene loci such as 8q23 and q25.3 have also been investigated for its association with MMD.(82, 83) A holistic theory on its etiology based solely on genetic factors is however not feasible as some studies have observed occurrence of MMD in only 1 of the set of monozygotic twins. (84, 85) This indicates that there could other environmental factors responsible for its acquisition

#### *Angiogenesis factors*

CSF analysis along with analysis of Intracranial and Extracranial arteries of MMD patients revealed a marked increase in certain protein levels such as basic fibroblast growth factor, hepatocyte growth factor, transforming growth factor β1, Endothelial progenitor cells, E-selectin and intercellular adhesion molecule type 1, in comparison to patients with ICA occlusion. (86-88)These growth factors are involved in the tight regulation of angiogenesis. In particular the hepatocyte growth factor has been associated with migration of smooth muscle cells into the intima thereby thickening the intima of the terminal carotid arteries which is a common histopathological characteristic of MMD vasculopathy.(88)

### *Immune factors*

Some studies have also stated infections such as *P.acnes* infection, leptospiral infection and tuberculosis meningitis of the head and neck to be a causative factor of MMD.(89-91) A study done by Yamada et al., found a relatively high antibody titer including high serum levels of IgA, IgM, elevated thyroid antibodies and α2M, in MMD patients infected with *P. acnes.* They performed in vivo studies in rats infected with *P.acnes* and found similar antibody profiling with histopathological changes characteristic of MMD such as exfoliation of intima with thickening of intimal wall.(91)

### *Radiation and other factors*

Moyamoya disease has been reported as a rare delayed complication after radiation therapy for patients with neurofibromatosis type 1 (NF-1) (92). More significantly, radiation therapy for NF- 1 in patients < 5 years of age seems to place them in a high risk category as they are prone to develop MMD disease at a latent stage (4 -20 years post therapy). One explanation for this is the higher probability of radiation induced vascular injury in these pediatric patients.(93) This topic needs further investigation as the exact radiation dosage capable of causing MMD is not known.

Moyamoya disease has been associated with multiple disorders in past literature. Despite of lack of etiological evidence, immunological disorders such as Grave's disease and thyrotoxicosis have been linked with Moyamoya disease. (94)In addition to this, congential abnormalities such as Downs syndrome, Marfan's syndrome and Turners syndrome have also been reported to have high relativity with MMD.(95) Hypertension and other associated vascular anomalies such as aortic infarction and cranial trauma are also speculated to be causes for Moyamoya Disease.

### Pathophysiology

It is well accepted that a markedly increase in the thickness of intima with increased concentration of smooth muscle cells is characteristic of MMD.(96) This is the cause of the occlusion of distal internal carotid arteries, anterior and middle cerebral arteries and posterior communicating artery. Lack of inflammatory infiltration and media attenuation is also found in all the cases. Lipid deposits occur occasionally in the stenosis. (97)The collateral vasculature in pediatric patients is dilated with signs of fibrosis where as it is stenotic in adult MMD patients due to the disease's progression and attenuation.(98)

## 1.3.2 Clinical Presentation of MMD

The clinical manifestation of MMD varies greatly according to the age of onset. The disease progression in children is dynamic when compared to static progression in adults. In the United States the adults who present with hemorrhage are approximately 10 times higher than incidences of hemorrhage in children.(99) In children, the most common symptom is cerebral ischemia recognizable as Transient Ischemic Attacks (TIA)

### *Cerebral Hemorrhage*

There are multiple types of intracranial bleeding such as i) intraventricular ii) intraparenchymal and iii) sub arachnoid hemorrhage, reported in MMD patients. Increased blood flow volume through the compensatory vasculature due to carotid artery occlusion leads to their rupture which thereby results in an intracranial hemorrhage Saccular aneurysms associated with MMD are generally found in the basilar artery bifurcation or basilar artery-superior cerebral artery junction of the CoW. Rupture of these microaneurysms is also held responsible for intracranial hemorrhage. Hemorrhage is a common clinical occurrence in adults due to medial attenuation and is rarely present in pediatric MMD patients.(100)

### *Cerebral Ischemia*

Cerebral ischemia, more specifically hyperventilation induced transient ischemia attacks (TIA) and infarctions are a common clinical symptom in pediatric Moyamoya patients. Ischemia caused by occlusion of carotid arteries in the frontal, parietal and temporal lobes of the brain may result in hemi/mono paresis, aphasia and cognitive impairment.(97) Patients may also present with syncope, seizures and visual deficits. In pediatric patients, with disease progression cerebral infarction accompanied by personality changes and/or mental retardation can also occur.(101)

Migraine like headaches and Choreiform gait demonstrations are also reported in a small percentage of MMD patients.(102)

## 1.3.3 Diagnosis of MMD

Diagnosis of MMD can be done using a number of imaging methods such as conventional DSA, MRA, and less commonly using CT and EEG. Diagnostic criteria vary according to the imaging method used, yet the common disease progression classification is standardized according to the Suzuki Grading System. In addition to the six stages of grading as laid out by Suzuki et al., in 1969, there have been different pathognomonic pathways described for Moyamoya disease,

- Basal Pathway refers to the abnormal dilation of perforating arteries in the basal ganglia and thalamus such as thalamo-perforating artery and lenticulostriate artery.
- B the second pathway involves extensive dilation of anterior choroidal and posterior pericallosal arteries.
- C known as the “Ethmoidal pathway”, this is characterized by the dilation of the anterior and posterior ethmoidal arteries that branch from ophthalmic artery to ACA branches

- D. The final pathway known as the “Vault pathway” causes abnormal vasculature in the cranial vault that supplies collateral blood flow from dural to pial arteries.(103, 104)

### Grading Systems

Suzuki grading system has been the standard grading classification followed by neurosurgeons worldwide. Their grading system classified Moyamoya disease progression among six stages as follows: I, narrowing of ICA apex; II, initiation of Moyamoya vessels (MMV; III, progressive ICA stenosis with intensification of MMV; IV, development of external carotid artery (ECA) collaterals; V, intensification of ECA collaterals and reduction of MMV; and VI, occlusion of ICA with disappearance of MMV.(102) Despite the worldwide acceptance of Suzuki’s method, some argue that the method has limited clinical applications and hence novel methods for disease staging are being investigated. Some examples are:

- Hung et al.,(105) color coded method based on maximal opacification between ICA and M2 segment of MCA showed significant clinical correlation to Suzuki’s method,
- Czabanka et al.,(106) method based on DSA & MRI imaging data as well as cerebrovascular reserve capacity (CVRC) helped stratify clinical symptomatology.
- Houskin et al., grading method solely based on MRA scores showed a significant correlation to Suzuki’s grading done with conventional angiography, thus laying an avenue for non-invasive diagnosis of MMD (105-107)

## *Cerebral Angiography*

### MRI and Magnetic Resonance Angiography

MRI imaging can be used as the initial step of diagnostic investigation for MMD patients. T2 weighted and Fluid-attenuated inversion recovery imaging (FLAIR) can be used to visualize ischemic and hemorrhagic lesions in the brain, stenotic lesions in the CoW and asymptomatic

microbleeds which might indicate an impending hemorrhagic stroke. (108)T1 weighted imaging can identify dilated Moyamoya vessels in the basal ganglia and thalamus. MRA is a powerful non-invasive screening tool which can detect Moyamoya in high accuracy in those patients with familial MMD links. It can be used as an adjunct diagnostic tool if done using a 0.5 to 1 T MRI.(109) If done with a 1.5T MRI or more, MRA and MRI can be used as standalone diagnostic tools provided it satisfies the diagnostic criteria as laid out by the Research Committee on Spontaneous Occlusion of the Circle of Willis (Moyamoya disease) of the Ministry of Health and Welfare, Japan which are as following i) stenosis or occlusion at the distal ICA or at the proximal ACAs and MCAs seen on MRA, ii) an abnormal vasculature in the basal ganglia with MRA; iii) an abnormal vasculature evident from ipsilateral flow voids in the basal ganglia seen with MRI; and iii) bilateral presentation of the above two findings.(97)

### Conventional Angiography

Conventional Digital Subtraction Angiography is the gold standard of diagnostic and post-operative Moyamoya imaging. Injecting a contrast dye into the cranial networks help visualize the stenosis/occlusion of the C1-C2 region of carotid arteries in addition to the hazy compensatory vasculature developing as a consequence of occlusion. .The diagnostic imaging guidelines for conventional DSA as laid out by the Research Committee on Spontaneous Occlusion of Circle of Willis (Moyamoya disease) includes i) Bilateral stenosis or occlusion at the terminal portion of ICA and/or at the proximal portion of the ACA and/or MCA. ii) Abnormal vasculature near the of the occlusive or stenotic lesions in the arterial phase.(97) Conventional angiography also gives us a precise idea of the pathognomonic collateral pathways involved. Imaging extracranial arteries is essential for surgical planning as collateral structure if existing, should not be disturbed. Microaneurysms and other associated vascular conditions such as AVMs if present need to be also considered in surgical planning and management of MMD. This is made possible by angiographic imaging.(102)

***Other methods***

Another diagnostic tool used to evaluate the "*buildup*" waves during hyperventilation and "*rebuildup*" waves post hyperventilation in pediatric MMD patients is Electroencephalography (EEG). This buildup and rebuildup presents with a small time difference in patients with MMD as compared to the normal individuals due to lower cerebral perfusion reserve.(110) Other tools such as SPECT/PET and CT have been used to observe the cerebral blood flow and areas of hypodensity suggestive of hemorrhage/stroke respectively, in MMD patients.(84, 102)

### 1.3.4 Treatment of Moyamoya Disease

Moyamoya is a progressive disease with no known treatments existing to reverse the disease process. The existing treatments are aimed at preventing occurrences of stroke and ischemia by improving cerebral blood flow and to alleviate the associated symptoms.

***Conservative Management***

Medical Therapy may be used for patients when surgery is considered high risk or for MMD patients in the initial staging of disease progression. Medical treatments have been used in combination with surgical treatment or standalone in ischemic Moyamoya patients to prevent imminent stroke from thromboemboli. Medical treatment has however not been proven to stop the progression of the disease by a large scale study where 38% of the 651 MMD treated with conventional medical therapy had to undergo surgical intervention ultimately due to progressive symptoms.(111) Common drugs used are.

- Antiplatelet and anticoagulants such as aspirin, argatroban, clopidogrel and thienopyridine are used to prevent stroke due to ischemic thromboemboli.
- Vasodilators to combat the stenotic lesions of basal internal carotid arteries.

- Common supportive medications to combat symptoms such as headache, numbness, hypertension and high blood glucose levels are also used.

There has been no randomized controlled trial to date to investigate the outcome of medical treatment in comparison against surgical treatment. Hence the Research Committee on Spontaneous Occlusion of Circle of Willis (Moyamoya Disease) recommends management of MMD by 1.Observation using standard cerebral angiography guidelines, 2.Medical Treatment based on the disease severity and 3.Surgical intervention (97)

### *Endovascular therapy*

Endovascular therapy uses methods such as angioplasty and wingspan stenting to treat the stenotic arteries with Moyamoya collaterals. The largest systemic review study for Moyamoya patients treated with endovascular therapy was done by Gross BA et al, in which 28 endovascular procedures (11 Wingspan stenting and 17 angioplasty) were considered for lack of clinical and angiographic recurrence. There was major intracerebral hemorrhage reported in 2 of the procedures with 3 of the procedures deemed unsuccessful due to incomplete dilation of the stenotic vessel. Other complications such as stenosis recurrence and thromboemboli events occurred in further 16 cases. With only a 25% procedural success, endovascular therapy was not recommended to stop disease progression. (112) However, due to the high risk of surgical clipping for MMD associated microaneurysms, endovascular embolization was considered favorable in a study done by J-L Yu et al., where almost 85% of the treated aneurysms thrombosed with no rebleeding at a 2 year follow-up.(113)

### *Surgical Revascularization*

The earliest reported surgical treatment of Moyamoya disease were ganglion ablation and cervical carotid perivascular sympathectomy with an aim of restoring blood flow to the ischemic hemispheres thereby offloading stress in the Moyamoya collaterals.(114) This has

not proven to be ineffective in stopping disease progression and surgical revascularization is the gold standard at improving neurological outcomes and alleviating clinical symptoms in MMD patients. There are different types of revascularization techniques practiced based of patient stratification characteristics such as age, gender, occluded region and other associated disorders such as presence of saccular or microaneurysms.(115, 116) The most commonly used techniques include direct revascularization, indirect revascularization techniques and combined direct and indirect method.

### Direct Revascularization

The etiology of Moyamoya is not clearly known but it only occludes the intracranial carotid arteries sparing extracranial arteries. In this method of treatment the surgeons perform craniotomy to suture the mobilized scalp artery (superficial temporal artery) to the intracranial middle cerebral artery known as STA-MCA anastomosis. In addition to mobilizing the STA for avoiding constriction, the cranial flap needs to adequately gouged out to prevent compression of the arterial graft. The surgery was first reported by Yasargil, M.G in 1972 and has since been proven effective in halting disease progression in MMD. (117) The Moyamoya Center at Stanford, one of the largest have reported a 95% graft patency with excellent post-operative outcomes for MMD patients treated with STA-MCA bypass. Direct revascularization has been reported by many to have promising outcomes in preventing recurring ischemia and reduced incidence of rebleeding. In a study done by Karasewa et al., reported a study with 17 MMD patients treated with STA-MCA bypass with and without Encephalomyosynangiosis (EMS). 83% of the patients were reported to have good to excellent results.(118) S Miyamoto et al., reported long term assessment (3-24 years follow up) of 113 MMD patients treated with direct bypass surgery out of which improvement was noted in 110 patients with complete cessation of ischemic events. (119) There are no conclusive multi-center large scale randomized study results available to prove the efficacy of STA-MCA bypass but there have been some promising advancements in the field. The

current technology which enables non-constrictive anastomoses in large cerebral vessels is called as excimer laser-assisted nonocclusive anastomosis (ELANA) technique in which an ELANA platinum ring is used to sew the donor vessel to the recipient vessel using a laser catheter.(120) This technique can only be used in cerebral vessels of diameter 2.6 mm or larger as there are no smaller ELANA platinum rings available. Research is underway to improve aspects such as laser catheter design ,size of platinum rings and going completely suture less (SELANA) to allow any caliber vessel to be anastomosed non-occlusively.(121)

Although considered effective with high rates of cerebral blood flow to the ischemic hemisphere, direct bypass surgery has been associated with significant peri-procedural and post-operative mortality. Mesiwala et al., reported procedural related mortality and morbidity rate of 4.61% and 12.3% respectively, in a group of 39 patients of which 86.2% underwent direct STA-MCA bypass.(122) Due to the sharp spike in the cerebral blood flow, symptomatic hyperperfusion may lead to neurological deterioration in some patients. This has especially been found true in pediatric MMD patients. (123).

### Indirect Revascularization

Due to high rates of peri-procedural complications associated with direct bypass procedures, indirect revascularization procedures are now being recommended for pediatric patients. Indirect procedures are considered to be safe and effective in children in establishing sufficient collateral pathways. As direct bypass is technically difficult to be performed in children due to the smaller size of their arteries, grafts are attempted in the soft tissues of the scalp or transplantation of omentum are used to reach new collateral channels on the cortical surface. There are a great variety of indirect revascularization techniques used either as a standalone bypass or in combination with other indirect/direct techniques to achieve sufficient revascularization pathway. Some of the techniques are as follows: Cervical sympathectomy (CS), Omental transplantation (OT), Multiple burr holes (MBH), Encephalo-myo-arterio-

synangiosis (EMAS), Encephalo-duro-arterio-synangiosis (EDAS), Encephalo-duro-arterio-myo-synangiosis (EDAMS), Encephalo-myo-synangiosis (EMS), Encephalo-arterio-synangiosis (EAS) and Encephalo-duro-synangiosis (EDS) used as an adjunct to EMAS/EDAMS/EDAS, and Encephalo-duro-galeo (periosteal)-synangiosis (EDGS) in Multiple Combined Indirect procedures (MCI) (124). Touho and his colleagues reported long term resolution of MMD symptoms in 5 children on whom OT was performed.(125) Takeuchi et al., reported that 75% of the 13 patients treated with EMS achieved more than one-third revascularization to the distal MCA region along with complete resolution of TIAs.(126) Matushima et al., described the EMAS procedure in detail with 88% of his 10 patients developing adequate revascularization at 25 months after surgery(127). EDAS is the most commonly performed indirect revascularization procedure done in combination with EDAS + pial synangiosis, EDAS + dural inversion and EDAS + split dura technique. Matsuhima T et al. reported a 75% success rate along with decreased complication rates than direct bypass in 12 pediatric patients. (128). The effectiveness of indirect revascularization has been well drafted for pediatric patients. However, indirect methods are not recommended for adult MMD patients since significant failure rates are commonly reported.(129) In addition to this, adequate development of collaterals is found lacking in certain pediatric patients undergoing traditional indirect revascularization surgery.

### Combined Revascularization

To combat the issues of peri-procedural complications and to ensure adequate revascularization is established to prevent ischemic and stroke related post-operative complications, combined direct and indirect techniques are practiced. Golby AJ et al., reported a 100% success rate in 12 patients who underwent direct STA-MCA bypass combined with EDAS.(130) Commonly reported combined revascularization procedures include STA-MCA anastomoses with EDAS, STA-MCA Anastomoses with EDAMS(131), STA-MCA bypass with concurrent EMS(128), and MMA-MCA anastomoses with EDAS.

Hayashi T et al., reported Occipital artery-PCA anastomoses combined with indirect revascularization to be successful in all 3 adult ischemic MMD patients with complete cessation of TIAs.(132). Esposito A et al., has defined a new multi-technique revascularization procedure consisting of STA-MCA anastomoses with EDMS and bifrontal encephalo-duro-periosteal-synangiosis (EDPS) with two of his eight patients having successful treatment outcome.(133) The benefits of multiple combined revascularization procedures are yet to be explored via multi-center randomized controlled studies in order to fully comprehend the disease etiology and progression.

Perfusion weighted imaging methods are used in diagnosis to obtain basic information regarding blood flow rate and perfusion pressure. Although such methods; MRA and CT are considered a viable alternative to much more invasive diagnostic methods, a flow quantification and visualization capability of cerebrovascular disorders is rudimentary. Computational Fluid Dynamics is a non-invasive simulation tool that can be used to develop patient specific three-dimensional models of the cerebrovascular disease. Blood flow is then simulated through the model to understand the hemodynamic characterization in each case.

# Chapter 2

# *Role of Computational Fluid Dynamics (CFD) in the management of Cerebrovascular Diseases*

## 2.1 Introduction

Computational Fluid Dynamics has been long since used in the study of hemodynamics of cerebrovascular disorders. It involves three-dimensional reconstruction of patient-specific/ideal disease geometry through the use of medical image segmentation software. The model is then exported to a meshing program which divides the model into smaller computational domains

### 2.1.1 Numerical Methods in CFD

The process of computational analysis of fluid flows involves the conversion of partial differential equations and auxiliary conditions into a system of discrete algebraic equations. This stage is commonly known as discretization stage. There are three popular discretization approaches in CFD

- Finite Difference Method
- Finite Element Method and
- Finite Volume Method

ANSYS, used for numerical simulation, is based on the Finite Volume Scheme which offers greater support for unstructured meshes which are the norm in patient specific geometries. The domain/geometry is discretized into a set of finite node-centered control volumes on which the Navier Stokes equation for conservation of mass, momentum and energy are applied individually.

$$\left.\begin{aligned} &\frac{\partial}{\partial t}(\rho u_{i)} + \frac{\partial}{\partial x_j}(\rho u_i u_j) = -\frac{\partial p}{\partial x_i} + \frac{\partial}{\partial x_j}\left[\mu\left(\frac{\partial u_i}{\partial x_j} + \frac{\partial u_j}{\partial x_i}\right)\right] \\ &\frac{\partial p}{\partial t} + \frac{\partial}{\partial x_j}(\rho u_j) = 0 \end{aligned}\right\} \quad (1)$$

where $i, j$ = 1, 2, 3; $x_1$, $x_2$, $x_3$ represents the coordinate axes, $u_i$, $u_j$ and $p$ are the velocity vectors and the pressure in the point of the fluid domain, respectively, $\rho$ and $\mu$ are the blood density and viscosity, respectively, and $t$ is the time.

For a cell p, having face f and nb adjacent cells the discretization equation can be simply expressed as

$$a_p\varphi_p + \sum_{nb} a_{nb}\,\varphi_{nb} = b_p \qquad (2)$$

where, $a_p\varphi_p$ is the gradient of solution variables of cell p, $a_{nb}\varphi_{nb}$ are the sum of solution variable gradient of cells adjacent to the control volume p, $a_p$ and $a_{nb}$ are coefficients of solution variable and $\phi$ is the conservative form of all fluid flow (X momentum-u, Y momentum-v, Z momentum-w and energy variable-h) and $b_p$ is the source term. All equations are solved until a solution converges with residual errors next to negligible. The results will then be available for visualization in post-processing software.

## 2.2 CFD in the management of Intracranial Aneurysms

Management of cerebral aneurysms is currently done solely based on clinicians' experience and knowledge. Computational fluid dynamics (CFD), a numerical method aims to provide data that will help in clinical decision making and in the treatment of cerebral aneurysms. Various research groups around the world are now trying to understand the underlying mechanisms leading to aneurysm initiation, development and rupture along with trying to determine the efficacy of surgical intervention.(134)A combined approach of applying principles of arterial mechanobiology, wall mechanics and blood flow dynamics is the archetype to understand the innate complexity the disease pathophysiology.(135)A detailed investigation of various morphological and hemodynamic parameters is necessary to understand the various factors that contribute to aneurysm rupture. In addition to this, CFD can

also be used to specifically determine the efficiency of the treatment such as stenting and flow diversion. Morphological parameters such as aneurysm size, shape, aspect and size ratio and inflow angle are believed to be important factors that contribute to the development and rupture of an aneurysm. Of these, previous studies have shown that the size ratio and aneurysm inflow angle are autonomous parameters that helps in the prediction of aneurysm rupture. Various hemodynamic parameters like flow velocity, pressure, wall shear stress, oscillatory shear index and energy loss are believed to play a crucial role in the growth and rupture of cerebral aneurysms(136)

### 2.2.1 Morphological parameters in assessment of risk of rupture

Cerebral aneurysms are mostly asymptomatic until they rupture which makes diagnosis and treatment of cerebral aneurysms harder. When an un-ruptured aneurysm is diagnosed in a patient, image-based morphological analysis of the aneurysm is still the most widely followed method for its treatment and management. Initial factors that are used by clinicians for assessment of rupture include the size, shape and location of the aneurysm.(137) For instance; larger or wide-necked fusiform aneurysms are believed to hold a higher risk of rupture than smaller aneurysms. The location of aneurysm occurrence, i.e. the artery in which the aneurysm occurs is also said to play a crucial role in increasing the risk of rupture. Conventionally, aneurysms occurring at a bifurcation site and sidewall aneurysms with curved parent artery were believed to be in a higher risk of rupture.

Aside from the image-based indicators several other morphological parameters are believed to contribute significantly. A wide range of parameters such as aspect ratio, size ratio, inflow angle, nonsphericity index, ellipticity index, ostium ratio and undulation index was defined by earlier research publications as important in determining the risk of rupture of an aneurysm.(137-139) Aspect ratio (AR) has achieved statistical significance as an important risk factor for rupture.(140) Aspect ratio is defined by the following equation

$$Aspect\ Ratio\ (AR) = \frac{Depth\ of\ the\ aneurysm}{Neck\ width\ of\ the\ aneurysm} \quad (3)$$

Increasing values of aspect ratio is agreed upon to increase the risk of rupture of an intracranial aneurysm. However, there have been discrepancies in determining the absolute threshold value of aspect ratio beyond which aneurysms are deemed to have a high risk of rupture.

Nader et al. in 2004 reported a mean aspect ratio of 2.7 for ruptured aneurysms. Weir et al. (2003) reported rupture for 7 per cent of aneurysms having an aspect ratio as small as 1.38. Dhar et al. (2008) reported an average value of 1.18 for ruptured aneurysms using images that were obtained using a 3D rotational angiography. In general, a value of 1.6 is predicted to be the lower threshold value of aspect ratio for ruptured aneurysms. (138, 141, 142)Hence aspect ratio, though believed to be an important risk factor for aneurysm rupture, cannot be taken as a standalone method for risk stratification. Other parameters such as undulation index and ellipticity index though statistically significant, are inter-dependent in serving as rupture risk indicators

Prediction of risk of rupture for intracranial aneurysm based on morphological parameters involves analysis of the properties of parent artery. As a result, inflow angle was looked into to serve as an indicator of rupture risk. Aneurysm inflow angle (IA) or vessel angle is defined as the angle of blood flowing from the parent artery into the daughter aneurysm. Baharoglu et al. (2012) demonstrated that apart from clinical risk assessment metric, $D_{max}$, Size and Aspect ratio, the Inflow angle is the only independent morphological feature that can be used to differentiate the rupture status of intracranial aneurysms.(143) Aneurysms with higher inflow angle have a greater tendency to have complex flow patterns which might lead to the development of blebs that act as rupture sites. Dhar et al. (2008) and Wong et al. (2012) have reported higher risk of rupture for vessel angles greater than 112 degrees and 180 degrees

respectively.(138, 144) Thus the risk of rupture is proved to increase with increasing inflow angle.

$$Size\ Ratio\ (SR) = \frac{Maximum\ aneurysm\ height}{Average\ vessel\ diameter} \quad (4)$$

Tremmel at al., (2009) found that size ratio (SR) can serve as an independent contributor to analyze the risk of rupture in cerebral aneurysms. They reported a threshold value of 2.0, beyond which it was proposed that aneurysms hold a higher risk of rupture(145). However, a more recent study done by Rahman et al (2010) reported a size ratio value of 2.76 for ruptured aneurysms from logistic regression method.(146) A multi-center study using larger cohorts is proposed to determine the size ratio value that can serve as an effectual risk index (147)

Currently, size ratio and aneurysm inflow angle are proven to be independent morphological risk assessment factors for aneurysm rupture. Further large scale studies are in order to further investigate the magnitude of these risk factors in rupture prediction.

### 2.2.2 Hemodynamic parameters in diagnosis and management of cerebral aneurysms

In addition to morphologic parameters, hemodynamic parameters play an important role in the rupture process of an aneurysm. Several hemodynamic factors have been studied in the past to identify their contribution to aneurysm rupture. Although extensive research is being done in this field, no conclusive pattern pertaining to aneurysm rupture has been established till now.

Pressure is an imperative hemodynamic factor that influences aneurysm rupture. Cebral et al. (2011) discussed the impact of intra aneurysmal pressure on rupture of an aneurysm. His paper discussed the effects of placement of flow diversion device on intra aneurysmal

pressure. They reported a drastic increase in the intra-aneurysmal pressure following flow-diverter placement. (148)There was a difference of about 25 mm Hg between ruptured and un-ruptured aneurysm. This high difference is cited to be due to the increase in the complexity of flow pattern in the aneurysm and presence of jet flow impingements. Although this statement appears cogent, clinically such difference in pressure is quite large in magnitude and hence considered implausible. A standard reference point for pressure needs to be specified where necessary to avoid such large pressure differences. Furthermore, CFD is capable of measuring only the pressure difference at specific points and not the absolute pressure at any given point in the aneurysm. This is noteworthy in order to derive a realistic inference that would help us understand the relationship between pressure and aneurysm rupture. There exists a moderate elevation in intra-aneurysmal pressure due to flow impingement which is discussed by Shojima et al. (2005) and Burleson et al. (1995). This leads to substantial changes in the wall shear stress distribution pattern thereby resulting in loss of aneurysmal wall integrity. (149, 150)

Wall shear stress (WSS) is another important indicator of aneurysm rupture. Wall shear stress also has a significant role in aneurysm initiation and growth. Research is being done to understand how wall shear stress contributes to aneurysm rupture. Wall shear stress in an aneurysm is calculated by the following equation

$$Wall\ shear\ stress\ (WSS) = \mu\omega_{wall} \quad (5)$$

where μ is the dynamic viscosity of blood and ω is the velocity gradient at the aneurysm wall (151)

An increase in the complex flow patterns and a flow impingement on the aneurysm wall is reported to cause wall shear stress which is due to the frictional force of the blood against the

wall.(152) Wall shear stress patterns have been analyzed for various aneurysms such as saccular and fusiform aneurysms at various locations. There is varied opinion of the way that wall shear stress influences the rupture process. Cebral et al. (2011) and Hashimoto et al. (1980) observed high values of wall shear stress inside the aneurysm that was almost twice the normal value. Cebral et al. (2011) also showed that high WSS with a small impingement region possessed statistical significance between the rupture and un-ruptured group for about 210 cerebral aneurysms in different locations.(19, 153) Lu et al. (2011) however, argues that a low WSS pattern compared to that of the parent artery was found in the bleb region. Thus they contribute low WSS to increasing the risk of rupture of aneurysm.(154) Xiang et al. (2011) stated that low wall shear stress triggers an inflammatory response in the aneurysm wall which leads to its heterogeneous remodeling. This in turn contributes to aneurysm growth that increases the size ratio thereby increasing the complexity of flow patterns which results in rupture of an aneurysm. (155)Different derivations of wall shear stress magnitude may also serve to accurately portray the role of wall shear stress in aneurysm dynamics. Wall shear stress gradient aims to illustrate the spatial distribution of the wall shear stress in the directions normal and tangential to the wall.(156) Goubergrits et al. (2012) attempted to determine the pattern of wall shear stress gradient by plotting statistical wall shear stress maps in ruptured and un-ruptured aneurysms that is believed to increase the sensitivity of rupture risk analysis (157). By considering wall shear stress magnitude and its directions we can better determine how wall shear stress induces aneurysm growth and rupture.

Oscillatory shear index (OSI) is another hemodynamic parameter that is speculated to influence the rupture of aneurysms. It defines the disturbance in the flow field.

Oscillatory shear index averaged over dome area is calculated by the following equation

$$OSI = \frac{1}{2}\left(1 - \frac{\left|\int_0^T wss_i\, dt\right|}{\int_0^T |wss_i|\, dt}\right) \quad (6)$$

This area has also been reported to be a region of low wall shear stress.(155, 158). Although the correlation between high OSI and low WSS is not reported in previous publications we believe that there exists an essential inter-dependence between the two parameters which could be investigated further. Jing et al., (2015) have reported that a high OSI indicated the initiation of thrombus in an aneurysm that was earlier treated with a flow diverter. Supplementary studies investigating the effect of oscillatory shear index is needed to understand the method of influence of this hemodynamic parameter.(159)

We defined Energy Loss (EL) as a parameter that measures the loss of energy by the aneurysm without the influence of the parent artery in our earlier publications. Energy loss is mathematically expressed as

$$EL = \frac{v_{in}A\left\{\left(\frac{1}{2}\rho v_{in}^2 + P_{in}\right) - \left(\frac{1}{2}\rho v_{out}^2 + P_{out}\right)\right\}}{V_n} \quad (7)$$

where $\rho$ is the fluid density $V_m$ is the volume of the measurement section and $A_{in}$ is the area of the test plane at the inlet of the measurement region. $v_{in}$ and $P_{in}$ represent the mean flow velocity and static pressure of the test plane at the inlet side, respectively, and $v_{out}$ and $P_{out}$ represent those at the outlet side, respectively. [Figure 2-1]

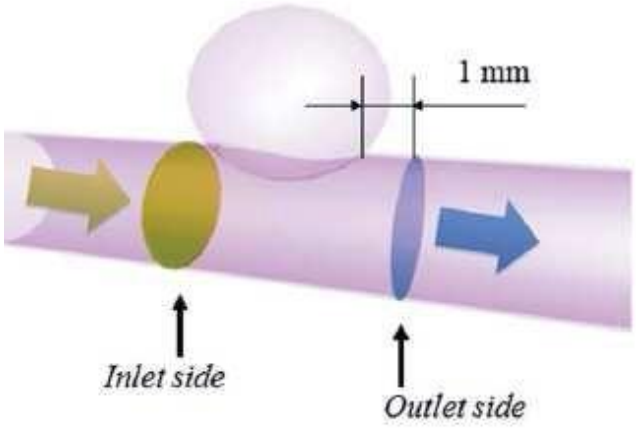


Figure 2-1 CFD Model of physical variable extraction site for defining energy loss

A study of 30 intracranial aneurysms consisting of 26 stable (mean aneurysm diameter 7.07mm) and 4 ruptured aneurysms (mean aneurysm diameter 6.05mm) for calculating energy loss were performed. The results of the study showed us that the energy loss for ruptured aneurysms were 5.02 times higher than that of energy loss of stable intracranial aneurysms. This proves that energy loss is a key hemodynamic parameter of statistical significance ($P<0.001$). The results of the study are shown in the figure 2-2(160, 161)

The discussed morphological and hemodynamic parameters are proven to influence the aneurysm growth and rupture although the statistical significance of each of them may be debated. Nevertheless, all these factors are believed to be interwoven and they collectively influence the rupture of an aneurysm. For instance, the low WSS which results in remodeling of the vessel wall causes aneurysm growth which in turn leads to complex flow patterns and impingement regions that lowers the WSS of the aneurysm wall. A collaborative study of morphological and hemodynamic factors of aneurysms would help us assess the inherent risk of rupture.

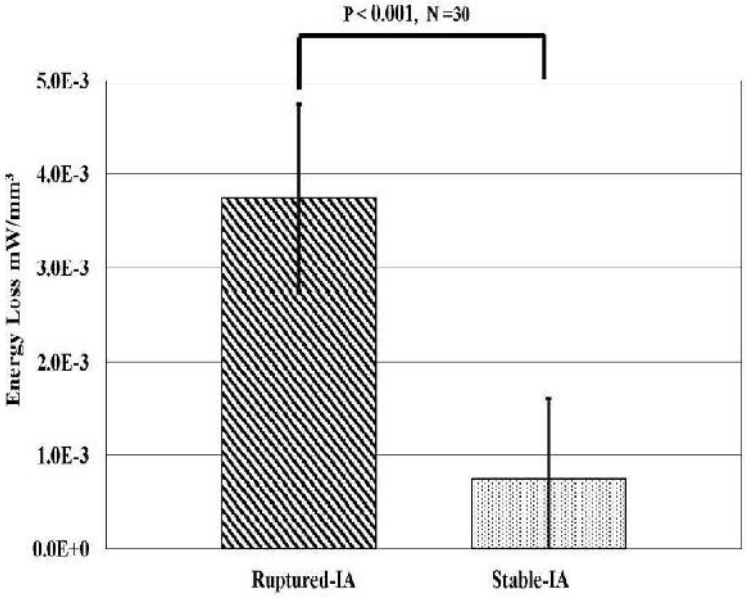


Figure 2-2 Energy loss difference between ruptured and unruptured aneurysms

In addition to prediction and stratification of aneurysm rupture risk; there have been quite a few hemodynamic studies to tackle the issue of treatment outcome and post-operative complications. Significant research into modeling treatment procedures such as coil embolization and flow diversion (FD) has been done in recent times and valuable the hemodynamic information obtained has helped shine light into development of post-operative complications such as rebleeding and aneurysm recanalization. Byun, H.S & Rhee, K., reported a simplistic partial coil filling locations in an ideal aneurysm model. Their results indicated that thrombus initiating hemodynamic environment, such as low WSS and smaller inflow was present in one of the four coil locations i.e. distal neck. (162) Wei et al., has also published a real-time coil embolization simulation method in a patient specific aneurysm model to help simulate a dynamic coiling plan. This has opened avenues for further inquiry into the fluid structure interaction post coil embolization(163)

CFD analysis of flow diversion treatment has been carried out by numerous researchers to understand the dynamic vessel wall remodeling post FD placement. A high fidelity virtual stenting (HiFiVS) method has been developed by Ding et al., for deployment of Pipeline

Embolization Device (PED) into patient specific aneurysm model. Although, reported as an accurate representation of real time flow diversion treatment, the simulation time is a serious limitation of HiFiVS and thus hinders its use in clinical application.(164) There have been successful efforts by various groups to model stent at neck methods and by using porous medium alternatives to develop a clinically relevant yet computational cost effect simulation method of flow diversion.(165-167) porosity of flow diverter, is the only hemodynamic parameter being usually analyzed to understand the mechanism of aneurysm recurrence and rebleeding. (168) Apart from this, traditional hemodynamic parameter such as intra aneurysmal pressure and WSS are studied in patients with failed flow diversion treatment to understand their significance (148, 169)

## 2.3 Hemodynamic Analysis of Moyamoya Disease

### 2.3.1 Radiological Methods used in hemodynamic analysis of MMD

Hemodynamic characteristics that contribute to disease progression of MMD had not been understood until the advent of advanced imaging techniques such as Single Photon Emission Computed Tomography (SPECT), Positron Emission Tomography (PET) and perfusion MRI that can measure the cerebral blood flow with increased accuracy.

Studies from these imaging studies show us distinctive styles of cerebral blood flow patterns in MMD patients. They have established that cerebral blood flow (CBF) and Cerebral Perfusion Pressure (CPP) are reliable hemodynamic indicators of treatment outcome in MMD patients. In a study done by Takahashi et al., the cerebrovascular reserve capacity (CVRC) and hemodynamic stress distribution (hdSD) patterns were measured between the asymptomatic and ischemic hemisphere in 8 MMD patients. Data showed a lower hdSD score post-operatively which corresponded with resolution of ischemic symptoms. (170) CVRC test is the gold standard to measure cerebral perfusion pressure in MMD patients. A lower

CVRC score in the ischemic posterior ICA region indicates decreased cerebral perfusion pressure (CPP). To compensate for the reduced CPP, there is an increase in the cerebral blood volume and oxygen extraction factor. Hence, the cerebral blood volume is most often high in the occluded ICA and its associated MMD vessels. If the CVRC shows a normal limit post revascularization surgery, it is expected that the cerebral blood volume is in the physiological range thereby stabilizing cerebral hemodynamics and metabolism. (171) Kawabori et al., found that lower CBF and lower CPP values were present in 29 pediatric MMD patients before surgery. 11 of them complained of severe frontal and temporal region headache The values normalized post-surgery accompanied with complete eradication of headache (172).

### 2.3.2 CFD in the hemodynamic analysis of MMD

From these studies we can understand that cerebral hemodynamics play a key role in disease progression and its associated clinical symptoms. Currently, CBF and CPP are the only hemodynamic parameters that can be obtained through imaging methods. Computational Fluid Dynamics are increasingly being used to uncover a wealth of hemodynamic parameters that be used to understand MMD disease progression and reversal. There have been only a handful of computational studies on MMD till date. The earliest was a two dimensional simulation of the ICA and PCA at the CoW, that was done by Seol, H.J et al., The WSS distribution was found to vary in the ICA region with lower levels of WSS noted in distal ICA which is the prime pathological region for MMD (173) Zhu, F.P., et al. analyzed eleven patients who underwent STA-MCA bypass surgery. They reported reduced flow resistance in the patent bypass at follow-up. (174). Recently Kim et al. studied the vascular tortuosity along with WSS and blood flow velocity, using the 3D rendering capability of CFD simulations. They found that ICA of MMD patients exhibited lower vascular tortuosity with lower angles of curvature than normal group ICAs. Also, significantly higher blood flow velocities and WSS were found in the ICA bifurcation of MMD patients. (175)

## 2.4 Research Aims and Objectives

The present study aims to identify reliable hemodynamic and morphological parameters that can assist in the management of cerebrovascular disorders such as intracranial aneurysms and Moyamoya disease. As discussed earlier in this chapter, CFD analysis of intracranial aneurysms is a putative field of research with standard flow parameters, such as flow velocity, WSS and EL, used in the prediction of aneurysm rupture risk. However, there aren't dedicated hemodynamic parameters that can be used in assessing treatment outcome or those that assist in optimum surgical planning of intracranial aneurysms. In comparison, application of CFD to MMD is a niche area of research, in order to provide effective treatment to stall and reverse MMD progression and relief of clinical symptoms a thorough understanding of the various hemodynamic parameters involved is indispensible. The objectives of the thesis is as follows

- To understand the regulation of flow inside the aneurysm after flow diverter placement and to investigate the impact angle of Flow Diverter curvature at aneurysm neck the associated metal coverage rate on aneurysm hemodynamics
- To explore application of CFD in Moyamoya disease and to effectively identify new hemodynamic parameters that can assist clinicians in treatment prognosis.

# Chapter 3

# *The influence of flow diverter's angle of curvature across the aneurysm neck on its hemodynamics*

Published As

Karunanithi, K., Lee, C. J., Chong, W., & Qian, Y. (2015). The influence of flow diverter's angle of curvature across the aneurysm neck on its hemodynamics. Proceedings of the Institution of Mechanical Engineers, Part H: Journal of Engineering in Medicine, 229(8), 560-569.

## 3.1 Summary

CFD analysis of intracranial aneurysms has yielded a wealth of information regarding aneurysm initiation and rupture. Wall shear stress and Flow velocity are believed to play a vital role in the origin and development of arterial aneurysms. There have been a few computational studies aimed at investigating flow dynamics inside the aneurysm post-endovascular treatment.(176) Prior to this study, our group had assessed hemodynamic indices of patients following flow diversion treatment. They found that the failure to occlude the aneurysm is due to lack of obliteration of incoming jet flow owing to lower FD flow resistance at the neck. The prime limitation of the study was the use of a porous medium model which does not accurately replicate changes to its geometry and positioning of porosity. This study aims at using real-life flow diverter geometry at aneurysm neck (SILK, Balt Extrusions, Germany) to observe flow impingement, WSS and Energy Loss reduction values post flow diverter treatment.(177)

## 3.2 Abstract

Flow diverter stents have provided a new method of endovascular reconstruction for large and complex aneurysms. Understanding the impact of the flow diverter's angle of curvature across the neck and its metal coverage rate on the hemodynamics of aneurysm is crucial to maximize the mass flow reduction inside the aneurysm, post-deployment. The aim of this study is to understand the correlation between the angle of curvature of flow diverter across the aneurysm neck and the metal coverage rate, and the aneurysm's hemodynamics, using computational fluid dynamics. Varying the flow diverter angle resulted in varying metal coverage rate across the aneurysm neck for two patient vessel geometries, A (straight artery) and B (curved artery) with aspect ratios of 3.1 and 2.9, respectively. The results indicate that there exists a relationship between the aneurysm's hemodynamics and the flow diverter's angle of curvature across its neck. Moreover, the calculations indicated that cases with a

moderately curved flow diverter, with an associated metal cover- age rate of 50%–60%, achieve maximum flow reduction inside the aneurysm due to a stable flow resistance in the direction normal to the blood flow.

## 3.3 Introduction

Cerebral aneurysm is a localized dilation of the blood vessel. It is a cerebrovascular condition where the blood vessel becomes enlarged to form a balloon-like structure due to weakness of the arterial wall. Although mostly stable, intracranial aneurysms some- times rupture leading to a subarachnoid hemorrhage (SAH), and other various complications.(178) Treatment of cerebral aneurysms is strongly based on their risk stratification. Intracranial aneurysms are treated either by surgical clipping/bypass or by endovascular methods. Endovascular flow diverters (FDs) are stents used to treat complex aneurysms. They have low porosity and effectively occlude the aneurysm by promoting thrombosis inside the aneurysm, due to reduced wall shear stress (WSS). This leads to vascular reconstruction of the parent artery. (179, 180) There are now several commercially available FDs including pipeline embolization device or PED (ev3 Neurovascular, Irvine, CA, USA), SILK (Balt Extrusion, Montmorency, France) and SURPASS (Stryker Corporation, Kalamazoo, MI, USA).

Wang et al.(181) observed that the metal coverage rate (MCR) of deployed SILK stent at the neck significantly influenced the occlusion rate in rabbit aneurysms in vivo. The strut dimensions of the FD change with the different angles of curvature at the neck, and this study investigates the alteration that the change in strut geometry brings forth the change in stent's MCR and its pore density. By regulating the angle of curvature and thereby the MCR at the aneurysm neck, the flow reduction inside the aneurysm can be regulated.

Computational fluid dynamics (CFD) is widely applied in cerebrovascular aneurysm research.(160, 182) CFD has been applied to two main areas of research in FDs.(183, 184)

First involves understanding the mechanism by which the low-porosity stent enables vascular reconstruction and occlusion of the aneurysm. The second involves optimization of surgical techniques for pre- venting a delayed rupture, thereby achieving higher success rate.

The hemodynamic modeling of FDs such as SILK and PED has been attempted. CFD modeling has also helped develop novel flow diversion devices such as the 'Sphere' designed specifically for bifurcation aneurysm.(185) CFD analysis of pre and post stent deployment has helped researchers understand the mechanism of occlusion in various patient-specific geometries.(183) The angle of curvature of the FD across the aneurysm neck is dependent on the radial force of deployment along with factors such as the geometry of the parent vessel and the pull/push force applied during the operation. In turn, it is argued that the radial force of deployment should not be greater than the artery wall's stress– strain curve in order to achieve vessel remodeling.(184) In this study, the SILK FD has been modeled across the aneurysm neck with varying angle of curvatures which resulted in different MCRs. Hence, it is proposed that the FD's angle at the aneurysm neck has an impact on the hemodynamics of the cerebral aneurysm as it alters the MCR percentage at its neck. By measuring conventional parameters such as mass flow rate (MFR) and percentage reduction of energy loss (EL), the relationship between the aneurysm's hemodynamics and the FD's angle of curvature (and its associated MCR percentage) can be predicted.

## 3.4 Methods

### 3.4.1 Image Processing

Computed tomography angiography (CTA) was per- formed on Patient A and Patient B which showed internal carotid artery (ICA) aneurysms with the following geometry measurements, at Monash Medical Centre, Melbourne (Table 1). The parent vessel of Patient A is relatively straight, whereas Patient B has a highly curved parent artery. The curvature of

parent vessel geometry has been found considerably influence flow regulation post endovascular surgery by Xu. J et al., (268) and hence two different parent vessel geometry; straight and curved, was chosen to understand how the angle of the stent at the free segment changes the MCR, thereby regulating the flow inside the aneurysm. Written patient consensus was obtained for both the cases. Three-dimensional (3D) volume reconstruction from acquired two-dimensional (2D) CTA images was done using commercially available segmentation software Mimics 14.0 (Materialise, Leuven, Belgium). Thresholding is done to convert the grey- scale image to binary pixels. Care is taken to prevent surface artefacts. Local smoothing is done on these images as they help keep the geometry as realistic as possible as opposed to global smoothing.(186)

Table 1Geometric measurements of aneurysms of Patients A and B

| Patient | Diameter (D), mm | Height (H), mm | Neck width (N), mm | Aspect ratio (H/N) |
|---|---|---|---|---|
| **A** | 17.8 | 12.5 | 4.1 | 3.1 |
| **B** | 16.5 | 15.2 | 5.3 | 2.9 |

### 3.4.2 Stent Modeling

SILK is a closed-cell flow diversion device with low porosity used for vascular reconstruction in cerebral aneurysms. It consists of 48 braided Nitinol strands and 35 mm platinum microfilaments,10 and each strut has a width of 0.25 mm and a length of 0.52 mm. SILK FD was modeled for this study using the commercial computer-aided design (CAD) software package Creo Elements Pro Schools Edition 4.0 (PTC, Inc., Needham, MA, USA). The flow diverter deployment was facilitated by assembling the patient and FD geometries in CREO Elements Direct Modelling Express 4.0 (PTC, Inc., Needham, MA, USA). The vessel centerline was computed for each patient to be used as a reference for FD alignment and the vessel wall was used as the outer boundary. For conserving computational power and to avoid the complications arising from the additional stress caused by struts lodged against the artery wall, the FD was cropped to fit at specific angles across the aneurysm neck. Numerous studies (164, 183, 187) have validated the stent at neck method, wherein the FD is cropped at the aneurysm neck, against full virtual deployment of FD. In comparison, the key hemodynamic parameters showed no significant difference between the two data sets.(165, 168)

In Creo Direct Modelling Express 4.0, For Case 1, the stent was placed straight at the aneurysm neck without any curvature (0°; Figures 3-2(b) and 3-3(b)), whereas for Case 2 and Case 3, a bend was introduced at the neck with a curvature of 10° (Figures 3-2(c) and 3-3(c)) and 25° (Figures 3-2(d) and 3-3(d)), respectively, was introduced. A case with no stent inserted was also included in this study as control (Case 4; (Figures 3-2(a) and 3-3(a)). The

angle was calculated between the plane directions using Creo Elements Direct Modeling Express 4.0 (PTC, Inc.) for all cases (Figure 3-1). The angle was calculated using the following formula

$$\theta = \frac{\sum \theta_{1-4}}{4} \quad (8)$$

Where, $\theta_1$, $\theta_2$, $\theta_3$ and $\theta_4$ are measured between the arterial centerline and the strut direction of the FD. This is done to evaluate the effect of the angle of curvature on the hemodynamics of the aneurysm post FD treatment.

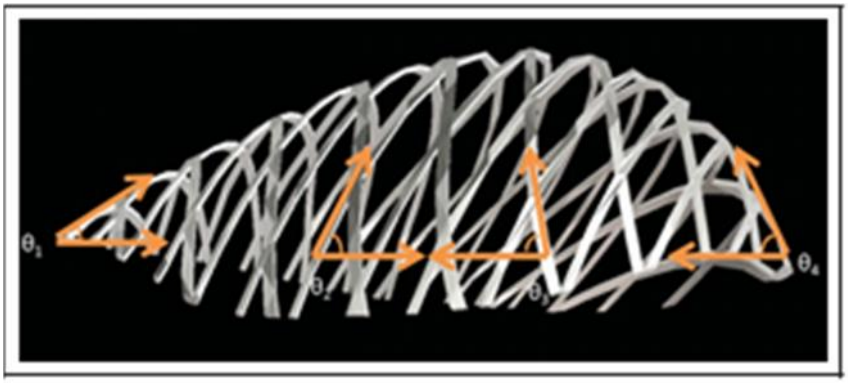

Figure 3-1 Illustration of measurement of FD's angle of curvature

The assembly was then exported to ANSYS ICEM CFD 14.0 (ANSYS, Inc., Canonsburg, PA, USA) mesh generation software. Due to complex nature of the geometry, unstructured tetra mesh with sizes from 0.3 mm for artery-aneurysm and 0.025 mm for FD was used with the mesh size of inlets and outlets being 0.1 mm. The total number of elements for all the cases ranged from 1,750,000 to 250,000. Grid-dependence tests, previously done by our research group, established that the EL became constant when the grid number is greater than 0.8 million.(188)

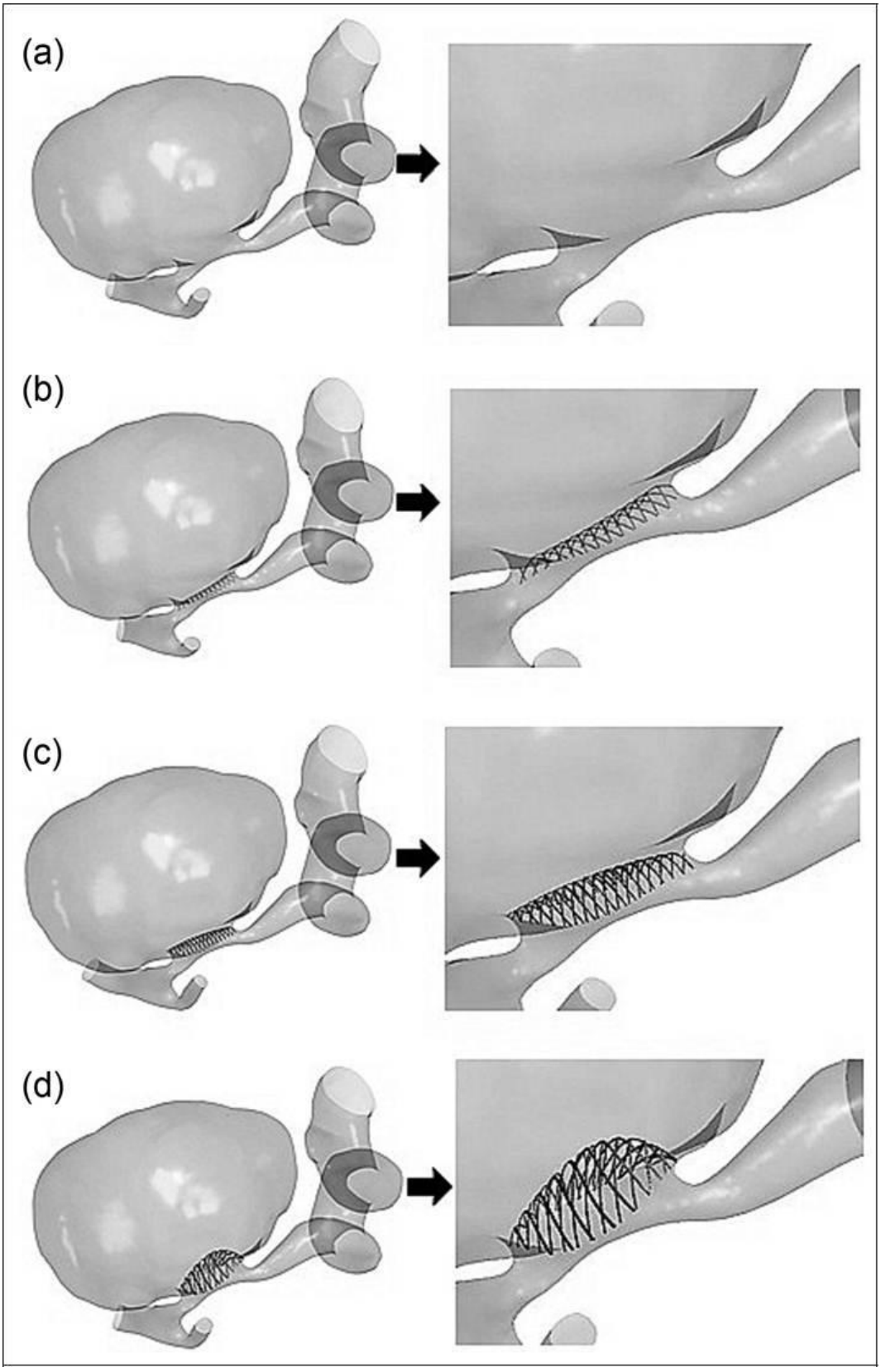


Figure 3-2 Flow diverter–aneurysm assembly for Patient A: (a) no stent, (b) 0° stent, (c) 10° stent and (d) 25° stent.

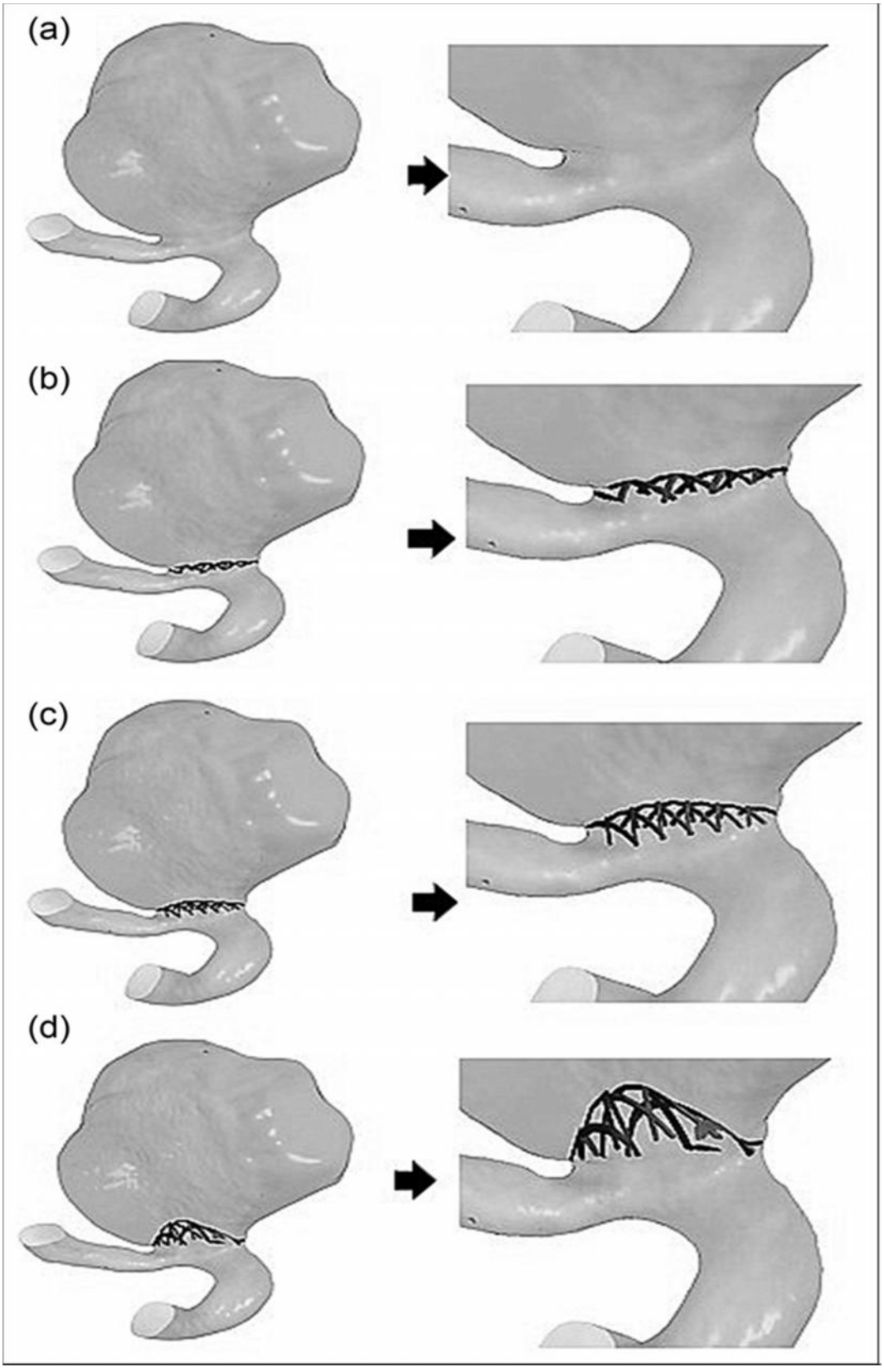


Figure 3-3 Flow diverter–aneurysm assembly for Patient B: (a) no stent, (b) 0° stent, (c) 10° stent and (d) 25° stent

### 3.4.3 CFD Simulation Methods

The meshed geometry was then exported to a commercial CFD solver called ANSYS CFX 14.0 (ANSYS, Inc.). The Navier–Stokes momentum and continuity equation which governs the fluid flow was solved for both cases (equation 1)

Blood was modeled as an incompressible Newtonian fluid with a density of 1050 kg/m3 and dynamic viscosity of 0.0035 Pa s. Cases 1–4 were run twice with the inlet boundary flow condition being fixed at a minima and maxima of 200 and 400 mL/min, respectively(189) which lie within the reported physiological flow window at the ICA. The outlet was extended to be 30 times of parent artery size and had a zero- pressure boundary condition specified there. Blood flow was assumed as having laminar flow under steady-state conditions. The artery wall was specified as rigid surface conforming to the no-slip condition. Convergence was assumed when the maximum residual for each of the equations was attained to a level below 1026. MCR, MFR and EL were calculated for all cases.

## 3.5 Study Parameters

### 3.5.1 Metal Coverage Rate

MCR percentage is defined as the ratio of the metal surface area to the total surface area. According to Wang et al.,(181) it can be calculated by the following simplified formula

$$MCR\ \% = \left[1 - \left(\frac{a}{A}\right)^2\right] \times 100 \quad (9)$$

where '*a*' represents the surface area of the stent across the neck of the aneurysm and *A* stands for the surface area across the aneurysm neck.

### 3.5.2 Mass Flow Rate

MFR is defined as the mass of fluid flowing through a section per unit of time. MFR is calculated from the following formula

$$MFR = A \cdot v \cdot \rho = Q \cdot \rho \quad (10)$$

where $A$ is the cross-sectional area, $v$ is the flow velocity and $\rho$ is the density of the fluid.

A study by Tang et al.(190)has shown that flow rates inside the aneurysm reduced up to 98% immediately post-stenting in idealized bifurcation aneurysm model treated with FDs having a porosity of 60%–75%. Although the results reported were based on ideal aneurysm model, nevertheless, it indicates that an optimal porosity can bring about maximum flow reduction inside an aneurysm.

### 3.5.3 Energy Loss

Qian et al.,(191) and Takao et al.,(192) defined Energy Loss as a parameter that measures the loss of energy by the aneurysm without the influence of the parent artery. It was reported that aneurysms with higher EL values had more chances of rupture. EL is mathematically expressed as

$$EL = E_{in} - E_{out} = Q_{in} \cdot P_{in} - Q_{out} \cdot P_{out} \quad (11)$$

Where E is the mechanical energy, $Q_{in}$ and $Q_{out}$ are the volume flow rate at inflow and outflow, respectively, and $P_{in}$ and $P_{out}$ are the total pressure at the inflow and outflow, respectively.

In our study, the aneurysm's EL calculated pre and post FD deployment is compared to predict its stability. According to Takao et al.,(192) we expect the EL of stented aneurysm geometry to be lesser than the no- stent aneurysm geometry. Percentage reduction in EL between stented and no-stent case is calculated using the following equation

$$\%\ EL\ Reduction = \left[1 - \left(\frac{EL_{stented}}{EL_{unstented}}\right)\right] \times 100 \quad (12)$$

This percentage reduction in EL between the stented and no-stent case is used as an indicator of delayed rupture risk, post-treatment.(191)

## 3.6 Results

### 3.6.1 MCR Percentage

The MCR decreases with the increasing angle of curvature. This is due to the change in the strut geometry resulting in stretching of FD across the aneurysm neck. The higher the angle of curvature, bigger is the change in strut geometry which leads to lower MCR percentage. The values of the MCR for different cases of both Patient A and Patient B are given in the Table 2. It is seen from the table that with the increase in the angle of curvature of FD at the aneurysm neck, the MCR at the neck decreases. This brought about by the change in the strut dimensions due to stretching. Case 3 with the highest curvature of 25° results in MCR values of just above 30% in both patient cases A and B (Table 2)

Table 2 Calculated metal coverage rate percentage of the flow diverter at the neck

| Case | Patient A (MCR %) | Patient B (MCR %) |
|---|---|---|
| **1 (0î Stent)** | 70 | 72 |
| **2 (10° Stent)** | 55 | 53 |

| | | |
|---|---|---|
| **3 (25° Stent)** | 32 | 38 |
| **4 (No stent)** | 0 | 0 |

MCR: Metal Coverage Rate

### 3.6.2 Mass Flow Rate

The MFR reduction percentage is an effective tool in gauging the success of the FD treatment post-surgery. Standard deviation was calculated for the averaged flow condition for all eight cases. From the results reported by Cebral et al., we can assume that lowering the percentage flow inside the aneurysm is favorable as it relates to lower velocity and WSS values which are contra-indicators of aneurysm rupture.(193, 194) Table 3 lists the MFR percentage reduction in both Patients A and B (Table 3):

Table 3 Mass flow percentage reduction in blood into aneurysm

| Case | Patient A (MFR %) | Patient B (MFR %) |
|---|---|---|
| **1 (0î Stent)** | 43.5 | 30.6 |
| **2 (10° Stent)** | 86.6 | 94.2 |
| **3 (25° Stent)** | 25.6 | 19 |

Patient A. The MFR percentage reduction post stent deployment is an indication of decreased flow through the aneurysm. The result showed that as little as 13% of the original flow was seen entering the aneurysm neck in Case 2 which had a 10° curved stent at the neck. Case 3 comprising extremely curved stent (25°) had flow reduction of 26%, lesser than Case 1 which had a percentage flow reduction of 43.5% (Figure 3-4).

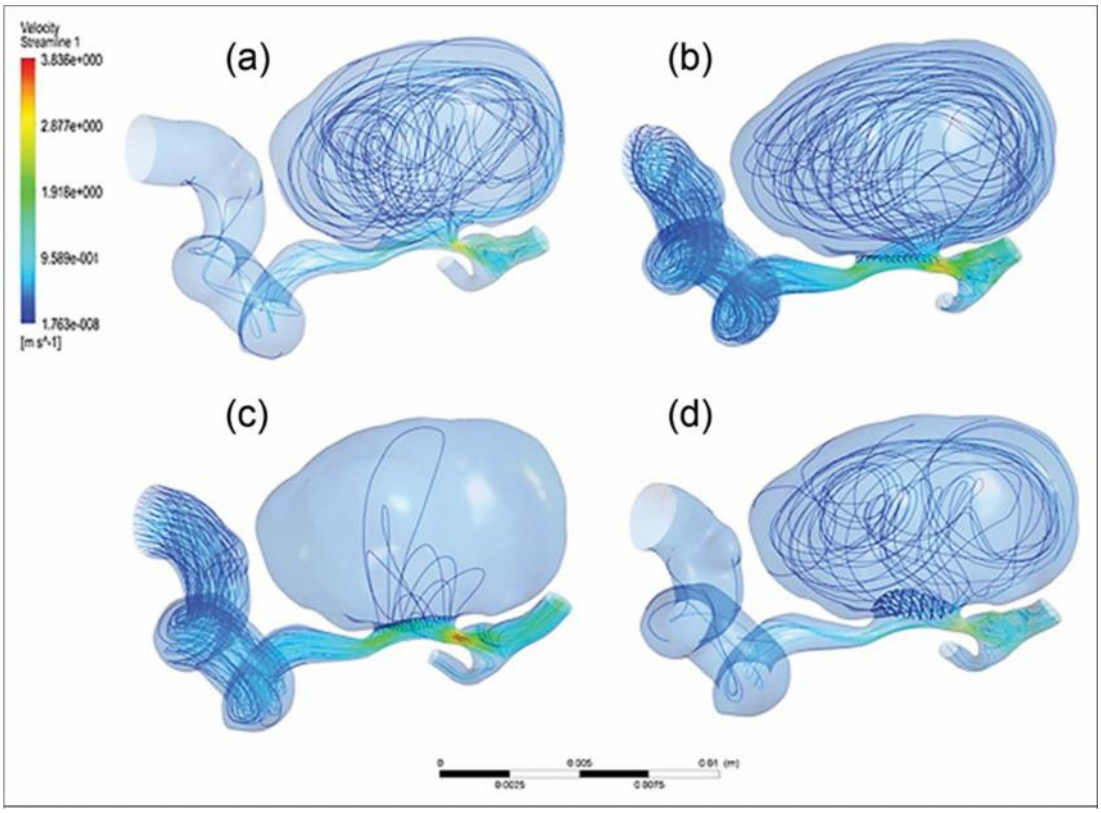


Figure 3-4 Blood flow streamlines for Patient A: (a) no stent, (b) 0° stent, (c) 10° stent and (d) 25° stent

Patient B. Due to the highly curved nature of the parent vessel, the highest percentage of MFR reduction of 94% was observed in Case 2 which had a FD deployed at the neck having a curvature of 10°. Case 3 with an extremely curved FD (25°) deployed had only a meager 19% reduction in the original flow when compared to the straight stent which reduced 30% of the original flow entering into the aneurysm (Figure 3-5).

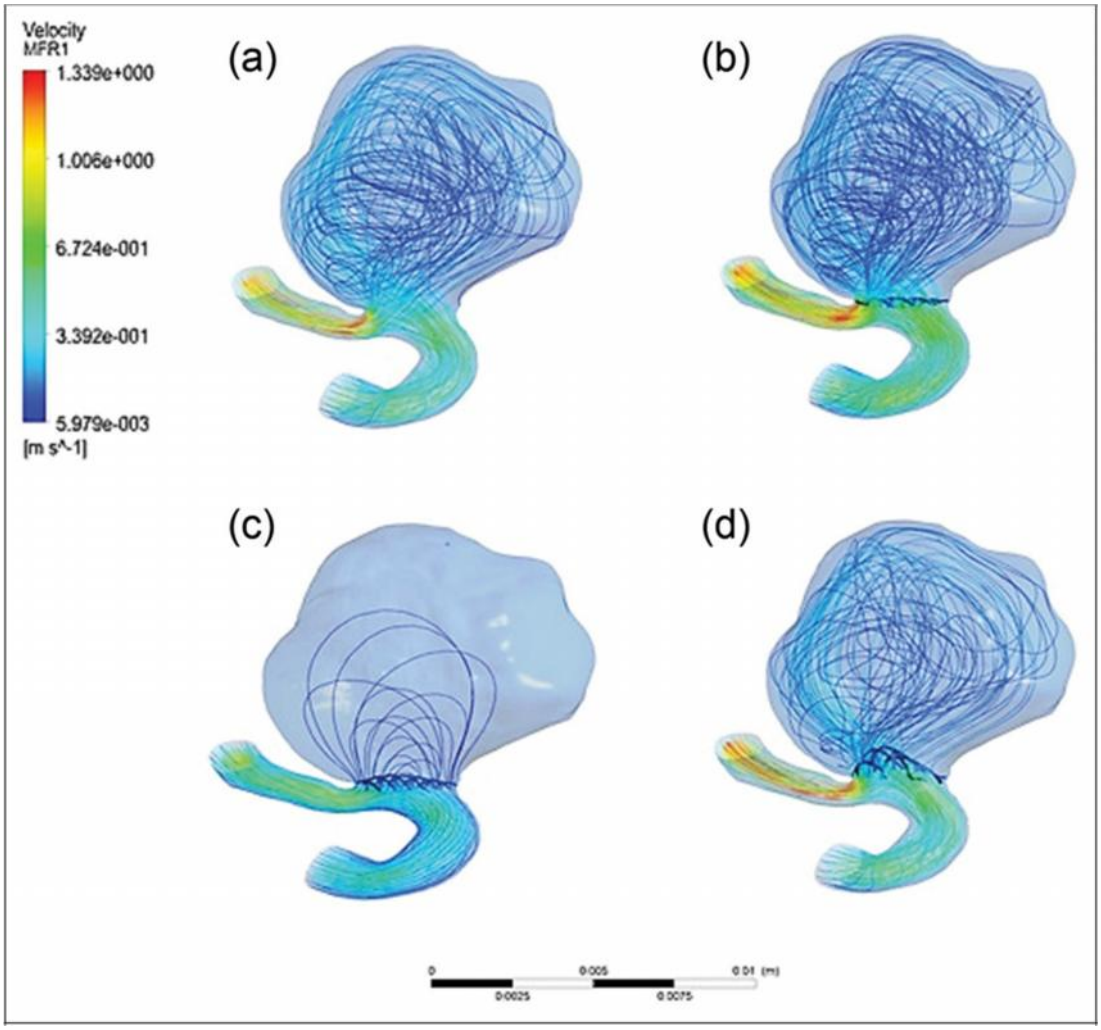


Figure 3-5 Blood flow streamlines for Patient B: (a) no stent, (b) 0° stent, (c) 10° stent and (d) 25° stent.

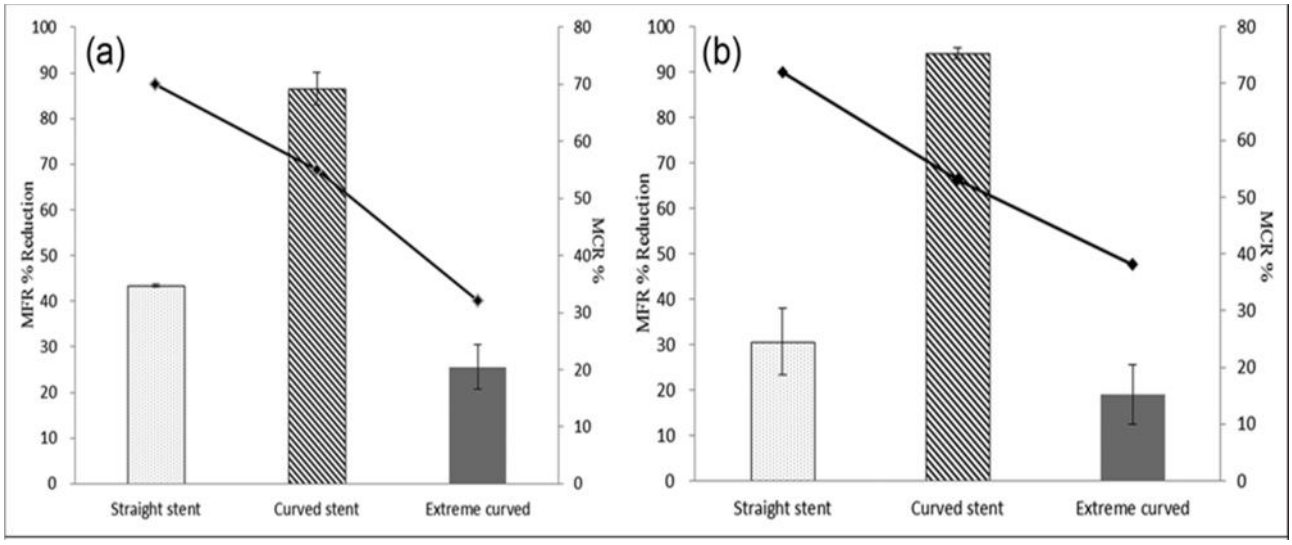


Figure 3-6 (a) Mass flow percentage reduction in blood inside the aneurysm post flow diverter deployment in Patient A and its correlation with MCR percentage and (b) mass flow percentage reduction in blood inside the aneurysm post flow diverter deployment in Patient B and its correlation with MCR Percentage

### 3.6.3 Energy Loss

We have discussed in our earlier research that higher EL leads to an increased risk of rupture for cerebral aneurysms.(160, 192, 195) The percentage EL reduction between pre- and post-deployment cases was averaged for min mum and maximum inlet flow conditions with the standard deviation error reported.

Patient A. A complex flow pattern is seen inside the aneurysm. There is an impingement zone of the side wall of the aneurysm as the outlet velocity is much higher than the inlet velocity. However, in Case 2 with a 10° curved FD at the neck, the impingement zone faded and the flow pattern becomes much less convoluted in comparison with the other cases. From the table, we can see that Case 2 with FD at a 10° angle with the aneurysm neck had the highest EL percentage reduction of 46% in comparison with the other 2 cases. Lowering the risk of rupture loosely translates to increased stability post-deployment (Figure 3-6).

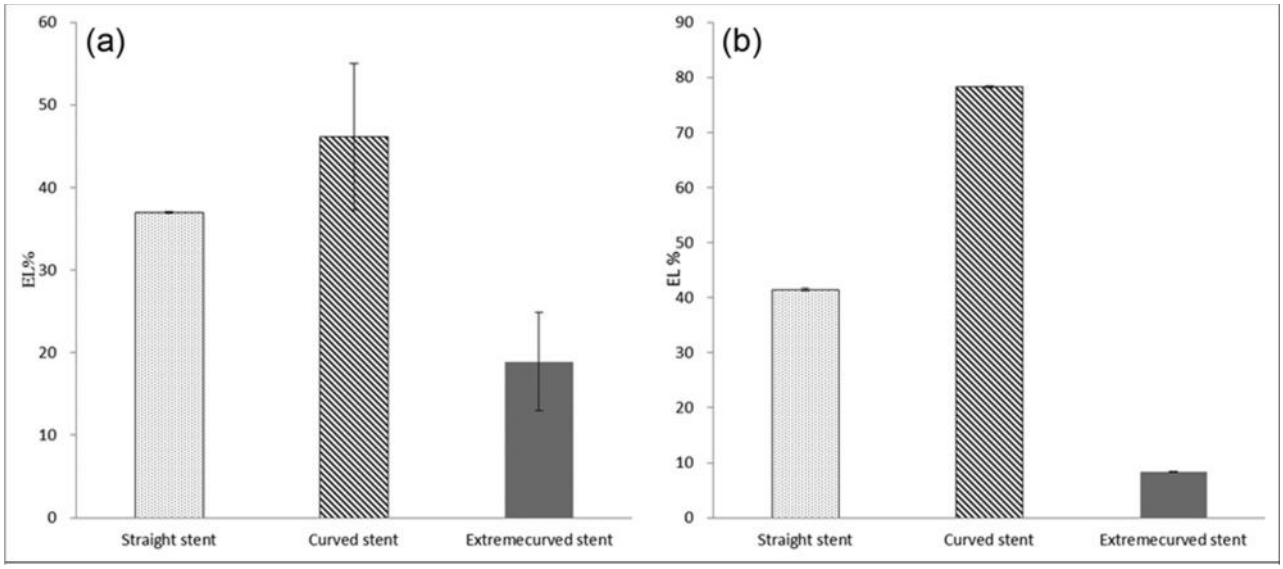


Figure 3-7 (a) Energy loss percentage of Patient A having flow diverters with varying (no stent, 0°, 10° and 25°) angle of curvatures across the aneurysm neck and (b) energy loss percentage of Patient B having flow diverters with varying (no stent, 0°, 10° and 25°) angle of curvatures across the aneurysm neck

Patient B. A high-velocity jet flow impingement was detected on the aneurysm bleb. Concurring with Patient A, Case 2 in Patient B shows a reduced jet flow and a simple flow pattern is observed. In addition to this, the velocity at the entrance of the aneurysm is much reduced in Case 2 in comparison with the other cases. In Patient B, the highest EL percentage reduction of 78% was calculated in Case 2. The other cases did achieve lower EL percentage reduction which is seen from Figure 3-7. Case 1 had significant EL value of 41.5% when compared to 8.3% in Case 3. This shows patency with the streamlines in Case 3 (Figure 3-5) where a complex intra-aneurysmal flow pattern with higher velocities is seen. An optimal vascular resistance has been calculated for Case 2 in both patient cases A and B (Figure 3-8)

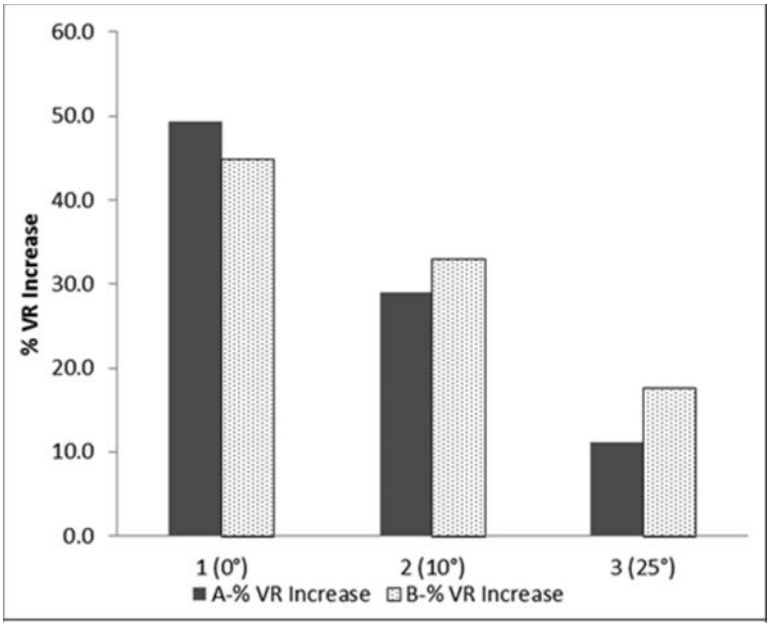


Figure 3-8 Vascular resistance percentage increase in Patient A and Patient B having flow diverters with varying (no stent, 0°, 10° and 25°) angle of curvatures across the aneurysm neck in comparison with no flow diverter inserted

In summary, it could be observed from the flow streamlines that patient A (Figure 3-4) with a relatively straight parent vessel geometry responds positively to curved FD sections as the flow entering the aneurysm appears to lower in Case 2 and Case 3 than Case 1. Whereas in Patient B (Figure 3-5) with the highly curved artery, the flow streamline in Case 3 with a highly angled FD section develops complex flow patterns with higher velocities inside the aneurysm when compared to Case 1 and Case 2. Wang et al.(181) have consistently reported MCR values of ≥35% to bring about maximum occlusion in rabbit aneurysms in vivo. To elucidate this further; our CFD calculations have established a desirable MCR percentage in the range of 50%–60% that brings about lowest intra-aneurysmal flow rate in Patients A and B. Despite both Patient A and Patient B having different parent vessel geometries, the highest percentage EL reduction is achieved in Case 2 for both patient cases. Yet for Patient B, the percentage EL reduction for Case 3 is negligible which might be resulting from complex flow patterns observed for Case 3 (Figure 3-5).

## 3.7 Discussion

Flow diversion has been recognized as an acceptable endovascular treatment for large and difficult-to-treat intracranial aneurysms.(179, 194) However, there have been cases of delayed aneurysm rupture and thromboembolic complications reported after flow diversion treatment.(196) In addition to the aneurysm/parent vessel geometry, this could be attributed to the suboptimal deployment of the FD in itself. This places emphasis that in addition to the FD itself, the surgical skill of the physician in positioning the FD across the aneurysm neck plays a key role in helping the treatment succeed. There have been a number of research publications involving CFD simulations that closely mimic the clinical stent deployment process in the past.(35, 164, 165, 187) These simulations aim to understand the general deployment process used and its function in the vascular reconstruction of the parent artery. It could also be used to understand the success or failure of the treatment and to identify the underlying hemodynamic parameters responsible for the same.

Decreasing the flow inside the aneurysm reduces the associated shear stress on the aneurysmal wall. This has been reported to promote the formation of thrombosis which is the key feature in the mechanism of aneurysm occlusion.(151, 197) In our study, no significant changes in WSS were observed among different angles of FD deployment cases for Patient A; in Patient B, there exists a maximum increase of 1 Pa (<10%) between Case 1 and Case 2 which could be attributed to the increase in EL percentage reduction by over 35%. CFD analysis of pre and post stent deployment has helped us understand the mechanism of occlusion in various patient-specific geometries.(148, 183, 198) A study of 30 intracranial aneurysms consisting of 26 stable and 4 ruptured aneurysms conducted by our group earlier18 showed us that the EL of ruptured aneurysms was 5.02 times higher than that of EL of stable intracranial aneurysms. It is to be expected that the EL for stented cases should be lower than the EL values calculated for untreated aneurysm geometry for increased stability. Therefore,

higher EL percentage reduction in treated aneurysms indicates lower chances of rupture which is seen in cases with a curved FD geometry, in both Patients A and B. Our study has taken into account two patient cases (A and B) with straight and curved parent vessel geometries, respectively. The key differences in the hemodynamic results (MFR and percentage EL reduction) between the two patient cases with differing parent vessel curvature were studied and reported in the results. In both patient cases A and B, Case 2 achieved the maximum flow reduction inside the aneurysm. This corresponded with the calculated EL as Case 2 had the highest percentage EL which implies that it will remain more stable post-deployment.

This is a preliminary investigation to provide clinically relevant data that explain the influence of the FD's angle at the aneurysm neck on its hemodynamics. Zhang et al.(177) reported that successful FD treatments are characteristic of possessing higher resistant forces, and in our hypothesis, we assume that a normalized angle of curvature of FD provides an ideal resistance force in the direction normal to that of the blood flow. In addition to this, curved FD at the neck decreases the MCR which has been established to have a positive correlation with volume flow reduction (VFR) percentage.3 this is consistently shown in our initial results, wherein Case 3 with the lowest metal coverage brought forth the least MFR percentage. The MCR percentage which is dependent on the FD geometry at the neck if regulated brings forth a desired flow resistance at the neck, as very high or very low increase in pulmonary resistance can destabilize the flow disrupting the occlusion process.(199) The results from this study show that there exists a correlation between the angles and the associated MCR of FD sections at the aneurysm neck and its hemodynamics. A preliminary attempt in understanding this correlation through the use of CFD indicates that a curved FD section might be able to bring forth a desired flow reduction inside the aneurysm.

The limitations of this study include an obvious lack of a wider patient sample size which is needed to establish the mechanism of influence of the FD's angle of curvature on the aneurysm's hemodynamics. Another possible limitation to this study is that along with the radial force of deployment, other features such as parent vessel geometry and aneurysm location have a strong hold on the deployed FD's angle of curvature at the aneurysm neck. In addition to this, the material properties of the constructed stent model are not reflective of the actual SILK flow diversion device, as the Nitinol and radio-opaque wires are not incorporated into the constructed FD model. This design limitation might lead to manipulation of angle of curvatures resulting in unrealistic FD sections which cannot be reproduced intra-operatively.

## 3.8 Conclusion

Despite the study limitations, this preliminary investigation has established a noticeable correlation between the angle of curvature of FD (and its associated MCR) on the hemodynamics of aneurysm. This basic study involving two different patient vessel geometries indicates that curved FD sections at the neck bring forth higher flow reduction. A key feature of significance is that although curved FD sections achieve higher percentage flow reduction, in substantially curved parent arteries, a highly curved FD section introduces complex flow patterns inside the aneurysm which is not desired. This study warrants further research in order to authenticate the mechanism of influence of the FD's angle of curvature across the aneurysm neck on intra- aneurysmal hemodynamics and to ascertain a statistical significance. It is nevertheless a promising approach to determine the success rate of FD treatment of large aneurysms on a case-by-case basis.

# Chapter 4

# *Identification of a hemodynamic parameter for assessing treatment outcome of EDAS in Moyamoya disease*

Published As

Karunanithi, K., Han, C., Lee, C.-J., Shi, W., Duan, L., & Qian, Y. (2015). Identification of a hemodynamic parameter for assessing treatment outcome of EDAS in Moyamoya disease. Journal of Biomechanics, 48(2), 304-309.

## 4.1 Abstract

This work is a novel attempt to incorporate computational fluid dynamics (CFD) techniques in the analysis of hemodynamic parameters of Moyamoya disease (MMD). Highly prevalent in Asian countries, MMD is characterized by progressive occlusion of the intracranial Internal Carotid Arteries (ICA). We intend to identify a reliable hemodynamic parameter that can be used to gauge treatment outcome. This will aid surgeons in the perioperative management of MMD patients. We carried out CFD analysis on eight patients (5 female, 3 male) with MMD treated by EDAS (Encephalo-duro-arterio-synangiosis) between 2011 and 2012. All the eight patients presented with hemorrhage, with subsequent 4–12 month follow-up done using Magnetic Resonance Angiography (MRA) to capture auto-remodeling. We calculated percentage change in flow rate and pressure drop index (PDI) across the Left and Right ICA. Pressure drop index (PDI) is defined as the difference of pressure reduction within the carotid arteries, measured at post-op and follow up, using patient specific inflow rates. The measured percentage flow change and pressure reduction showed an increase at follow up for improved patients (characterized by angiography according to the method of Matsushima), who did not develop any complications after surgery. The inverse was observed in patients who were clinically classified as no change and retrogressed (according to the method of Matsushima) cases post-operation. This elucidates that our findings have instituted a new parameter that may well play a critical role as an assistive clinical decision making tool in MMD

## 4.2 Introduction

MMD is a cerebrovascular condition that predisposes affected patients to stroke, in association with progressive stenosis of the intracranial internal carotid arteries and their proximal branches. It has a characteristic appearance of the associated network of abnormally dilated collateral vessels on angiography. This was later likened to “something hazy, like a puff of cigarette smoke,” which, in Japanese, is Moyamoya(200). Reduced blood flow in the

major vessels of the anterior circulation of the brain leads to compensatory development of collateral vasculature by small vessels near the apex of the carotid. Disease progression is not uncommon in adult MMD if untreated(201). The natural course of MMD is poorly understood but revascularization surgery is believed to be an effective procedure for preventing the progression of clinical symptoms(202, 203). Although various surgical techniques like direct Superficial Temporal Artery-Middle Cerebral Artery (STA-MCA) bypass surgery and indirect revascularization techniques (EDAS, EMAS (encephalo-myo-synangiosis) and Omental transposition) exist, post-surgical morbidity and mortality rates of 4–17% have been reported(204-206).

CFD has been widely applied to understand the hemodynamics of cerebral aneurysms. It has helped unravel a great deal of information regarding the genesis, development and rupture of intracranial aneurysms. The same cannot be said its application in other cerebrovascular diseases. Studying the hemodynamics of Moyamoya disease could benefit the way we diagnose and treat MMD patients. To align with the research objective, CFD techniques were applied to indirectly revascularised MMD patients and the hemodynamics at the CoW, particularly at the left and right ICA-site of occlusion were analyzed. The proposed aim of this study is to evaluate hemorrhagic MMD patients treated with revascularization surgery via the use of computational fluid dynamics (CFD) and analyze the pressure reduction in the left and right ICA arteries before and after treatment to understand how hemodynamic parameters such as flow rates and pressure reduction play a defining role in determining the success or failure of the treatment. A known pressure reduction has been established when fluid flows through a pipe according to Bernoulli’s equation. There also exists an acceptable range of pressure reduction or energy loss when blood is flowing through a normal healthy artery(207, 208). Hemorrhage on presentation is a major risk for morbidity and mortality, and revascularization surgery in hemorrhagic MMD patients aims to reduce the hemodynamic stress on abnormal collaterals. So measuring the pressure reduction across the artery post-

operatively and at follow up should serve as an effective indicator of treatment status. The effect of surgery associated complications such as rebleeding or infarction is not reflected in the Digital Subtraction Angiography (DSA) blood flow measurements carried out at follow up, thereby bringing into question its critical role in the treatment status classification. Hence, a reliable fluid flow parameter that could be calculated computationally is essential to gauge treatment outcome that will assist surgeons in the perioperative management of MMD patients. We carried out CFD analysis on eight MMD patients treated by EDAS wherein the branch of the STA is laid on the brain surface which vascularizes eventually providing a stable blood flow, with subsequent follow-up by MRA to capture auto-remodeling and calculated PDI and percentage flow change across the left and right ICA.

## 4.3 Methods

### 4.3.1 Patient Information

Eight adult patients (five female and three male) with ages ranging from 23 to 48 years were examined by MRA after undergoing revascularization surgery and at 4 to 12 months following surgery. All patients presented with hemorrhage as initial symptoms and were subsequently diagnosed with MMD. All patients were treated by EDAS on both left and right ICA from 2011 to 2012. All protocols were approved by the Institutional Research and Ethics Committee prior to the treatment. Although EDAS is rarely used to treat adult MMD patients (the method is more commonly used for pediatric MMD cases), we have shown that in adult patients with serious medical comorbidities, EDAS was effective in reducing the incidence of subsequent strokes along with preserving their functional independence(209). The demographic features of patient details are listed in Table 4. Also listed is the clinical treatment status for each patient at follow up classified according to the method described by Matsushima et al. (1992): improved

(III)= the postsurgical collateral vessels presented revascularization of two thirds of the MCA distribution; no change (II) = the postsurgical collateral vessels presented revascularization of one to two thirds of the MCA distribution; retrogressed (I) =the postsurgical collateral vessels presented very little or no revascularization. Each participant provided written informed consent. Three-dimensional (3D) geometries were reconstructed and segmented via use of commercial software package—MIMICS (Materialise, Belgium) so it can be computationally meshed in preparation for CFD calculation.(210)

Table 4 Patient demographics and follow up period

| Patient | Sex | Age | Status of treated left and right | Follow-up |
|---|---|---|---|---|
| **1** | F | 42 | Both sides improved | 13 |
| **2** | F | 30 | Left ICA—improved<br>Right ICA—retrogressed | 5 |
| **3** | F | 23 | Left ICA—retrogressed<br>Right ICA—improved | 4 |
| **4** | F | 36 | Both sides had no change | 5 |
| **5** | M | 38 | Both sides had no change | 8 |
| **6** | M | 25 | Both sides retrogressed | 12 |
| **7** | M | 42 | Both sides retrogressed | 5 |
| **8** | F | 48 | Both sides retrogressed | 4 |

### 4.3.2 CFD Modeling

3D geometry bypass model was reconstructed via generation of two-dimensional contours from grey scales of pixels, and by subsequent interpolation in a normal direction. This method prevents the intrusion of surface noise. Surface smoothing was kept to a minimum and limited to few localized areas to keep the surface roughness as close to the real vessel surface as possible. This method exhibited an average error of approximately one-third of a pixel in size(186).

Navier-Stokes equations (equation 1) for 3D flow with rigid walls were solved using ANSYS CFX 14 (Ansys Inc., Canonsburg, PA, USA), under steady state flow conditions. It has been established that steady state simulation adequately provide similar time- averaged results for pulsatile calculations over a cardiac cycle(211), which justified the use of steady state flow

condition rather than pulsatile condition. The inflow boundary conditions were measured for each patient at post-operation and follow-up by using Trans-Cranial Doppler Ultrasound (TCD Ultrasound). Blood flow was modeled as a laminar Newtonian flow with a density and dynamic viscosity of 1050 kg $m^{-3}$ and 0.0032 Ps respectively.

In order to simulate peripheral capacitance(212), the outlet of the vessel was extended distally in the normal downstream direction to 100 mesh layers, sufficient for the recovery of blood pressure(213), and zero pressure condition was applied at the outlets. In order to form a fully developed flow boundary layer at the proximal inlet, the domains were extended in an upstream direction to 100 times the size of ICA, so that fully developed velocity profiles were able to form in the boundary layer. Grid independence validations have been carried out in our previous work(191, 214). The total number of elements ranged between 800,000 and 1000,000. The grid size for the inlet/outlet interfaces were fixed at 0.01 mm and the rest of the computational domain had a maximum size of 0.03 mm.

### 4.3.3 Pressure Drop Index and Percentage Flow Increase

In two previous studies, Young and Tsai have investigated the flow characteristics in arterial stenosis through an extensive series of model experiments. On the basis of both steady- and unsteady-flow tests, they have found that the major factors controlling the pressure reduction across a stenosed artery can be estimated using factors such as tube length, instantaneous velocity across the tube and the fluid density and viscosity(215, 216). It has already been demonstrated that blood flow obeys pipe flow theory(208). In the current study, we hypothesize that PDI, calculated as the difference between pressure reduction at post-operation and follow-up, can serve as a figurative indicator of treatment success. Based on Bernoulli's equation, the pressure reduction is calculated as the difference between the total pressure at the inlet and outlet, at post-operation as well as at follow up. PDI is then calculated by the following equation:

$$PDI = \Delta P_f - \Delta P_p = (P_{if} - P_{of}) - (P_{ip} - P_{op}) \quad (13)$$

Where, PDI is a difference of pressure reduction measured at post-operation and follow up, $\Delta P_f$ and $\Delta P_p$ are the calculated pressure reduction at follow-up and post- operation respectively. $P_{if}$ and $P_{of}$ are the follow up total pressure values calculated at the inlet and outlet planes, respectively, and $P_{ip}$ and $P_{op}$ are the total post-operative pressure values calculated at the inlet and outlet planes, respectively (Fig. 4-1). All units are measured in Pascal (Pa).

In this study, we calculated the pressure reduction or head loss between the inlet and the outlet of each left and right ICA in all eight patients using CFD results. In order to eliminate error owing to segmentation, the pressure reduction in the left and right ICA were calculated between fixed co-ordinates at the inlet interface and the proximal end of the outlet, in both post-operative and follow up models in all patients (Fig. 4-1). The difference between the pressure reduction at post- operation and follow up was calculated as PDI which was then compared to the clinical classification (based on DSA and MRA measurements). Percentage flow change is calculated for this study by utilizing the TCD Ultrasound inflow rate measurements at the post-operative and follow up mode (Table 2). The rate of flow change at follow up and the calculated PDI values were then analyzed.

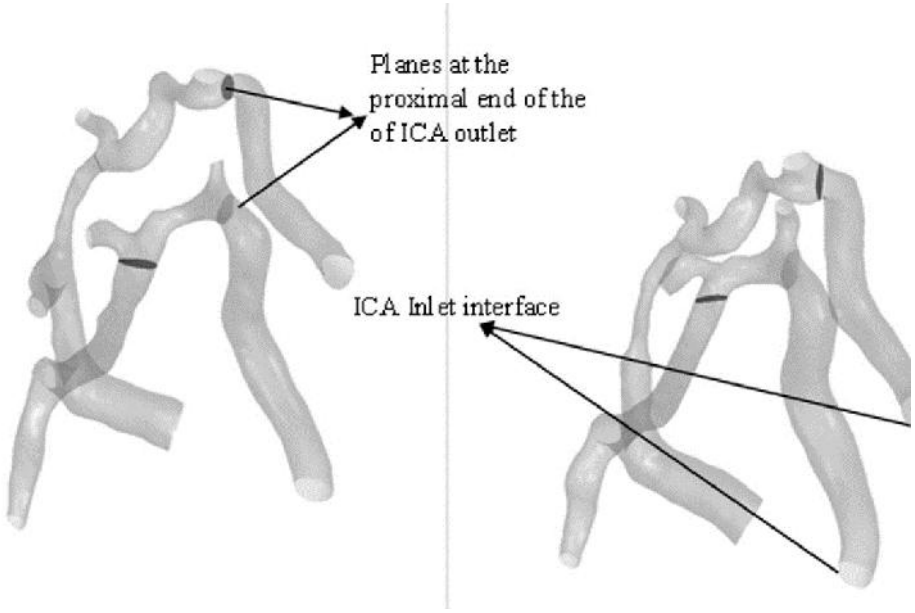


Figure 4-1 Segmented Moyamoya model with the inlet/outlet interfaces shown for pressure reduction measurement [Inserted plane at the proximal end of ICA outlet]

## 4.4 Results

### 4.4.1 Flow Changes

The inflow rates at post-operation and follow up were com- pared for all the cases and the % flow rate change in both left and right ICA were calculated which is displayed in Table 5 and Fig. 4-2. It was observed that for clinically classified as improved cases (III), there was an average increase of 14% in the inflow rate at follow up, whereas for no change cases (II), the flow decreased by up to 17%. In cases which were classified as retrogressed (I), the average % flow dropped greatly by 26% at follow up resulting in comparably lower blood flow through the carotid arteries than post-operation. This means that the volume flow of blood into the left and right ICA was decreased than at post-operation.

Table 5 Calculated percentage flow rate change between post-op and follow up in both left and right ICA for eight patients

| Patient number | Flow rate change %-left-ICA | Flow rate change %-right-ICA |
|---|---|---|
| **1—III** | 27.4 | 20.7 |
| **2—III** | 17.9 | 2.8 |
| **3—III** | 6.9 | 7.2 |
| **4—II** | −25.0 | −48.6 |
| **5—II** | −9.0 | 16.4 |
| **6—I** | −3.2 | −18.0 |
| **7—I** | −27.9 | −26.0 |
| **8—I** | −59.0 | −21.6 |

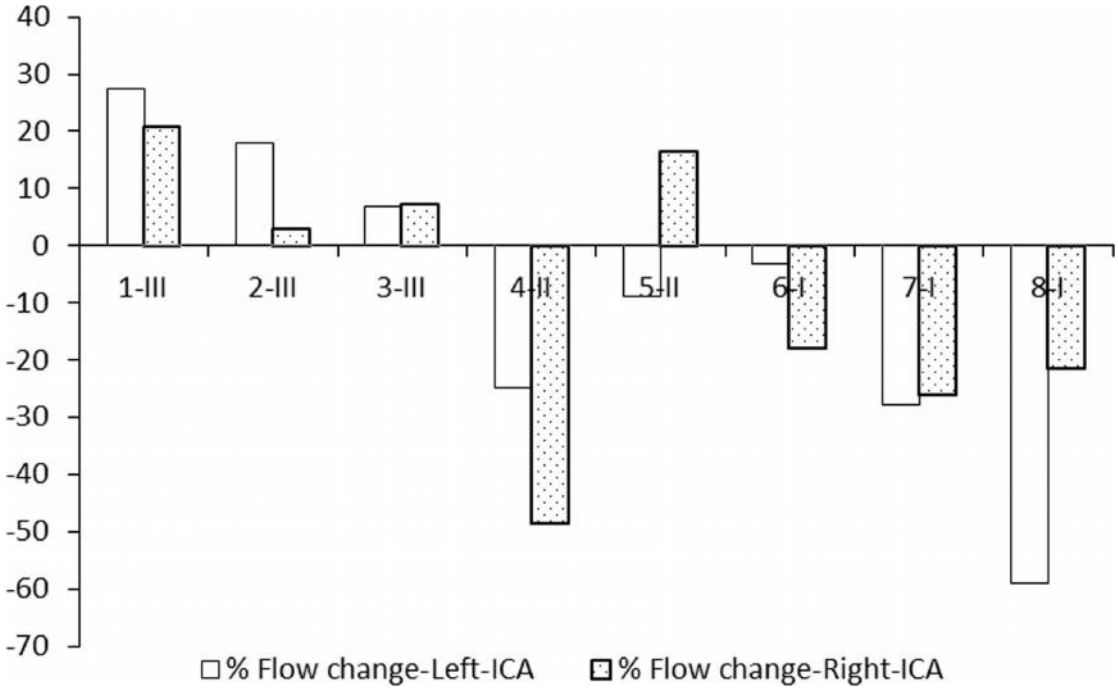


Figure 4-2 Calculated % flow rate change between post-op and follow up in both right and left ICA for eight patients

### 4.4.2 PDI Analysis

The difference in pressure reduction at post-operation and follow up (PDI) was plotted for all eight cases (Fig. 4-3), which shows that, in general, PDI is negative for improved cases and increases linearly for no change and retrogressed cases.

An average PDI for improved cases lied well within the negative band of -180.39 Pa. This shows that pressure reduction at follow up is much greater than the pressure reduction post-operation. In comparison, the average PDI value for no change cases and retrogressed cases were 48.49 Pa and 193.08, respectively. This is expected owing to the increase in mass flow rates at follow up. In no change cases, the relatively smaller decrease in flow rate (15–17%) at follow up than improved cases resulted in marginal decrease of pressure reduction at follow up in comparison to post- operation. There were a few interesting cases. For example, patient 2, who showed success in regaining blood flow in the left hemisphere but not the right, PDI lies in the negative band for left ICA whereas PDI in right ICA was calculated to be in the positive band at 76.02 Pa (Fig. 4-2). Patient 3 showed similar results, whose right ICA proved successful post treatment with PDI.

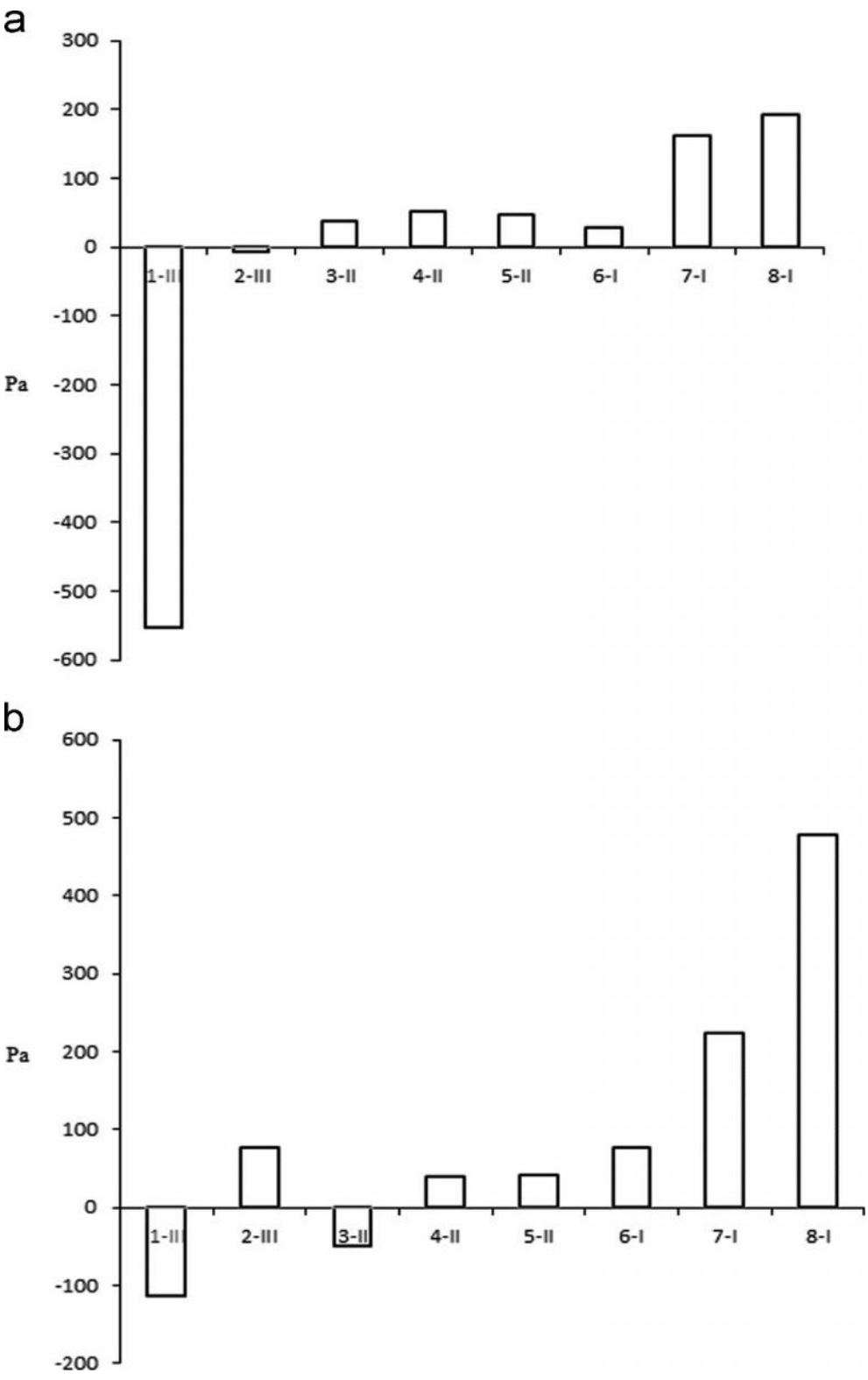


Figure 4-3 (a) PDI values of eight patients calculated for left ICA between post-op and follow up (Pa), I—retrogressed, II—no change, III—improved. (b) PDI values of eight patients calculated for right ICA between post-op and follow up (Pa)), I—retrogressed, II—no change, III—improved

The PDI values of all eight patients were plotted and a discernable increase in pressure at follow-up was observed in the pressure contours of all retrogressed and no change cases due to vessel narrowing in the Circle of Willis (Fig. 4-4). For patients 2 and 3 (Fig. 4-4b and c), the pressure contours showed an unambiguous trend wherein, the right and left ICA (deemed retrogressed) showed higher values of total pressure at follow up than post-op. Fig. 4-4b and c also reveal the pressure contours for the successful hemisphere of patient 2 (left ICA) and 3 (right ICA) have lower pressure values at follow up, due to successful vessel remodeling. For patient 8 (Fig. 4-4h), the development of a possible aneurysm in the right anterior cerebral artery could be responsible for the anomaly wherein the pressure contours at follow up are lower than the values at post-operation.

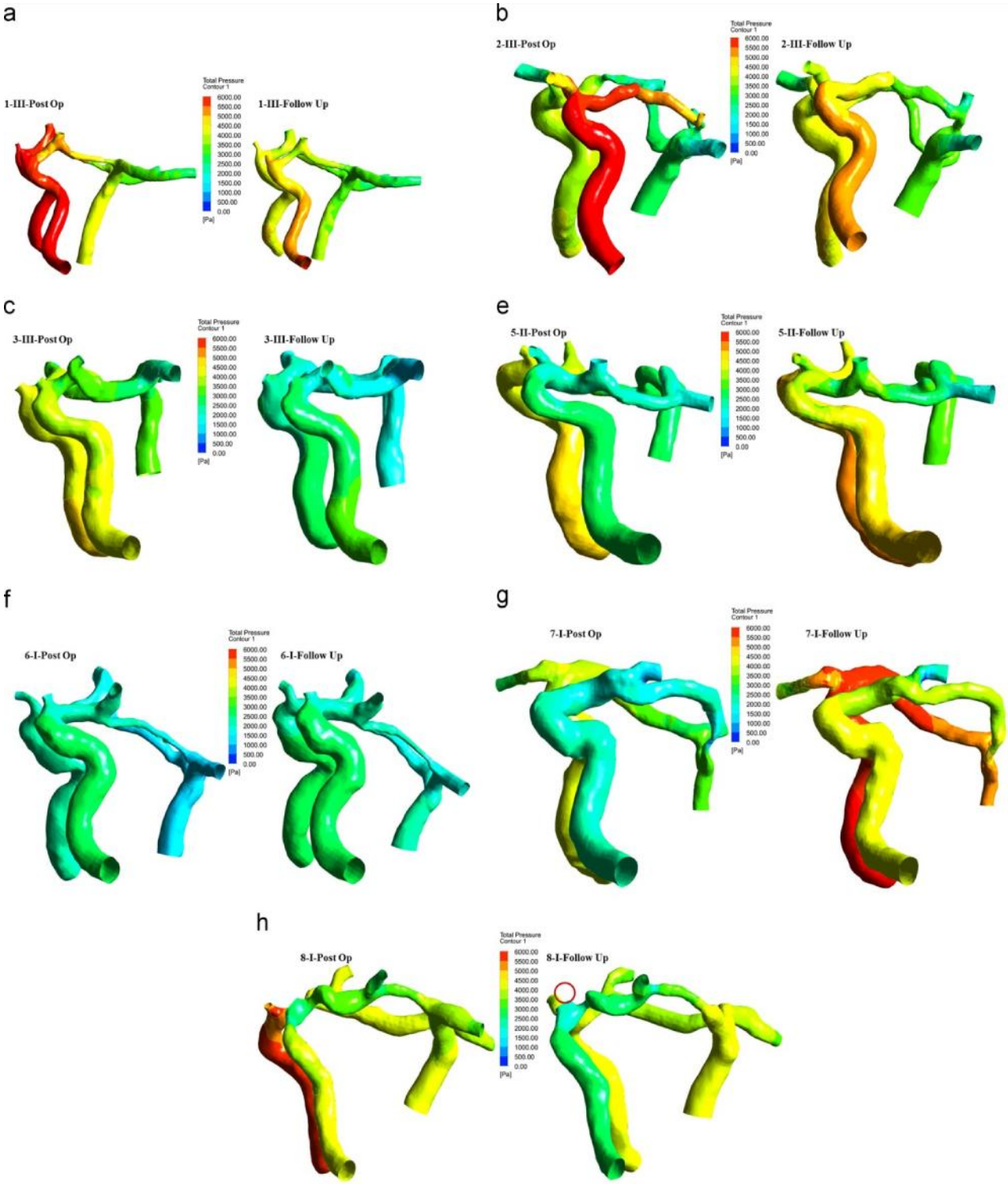


Figure 4-4 (a-h) Pressure contours for Patient 1-8 respectively at Post-op and Follow up

## 4.5 Discussion

Recent advances in angiographic techniques and increased routine health check-ups have raised our awareness of the presence of symptomatic and asymptomatic MMD(217). Symptomatic MMD is treated either by direct revascularization methods which have a

reported failure rate of 28.3%(218), or by indirect revascularization surgery. The study done by Karasawa et al. (1992) has a reported complication rate of 17% for 104 patients who underwent temporal-to-middle cerebral artery anastomosis and/or encephalo-myo-synangiosis(219). Iwama et al. (1997) reported a rebleeding and hemorrhage rate of 23% of the 129 patients treated with revascularization surgery. Their result indicated that intracranial bleeding might occur as a result of rupture of a tiny aneurysm at the periphery of collateral vessels.(220) In other cases, bleeding occurs at different sites from the initial site. They are considered to be a result of ruptured weak Moyamoya vessels which are forced to act as collateral pathways and are under unusually increased hemodynamic stress. This is evidenced by higher local cerebral blood flow rates in MMD patients(221). Prevention of rebleeding is one of the major goals in the treatment of MMD as patients who experience rebleeding tend to have worse outcomes(222). Direct surgical bypass is preferred in patients presented with cerebral ischemia whereas indirect revascularization is carried out in pediatric patients (103), but there have been no randomized clinical trials so far to assess the efficacy of the two surgical methods and support one technique over the other until now. Recently endovascular treatments such as angioplasty and stenting have also been investigated but without much success(223). Lack of comprehension about the mechanism of rebleeding, stenosis and rupture in MMD patients and also nil presence of indicative/ predictive measures of treatment outcome poses a serious health hazard. Hence strict perioperative and long term management of treated patients is indispensible to reduce the morbidity and mortality resulting from adverse complications.

CFD is applied widely in cerebrovascular aneurysm research. Various research groups around the world are now trying to understand the underlying mechanisms leading to aneurysm initiation, development and rupture along with trying to deter- mine the efficacy of surgical intervention (138, 224, 225). In our analysis, we sought CFD based risk factor identification, in addition to existing clinical image based methods, which would assist clinicians in

stratifying MMD patients placed in high risk category post- surgery. The measured patient specific inflow rates showed an increase at follow up for improved patients, who did not develop any complications since surgery. A decrease in ICA inflow rates at follow up implied that much of the Cerebral Blood Flow output (CBF) was still flowing through the collateral vessels. Thin and narrow walled collateral vasculature has been linked to rupture/ hemorrhagic events in MMD patients(220). Analysis of calculated PDI values showed us that negative PDI value (wherein the pressure reduction values at follow up are lower than the post-operative pressure reduction values) pointed to a risk of rebleeding/ischemia caused by collateral vessels rupture. The association of negative PDI with post-surgical complications is consistent in patients 2 and 3 wherein only one of the ICA vessels was successful in gaining normal CBF output in the long term.

This is a pilot study for hemodynamic analysis of treated MMD patients using CFD techniques where we quantitatively identify a parameter for effective risk stratification of treated MMD patients based on MRA images. Our results strongly suggest a distinctive correlation between treatment classifications; % flow change and PDI may thus be used in the long run to assist clinicians in long term on going care for treated hemorrhagic MMD patients. This research analyzed MMD cases primarily in terms of hemodynamics, rather than DSA or other image-based clinical classification. Other clinical factors resulting due to vessel auto remodeling, such as collateral development from indirect revascularization, were not distinguishable in this study. Another limitation of this study is that the number of cases is small. To fully elucidate the influence of PDI and to establish its statistical significance, further investigation with an exhaustive patient sample size is required. Nonetheless, our findings have instituted a new parameter that may well play a critical role as an assistive clinical decision making tool in MMD.

## 4.6 Conclusion

This work is an original attempt to incorporate CFD techniques in the analysis of hemodynamic parameters of MMD. We identified a new parameter PDI, trending conspicuously with treatment status classification. We computed PDI values for eight patients (three improved, two no change and three retrogressed cases). The pressure reduction increased considerably for three improved patients at follow up than their post-operation counterparts. The pressure reduction at follow up decreased linearly for the other five patients who were classified as no change and retrogressed based on DSA of the right and left ICA. This inference warrants further research into PDI as a causative factor for post-surgical complications in treated MMD patients. PDI has a potential to serve as a supplementary tool in assisting clinicians for confident risk stratification of MMD patients for long term follow up. In addition to this, PDI can shed some light into the underlying hemodynamic mechanism which is believed to bring about rebleeding/hemorrhage in MMD patients.

# Chapter 5

# *Assessing Surgical Treatment Outcome Following Superficial Temporal Artery to Middle Cerebral Artery Bypass based on Computational Hemodynamic Analysis*

Published As

Zhu, F., Karunanithi, K., Qian, Y., Mao, Y., Xu, B., Gu, Y., Morgan, M. (2015) Assessing surgical treatment outcome following superficial temporal artery to middle cerebral artery bypass based on computational hemodynamic analysis. Journal of Biomechanics, 48(15), 4053-4058.

## 5.1 Abstract

To estimate hemodynamic modification of Internal Carotid Artery (ICA) after bypass surgery using computational fluid dynamic (CFD) technology and thereby aid in our understanding of the influence of hemodynamic parameters on the outcomes of bypass operations. 18 patients who underwent superficial temporal artery to middle cerebral artery bypass and encephaloduroarteriomyosynangiosis surgery were included. Reconstructed three-dimensional vessel geometries from MRA were segmented to create computational domains for CFD simulations. All cases were classified as three groups according to the proportion of the MCA area of distribution supplied by revascularization: A, more than two thirds; B, between two thirds and one third; and C, less than one third of the MCA distribution. Pre-operative and follow-up hemodynamic parameters, especially volume flow rate and pressure drop index (PDI) in ICA were compared. For all cases, PDI and volume flow rate in the surgical-side ICA decreased significantly at follow-up ($P < 0.05$). For the cases of group A, volume flow rate in surgical-side ICA decreased by average 24.2%, whilst for the cases of group B and C, flow rate reduced by 10.5% and 3.7%, respectively. An average PDI for cases in group A was -1.67mmHg, conversely average PDI values of group B and C were -0.53 and 0.82mmHg, respectively. The remodeling of ICA after bypass was associated with reduction in the volume flow rate and pressure drop. Good correlation with angiographic treatment outcomes suggested that PDI might play a critical role as a hemodynamic indicator for clinical decision making during the follow-up of MMD patients.

## 5.2 Introduction

Moyamoya disease (MMD) is characterized by stenosis or occlusion at the terminal internal carotid artery (ICA) or proximal portions of anterior cerebral arteries (ACA) or middle cerebral arteries (MCA). It leads to formation of a fine vascular network at the base of brain which looks like “puff of smoke” in angiogram, which is why it is named Moyamoya (puff of

smoke in Japanese) disease(104). Arterial stenosis around the circle of Willis induces blood flow reduction in the brain and formation of fragile Moyamoya vessels (220). Surgical revascularization, including direct methods, e.g. superficial temporal artery – middle cerebral artery (STA-MCA) bypass, and indirect methods, e.g. encephaloduroarteriosynangiosis (EDAS), encephalomyosynangiosis (EMS), encephaloduroarteriomyosynangiosis (EDMS) and multiple burr holes surgery, are common treatments for reconstructing cerebral blood flow of MMD patients. Many observational studies indicated that direct and/or indirect bypass could reduce the risk of cerebral ischemic stroke by flow augmentation for patients with MMD (226-228). Angiographic diminishment of Moyamoya vessels was observed after EC-IC bypass surgery, which was regarded to result in decreased hemodynamic stress to pathological Moyamoya vessels(109, 180, 229).

Computational fluid dynamic (CFD) technology has been applied widely in many cerebrovascular diseases for quantitative hemodynamic analysis, especially for aneurysms and intracranial artery stenosis (230-232). In the past, CFD techniques have been employed to look into maintaining the patency of high flow bypass (233). Our previous study revealed STA-MCA bypass has a characteristic auto-remodeling after surgery using CFD (174). The decrease of ICA pressure drop index (PDI) was also observed for successfully treated cases, at follow-up after indirect bypass surgery (EDAS) (234). There have been many reported anatomical variations of the Circle of Willis from a number of autopsy studies.(235, 236) These variations are genetic in origin and the most commonly found variation is a disconnected Circle of Willis wherein the Left and Right ICA function as individual arterial hemispheres.(237) In this study, we have computationally analyzed the hemodynamics of MMD patients with an incomplete CoW that were treated with combined STA-MCA bypass and EDMS surgery. The study aims to estimate the hemodynamic modification of ICA after combined revascularization surgery in the treated hemisphere. Additionally, Pressure Drop Index has been calculated and the correlation of PDI with direct revascularization treatment

outcome has also been evaluated to determine if it follows an analogous pattern to our previous work.

## 5.3 Materials and Methods

### 5.3.1 Subjects

18 patients were diagnosed with MMD and treated with combined STA-MCA bypass and EDMS in Huashan Hospital from 2010 to 2013. MMD was diagnosed according to the criteria of the Research Committee on Spontaneous Occlusion of the Circle of Willis (Moyamoya Disease) of the Ministry of Health and Welfare, Japan(97). The circle of Willis was incomplete and bypass surgery was performed on one hemisphere for each patient. All patients were routinely examined by magnetic resonance angiography (MRA) and duplex ultrasonography preoperatively and at follow-up. The study was approved by ethical committees of Huashan Hospital, Fudan University and Macquarie University. Written informed consent was obtained from each patient.

### 5.3.2 Surgical Procedures

Surgical intervention for MMD was indicated after comprehensively evaluating the digital subtraction angiography (DSA), clinical manifestations and brain perfusion or metabolic findings in our department, detailed surgical indications were described before(229, 238). Combined direct STA-MCA bypass along with indirect encephalo-duro-myo-synangiosis (EDMS) was performed on all patients. This is in contrast to the standalone indirect encephalo-duro-arterio-synangiosis (EDAS) that was performed in our previous study. Anterior and/or posterior branch of STA were anastomosed to the cortical branch of MCA in end-to-side fashion using a single 10-0 nylon suture. EDMS, the indirect bypass procedure has been described in our previous study (238). Fifteen cases were operated by Professor B Xu, and three cases were operated by Professor YX Gu from Huashan Hospital.

### 5.3.3 MRI Scanning and Ultrasonography

MRA scans (4 slabs , 40 slices per slab; TR, 22 ms; TE, 4.2ms; flip angle, 18; matrix size, 365×384; slice thickness 0.5mm; field of view 181× 200 mm2) were obtained with 3.0 T MR Systems console (Verio, Siemens Medical Systems, Erlangen, Germany).

Duplex ultrasonography was performed to measure the blood flow of ICA using an L9-3 linear probe (bandwidth, 3-9 MHz) (bandwidth, 1-5 MHz) on a high-end ultrasound device (Philips Healthcare, Andover, MA) (239).

### 5.3.4 CFD Modeling

Three-dimensional (3D) geometries of ICA were reconstructed and segmented by using a commercial software package - MIMICS (Materialise' Interactive Medical Image Control System, Belgium) to create domains for CFD computation. Instead of using "global smoothing", we used manual "local smoothing" to keep the 3-D geometry as realistic as possible. Mesh generation yielded elements ranging from 0.8 to 1.4 million. The conservation equations for 3D steady flow with rigid walls were solved by using the ANSYS CFX 15.0, a finite-volume-based CFD solver (ANSYS Inc., Canonsburg, PA, USA). Patient specific inflow boundary conditions of blood flow were measured by duplex ultrasonography. A zero static pressure was specified as outlet boundary condition. Blood flow was modeled as a laminar Newtonian fluid with a density and dynamic viscosity of 1050 kg $m^{-3}$ and 0.0032 Pas, respectively.

### 5.3.5 Pressure Drop Index (PDI)

PDI was calculated as the difference in pressure reduction along the ICA at pre-operation and follow-up. PDI can be calculated using the equation 13 as shown in chapter 4.

The positions of proximal (inlet) and distal (outlet) planes where we measured the pressure values are the same between pre-operative and follow-up models. All units are in mmHg.

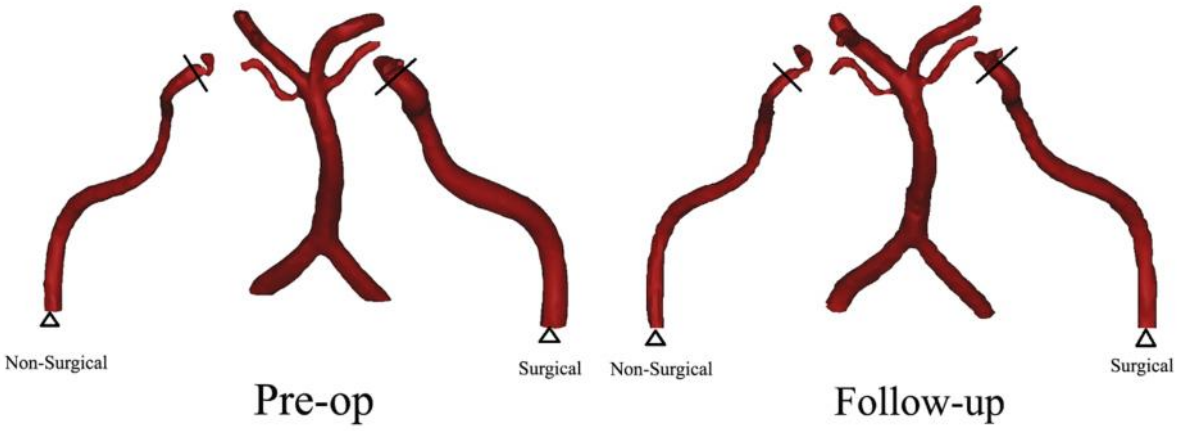


Figure 5-1 Illustration of planes for pressure measurement in the pre-operative and follow-up CFD models Inlet measurement plane is marked with triangle, outlet measurement plane is labeled using black line.

### 5.3.6 Inflow conditions and Volume flow rate change

Velocities were measured at the proximal end of ICA by ultrasonography and were used as inflow conditions in CFD simulation. The volume flow rate of ICA was measured by utilizing the mass flow from CFD. The percentage of volume flow rate change was calculated by using the formula.

$$\text{Percentage of volume flow rate change} = \left(F_f - F_p\right)/F_p \times 100\% \quad (14)$$

Where, $F_p$ and $F_f$ are the measured mass flow of ICA at pre-operation and follow-up respectively.

### 5.3.7 Angiographic treatment outcome

All cases are classified as three groups according to angiographic outcomes from surgery by the criteria proposed by Matsushima(240). This grading was the proportion of the MCA area of distribution supplied by the surgical revascularization: A, more than two thirds of the MCA distribution; B, between two thirds and one third of the MCA distribution; and C, less than one third of the MCA distribution. The angiographic treatment outcome was evaluated by 2 independent neurosurgeons who were blinded to this study.

### 5.3.8 Statistical Analysis

The normality of hemodynamic parameter distributions was checked. Mean and standard deviation were calculated to represent the normal variable, and non-normal distribution variables were represented as median and quartile. Two-tailed paired Student's t-test was applied to compare the results of pre-operative and follow-up parameters both in the surgical side and non-surgical (contralateral) side of ICA. Nonparametric analysis was used among non-normal variables. A significance level of 0.05 (P-value) was selected for the test to verify if the changes in the hemodynamic parameters were statistically significant. Statistical analyses were performed using SPSS 17.0 software (IBM Corp, USA).

## 5.4 Results

### 5.4.1 Surgical Outcome

There were seven males and eleven females diagnosed of MMD with a mean age of 34.8 ± 8.38 years, ranging from 18 to 50 years. Demographic features of patients' details are listed in Table 6. The 18 patients were followed up for 3-13 months, an average of 6.2 months. Preoperative symptoms were improved in all cases. There was no new cerebral infarction or bleeding during the follow-up observation. Eleven, four, and three cases were classified as group A, B and C respectively.

Table 6 Demographic and clinical characteristics of the patients

| | |
|---|---|
| **Age (Years)** | |
| *Mean ± SD* | *34.8 ± 8.38* |
| *Range* | *18-50* |
| **Gender** | |
| *Male* | *7 (38.9%)* |
| *Female* | *11 (61.1%)* |
| **Surgical Side** | |
| *Right* | *10 (55.6%)* |
| *Left* | *8 (44.4%)* |
| **Clinical presentation** | |
| *Cerebral infarct* | *8 (44.4%)* |
| *Transient Ischemic Attack* | *5 (27.8%)* |
| *Haemorrhage* | *5 (27.8%)* |

### 5.4.2 Volume Flow Rate Change

In this study, the volume flow rate in ICA at pre-operation and follow-up were compared, and the percentage of volume flow rate change in both sides of surgical and non-surgical ICA were calculated. At the follow-up observation, the volume flow rate of surgical ICA significantly decreased from 157.77 ± 50.14 ml/min to 131.28 ± 51.78 ml/min ($P < 0.01$) (Figure 5-2). While, in the non-surgical ICA, the volume flow rate insignificantly increased (157.18 ± 55.74 ml/min at pre-operation, 175.58 ± 106.51 ml/min at follow-up, $P > 0.05$). The changes of volume flow rate in the surgical and non-surgical ICA appeared significantly different ($P < 0.05$). Table 7 summarizes the change of volume flow rates at the conditions of pre-operation and follow-up. For cases classified in group A, as a result of the good auto-

remodeling of ICA (e.g. stenosis progression of terminal ICA, reduction in diameter), the flow rate in the surgical ICA was decreased by 24.2%, whilst for cases of group B and C, blood flow reduced by 10.5% and 3.7%, respectively.

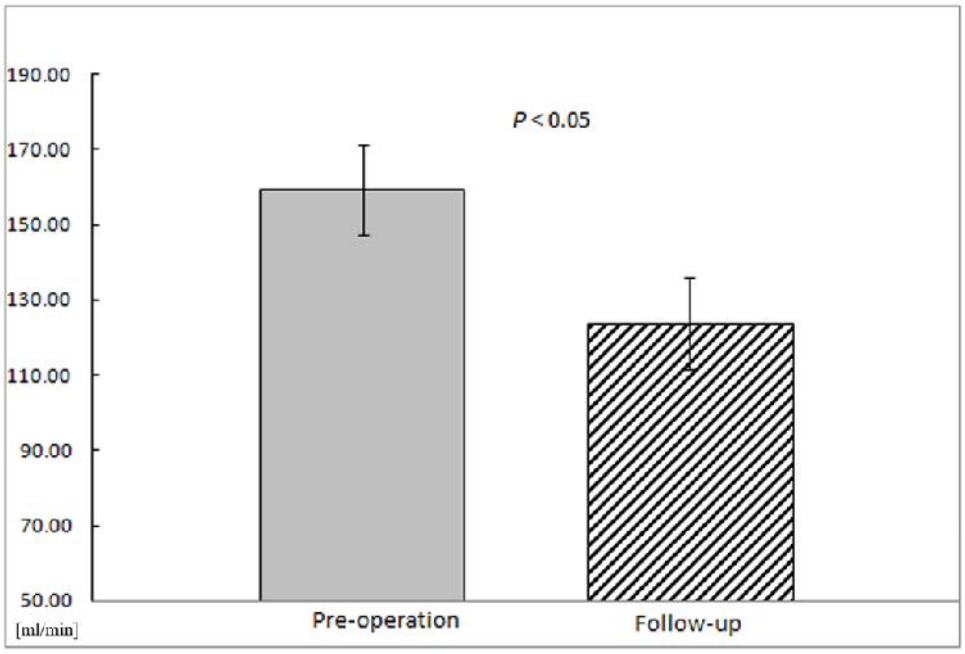


Figure 5-2 Volume flow rate of surgical ICA at pre-operation and follow-up

Table 7 Mean volume flow rate, Percentage volume flow rate change of surgical and non-surgical ICA in different groups classified according to follow-up angiographic changes

| Grading | No | Surgical ICA | | | Non-surgical ICA | | |
|---|---|---|---|---|---|---|---|
| | | Pre-operation (ml/min) | Follow-up (ml/min) | Percentage change | Pre-operation (ml/min) | Follow-up (ml/min) | Percentage change |
| **A** | 11 | 159.33 | 123.75 | -24.2% | 158.76 | 184.18 | 6.2% |
| **B** | 4 | 155.12 | 138.91 | -10.5% | 154.59 | 166.28 | 2.2% |
| **C** | 3 | 155.55 | 148.71 | -3.7% | 154.84 | 156.43 | 2.5% |

### 5.4.3 Pressure Drop Index

The difference in pressure drop between pre-operation and follow-up, named as PDI, was calculated for all cases. For all cases, pressure drop in the surgical ICA was significantly decreased from 4.41（2.37-5.95）mmHg to 3.23（1.89-4.73）mmHg ($P < 0.01$). In the non-surgical ICA, pressure drop showed insignificant change from 3.09（2.29-4.21）mmHg at pre-operation to 3.29（2.12-4.61）mmHg at follow-up ($P > 0.05$). An average PDI of surgical ICA and non-surgical ICA for all cases was -1.00 and 0.51 respectively, and the change of PDI in the surgical ICA was significantly different from that in the non-surgical ICA ($P < 0.01$). Table 8 summarizes the change of pressure drop and PDI at pre-operation and follow-up. An average PDI of the surgical ICA for cases in group A was -¬1.67 mmHg. The result indicated that the pressure difference at the terminal ICA was significantly decreased during the follow-up period. This is expected owing to the decrease in flow ratio during the follow-up period. By observing the structural and hemodynamic changes of the surgical ICA, we found diameter and vascular tortuosity of the ICA trunk were decreased. On the other hand, however, the wall shear stress (WSS) didn't change (illustrated by case 13 in group A, Figure 5-4). In comparison, the average PDI values for the cases of group B and C were - 0.53mmHg and 0.82mmHg, respectively. The pressure difference at the terminal ICA was

increased for the cases of group C. Following the observation of ICA changes in cases of group C between pre-operation and follow-up, we found that the diameter of ICA did not change. However, there was a new and severe stenosis in the ICA trunk and the WSS at the terminal and stenotic portions of the ICA were quite different (illustrated by case 11 in group C, Figure 5-5).

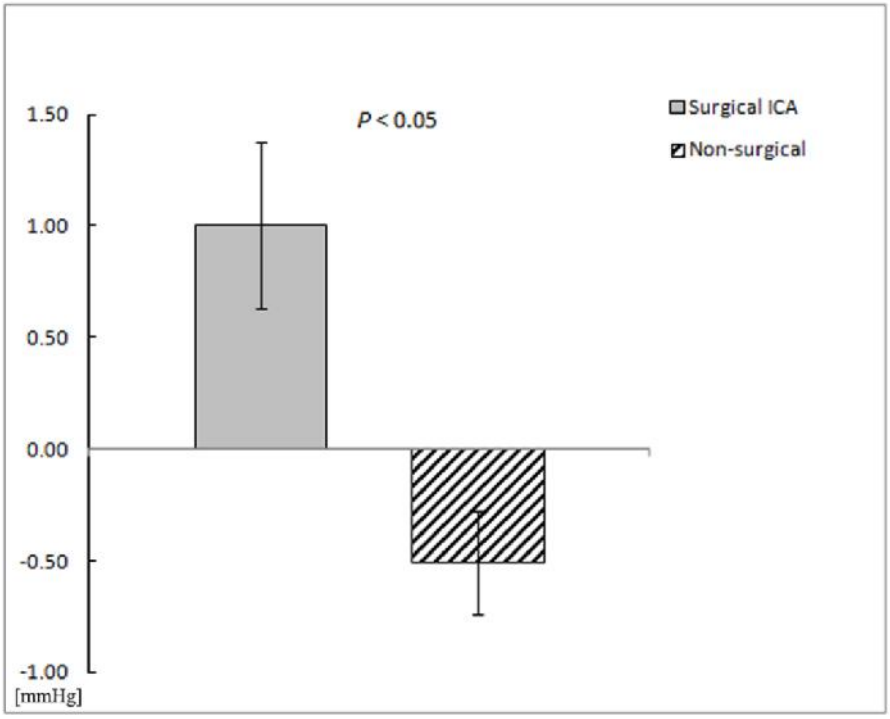


Figure 5-3 Pressure drop index (PDI) of surgical and non-surgical ICA

Table 8 Pressure drop, PDI of surgical and non-surgical ICA in different groups classified

| Grading | No | Surgical ICA | | | Non-surgical ICA | | |
|---|---|---|---|---|---|---|---|
| | | Pre-operation (mmHg) | Follow-up (mmHg) | PDI (mmHg) | Pre-operation (mmHg) | Follow-up (mmHg) | PDI (mmHg) |
| **A** | 11 | 6.74 | 5.07 | -1.67 | 4.00 | 4.57 | 0.57 |
| **B** | 4 | 3.56 | 3.03 | -0.53 | 2.69 | 3.31 | 0.62 |
| **C** | 3 | 2.89 | 3.30 | 0.82 | 3.94 | 4.07 | 0.14 |

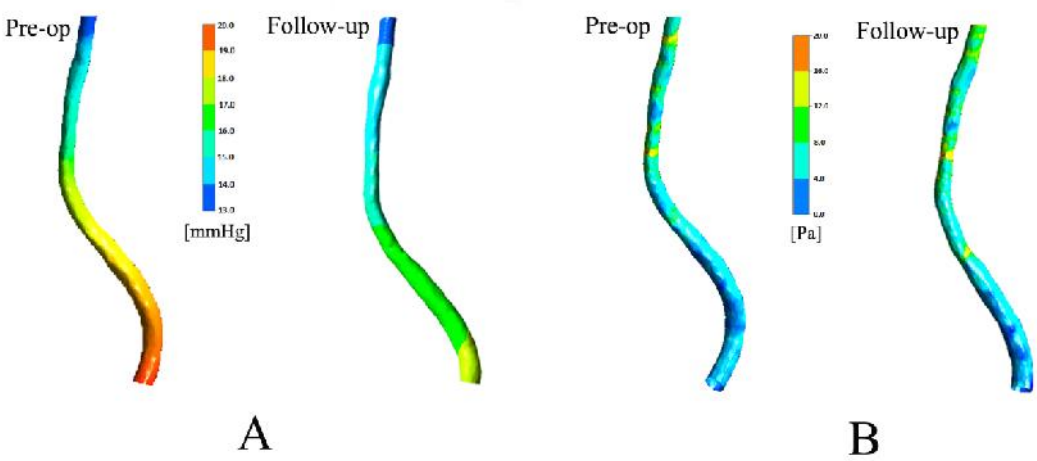


Figure 5-4 Pressure and wall shear stress (WSS) distribution of illustrative case in group A; A, Pressure contours and B, Wall shear stress contours of surgical ICA at pre-operation and follow-up, representing the characteristic vessel remodeling of ICA. ICA shrunk the diameter and vascular tortuosity of ICA trunk decreased. WSS of ICA trunk didn't change obviously

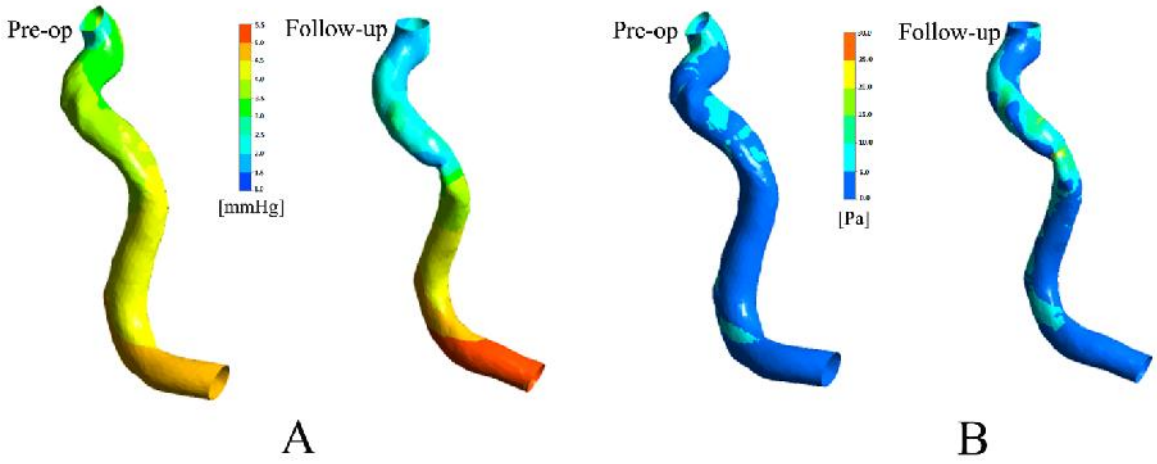


Figure 5-5 Pressure and wall shear stress (WSS) distribution of illustrative case in group C; A, Pressure contours and B, Wall shear stress contours of surgical ICA at pre-operation and follow-up. The pressure drop increased, and the diameter of ICA did not change obviously, however, there was new and severe stenosis in the ICA trunk. WSS at the stenotic portion of ICA were higher than the pre-operative model

## 5.5 Discussion

MMD is a rare cerebrovascular disease characterized by multiple steno-occlusive changes around the circle of Willis, leading to ischemic and hemorrhagic stroke. Although more prevalent in Asian countries, studies have shown that MMD also occurs amongst patients of non-Asian backgrounds(241).

There is still debate on the best treatment for occluded cerebrovascular disease; however, direct STA-MCA bypass with or without indirect revascularization is routinely performed for Moyamoya patients for the potential benefit of flow augmentation, hemodynamic stress relief, and relatively low surgical complications(104, 229). Development of collaterals circulation, reduction in Moyamoya leptomeningeal collateral vessels, improvement of dilation and branch extension of the anterior choroidal and posterior communicating arteries can be

observed among ischemic and hemorrhagic Moyamoya patients after bypass surgery, leading to surgical benefit and decreased risk of recurrent infarction and bleeding (229, 242, 243).

A few studies have been performed to investigate the vascular morphology associated with MMD. Narrowing of the outer diameter of the ICA bifurcation, high wall shear stress of the ICA bifurcation, progressive stenosis of PCA all have been identified in MMD (104, 175, 244). However, no computational quantitative methodologies were used to analyses the hemodynamic benefit after bypass surgery of MMD patients. Our previous study, using CFD technique, revealed that bypass graft has a characteristic remodeling after combined direct and indirect bypass surgery that usually reduces flow resistance. The initial morphology of bypass has a significant effect on the outcome of vessel remodeling and bypass patency(174). To the best of our knowledge, there is no study of vessel remodeling of ICA after combined direct and indirect bypass.

This is a pilot study using CFD technique for hemodynamic quantification analysis of MMD patients, with an incomplete Circle of Willis, treated using combined direct and indirect bypass. For all cases, the pressure drop and volume flow rate of the surgical ICA decreased significantly at follow-up ($P < 0.05$). Whereas in the non-surgical ICA, both pressure drop and volume flow rate showed insignificant changes ($P > 0.05$). Our data illustrates that the ICA has a characteristic vessel remodeling after bypass surgery that usually decreases pressure drop and volume flow rate. The inverse hemodynamic changes of the surgical and non-surgical side of ICA might be owing to the fact that MMD usually affects bilateral sides of the brain. Further study on the hemodynamic changes after bypass surgery for MMD cases in which the circle of Willis is complete is currently being conducted.

Since the preoperative symptoms varied, it was difficult to quantify the clinical functional treatment outcome with uniform standard. This research classified cases into three groups

according to angiographic findings rather than functional outcome of patients. In group A, the pressure drop decreased significantly and average PDI was -1.67 mmHg. This shows that pressure drop at follow up is much greater than the pressure drop at pre-operation. This might be expected owing to the structural shrinkage of ICA as a whole, decrease in diameter of ICA and reduction in flow rates at follow-up. Though the numbers of cases in groups B and C are small, the PDI value is shown to correlate with the angiographic treatment outcome. The average PDI values for cases in groups B and C were - 0.53 and 0.82 mmHg, respectively. These results suggest that the reconstructed flow from direct and indirect bypass can influence the hemodynamic state of the ICA and lessen its hemodynamic stress. PDI might be potentially used as a hemodynamic indicator for treatment outcome classification (234). The result is corresponding with our previous study, in which we identify PDI correlated with treatment classification after indirect bypass surgery.

In this study, MRA was used to create 3D vessel geometry for creation of CFD computational domains. It is much less invasive and more suitable for follow-up compared with DSA for the absence of radiation exposure to patients and complications induced by catheter angiography procedures. Although the number of cases in this study is limited, hemodynamic analysis based on MRA might be a potential non-invasive quantitative method for follow-up of MMD patients after bypass surgery.

In this study, treatment outcome was classified by angiography. However, functional benefit was still regarded as the crucial standard to judge medical treatment outcome. The computational hemodynamic analysis of ICA is an adjunct tool rather than replacement of careful and thorough assessment of patients' neurological function in the follow-up of MMD patients after bypass surgery. The angiographic changes observed could not be determined as cause or a result of the ICA vessel remodeling through this study. The main limitation of this study is that the small number of cases. However, to the best of our knowledge, this is

currently the largest case series study of hemodynamic analysis of bypass surgery for MMD patients using CFD technology. Furthermore, follow-up is short for a disease that is chronic and gradually progressive. To elucidate the nature of auto-remodeling, further investigations of more cases with a longer follow-up will be required in the future.

## 5.6 Conclusion

The ICA has a characteristic vessel remodeling after combined direct and indirect bypass surgery that usually decreases both pressure drop and volume flow rate. Detailed analysis of hemodynamic changes in the ICA using CFD technology might prove to be a potential non-invasive quantitative method of treatment outcome classification for the follow-up of MMD patients after bypass surgery.

# Chapter 6 *Hemodynamic Assessment of Surgical Treatment Outcome on Moyamoya Disease Patients with Complete Circle of Willis Following Revascularization Surgery*

Submitted As

Karunanithi, K., Zhu, F.P., Mao, Y., Qian, Y., Characterization of Pressure Drop Index (PDI) in MMD patients treated with combined direct & indirect revascularization surgery, Journal of Medical Engineering and Physics-Accepted

## 6.1 Abstract

. Moyamoya disease is signified by chronic occlusion of distal Carotid arteries with abnormally dilated collateral vessels, with surgical revascularization as the stand- alone treatment. Pressure Drop Index (PDI) defined as the difference in head loss between post and pre-operation indicates a suggestive correlation with encephalo- duro-arterio-synangiosis (EDAS) outcome of MMD patients in our previous research. In the current investigation, we aim to further elucidate the link by analyzing the hemodynamic parameters of eight hemorrhagic MMD patients (4-Male and 4- Female) who were treated unilaterally by combined direct STA-MCA bypass and encephalo-duro-myo-synangiosis (EDMS). Four of them were clinically classified significant improvement and the rest as limited improvement based on Magnetic Resonance Angiography (MRA) findings at post-operation. PDI and percentage flow decrease were calculated for all eight cases and compared against the clinical outcome. The results indicate that an inverse correlation exists between PDI and treatment outcome; negative PDI in significant improvement cases and positive PDI for limited improvement cases, thus validating the results from our preliminary analysis.

## 6.2 Introduction

Moyamoya disease is a cerebrovascular condition characterized by bilateral progressive occlusion of distal internal carotid arteries and/or proximal anterior and middle cerebral arteries leading to ischemia(245). Angiogenesis to compensate ischemia establishes a network of collateral vasculature which when observed in MRA, appears in the form of “puff of smoke” known as Moyamoya(200). MMD is treated with various types of revascularization procedures, all of which involve in combating high blood flow to the relatively smaller collaterals.(246) Based on the clinical characterization, the recommended method of revascularization treatment varies. Despite the lack of large-scale clinical trials, there have been various studies that have established direct extracranial-intracranial (EC-IC) bypass

revascularization procedure to be effective for adult patients presenting with intracerebral hemorrhage.(203, 247) Alternatively, pediatric MMD patients who undergo indirect revascularization are believed to have better prognosis with almost 100% rate of change in Moyamoya vessels.(248, 249) In adults, recurring hemorrhage poses significant problems post revascularization and severe morbidity and mortality rates have been reported due to rebleeding and cerebral hyperperfusion syndrome (CHS- in terms of direct STA-MCA Bypass).(250, 251)

To combat recurrent intracranial hemorrhage (ICH), a united approach consisting of both direct and indirect revascularization procedure have been proven effective in recent times.(252) STA-MCA bypass combined with EDMS has been reported to reduce the risk of rebleeding by up to 15%.(129) The EDMS is an indirect bypass combining the encephalo-duro- and encephalo-myo- synangioses. The combination treatment works well for adults as the middle meningeal artery, temporal muscles and STA are dominant blood suppliers thereby reducing the blood flow throughput to the cerebral vessels and any remaining cerebral ischemia if present becomes a driving factor for neovascularization via indirect method.(253)

Although the underlying mechanism by which direct revascularization surgery proves effective for adult MMD patients has not been documented through randomized large scale clinical trials, a recent initiative by Japan to conduct a large scale, randomized, multi-center adult Moyamoya trial to review the long-term efficaciousness of EC-IC bypass in underway.(254) The primary causative of rebleeding is the rupture of micro- aneurysms that develop in the compensatory vasculature due to increased hemodynamic load.(129) Hence we propose Computational Fluid Dynamics (CFD) technology to determine if there occurs a decrease in blood flow, thereby loss of energy, in the Moyamoya vessels. CFD simulations of treated MMD patient geometry will help us analyze hemodynamic patterns in the Circle of Willis pre- and post- operatively. This study is a sequel to our previous research to study the

influence of anatomical variations of CoW on the Pressure Drop Index. An anatomically intact CoW with connecting cerebral arteries has been found to maintain balance in the cerebral blood flow in the event of unilateral ICA stenosis. Any variations in the morphology of CoW have been known to disrupt the flow.(255, 256) Presence of anomalies in CoW have also been linked with development of cerebrovascular disorders such as aneurysms by altering the ACom artery hemodynamics.(257) Previous chapter had looked at PDI in MMD patients with an incomplete CoW whereas in this chapter, we aim to calculate PDI for MMD patients with a complete CoW and further delineate the impact of CoW anomalies on PDI. Our earlier CFD investigations of MMD have paved way to the current study where we aim to standardize PDI as an indicator of treatment outcome for MMD patients treated via combined revascularization approach in addition to investigating the influence of morphological variations of CoW on PDI.

## 6.3 Methods

### 6.3.1 Patient Demographics

Eight adult patients (four-Female and four-Male) aged 14-47 years were selected from the patient database. Inclusion criteria were as follows, MMD patients with complete Circle of Willis who presented with hemorrhage as initial symptoms and treated unilaterally with combined direct (STA-MCA Bypass) and indirect revascularization procedures at the Huashan Hospital, Shanghai, China between 2010 and 2012. Five cases were operated by Professor B Xu, and three cases were operated by Professor YX Gu. The treatment procedure combined STA-MCA direct bypass and EDMS method in unilateral hemisphere (Table 9). We specifically selected the patients who possessed the complete Circle of Willis, in order to analyze the hemodynamic alternation during the artery remodeling after MMD treatment. All patients were examined by MRA, a potential non-invasive quantitative method, and Doppler Ultrasound both at pre- and post-operation. Treatment outcome was clinically classified into

A- Significant Improvement, B-Limited Improvement from the MRA measurements by two independent neurosurgeons blind to the study(210): Significant improvement- the postsurgical collateral vessels presented revascularization of two thirds or more of the MCA distribution and Limited Improvement- the postsurgical collateral vessels presented from no/ little to two thirds revascularization of the MCA distribution. All participants provided written informed consent. All surgical protocols were approved by the Institutional Research and Ethics Committee prior to the treatment. Three-dimensional (3D) reconstruction and segmentation of patient geometries was done via use of commercial software package—MIMICS (Materialise, Belgium) for computational meshing in preparation for CFD calculation.

Table 9 Patient Demographic and Treatment Outcome

| **Case** | **Sex/Age** | **Surgical side (Left/Right ICA)** | **Treatment Classification** |
|---|---|---|---|
| **1** | Female/47 | Right | A |
| **2** | Male/45 | Left | A |
| **3** | Female/14 | Left | A |
| **4** | Female/26 | Right | A |
| **5** | Male/35 | Left | B |
| **6** | Male/46 | Right | B |
| **7** | Male/37 | Left | B |
| **8** | Male/36 | Left | B |

*A- Significant Improvement, B-Limited Improvement*

### 6.3.2 CFD Modeling

3D geometry of Circle of Willis including Left, Right Internal Carotid Artery (ICA) and Basilar artery (BA) of all eight patients were reconstructed via generation of two-dimensional contours from grey scales of pixels, and by subsequent interpolation in a normal direction. This method prevents the intrusion of surface noise. Surface smoothing was kept to a

minimum to avoid distortion and limited to few localized areas to keep the surface roughness as close to the real vessel surface as possible. This method has been proven to display an average error of one-third of a pixel in size approximately.(186)

Navier-Stokes equations for 3D flow with rigid walls were solved using ANSYS CFX 14 (Ansys Inc., Canonsburg, PA, USA), under steady state flow conditions. Steady state simulations have been proven to adequately provide similar time-averaged results for pulsatile calculations over a cardiac cycle, which justified the use of steady state flow condition rather than pulsatile condition(211). The inflow boundary conditions at pre- and post- operation were measured individually for each patient using Trans-Cranial Doppler Ultrasound (TCD). Blood flow was modeled as a laminar Newtonian flow with a density and dynamic viscosity of 1050 kg $m^{-3}$ and 0.0032 Pa s, respectively.

To mimic venous capacitance and to allow sufficient recovery of the blood pressure the vessel outlet was extruded distally in a direction normal to the blood flow downstream to 100 mesh layers.(191, 212) Patient specific inlet boundaries, based on Ultrasonography flow measurements were set and zero pressure condition was applied at all the outlets. Fully developed velocity profiles aping the measured flow rates should be achieved at the proximal inlet boundary layer and for this reason the domains were extruded in the upstream direction to 100 mesh layers. Corresponding grid independence validations have been carried out in our previous work.(191, 258) The total number of elements ranged between 1000,000 and 1400,000. The grid size for the inlet/outlet interfaces were fixed at 0.01 mm and the rest of the computational domain had a maximum size of 0.02 mm.

### 6.3.3 PDI and Percentage Flow Change

In our pilot study, we identified a new hemodynamic parameter; Pressure Drop Index (PDI) which indicated a suggestive correlation with EDAS treatment outcome in MMD

patients.(234) Ideally, decreased hemodynamic stress through Moyamoya vasculopathy post-surgery should lead to significant head loss and thereby pressure reduction; PDI was calculated as the difference between pressure reduction at pre-operation, post-operation and follow-up can help us establish the treatment consequence on an MMD patient. According to Bernoulli's equation, the pressure reduction is calculated as the difference between the total pressure at the inlet and outlet, at pre-operation as well as at post-operation. PDI is then calculated by the following equation:

$$PDI = \Delta P_{post} - \Delta P_{pre} = \left(P_{in} - P_{out}\right)_{post} - \left(P_{in} - P_{out}\right)_{pre}\Big] \quad (15)$$

where, PDI is a difference of pressure reduction/ head loss measured at post-operation and pre-operation, $\Delta P_{post}$ and $\Delta P_{pre}$ are the calculated pressure reductions at post-operation and pre-operation respectively. $P_{in}$ and $P_{out}$ are the total pressure values calculated at the inlet and both the outlet planes, at pre and post-operation. In this report, we calculate the difference in pressure at the inlet and outlet of the carotid arteries for all eight patients computationally. In order to eliminate human error owing to segmentation, the pressure reduction in the left and right ICA were calculated between fixed co-ordinates at the inlet interface and the proximal end of the outlet, in both pre-operative and post-operative geometries in all patients (Figure 6-1). The difference between the pressure reduction at pre-operation and post-operation was calculated as PDI which was then compared to the clinical classification (based on DSA and MRA measurements). Percentage flow change is calculated by utilizing the Ultrasound inflow rate measurements at the pre-operative and post-operative model. The rate of flow change at post-operation and the calculated PDI values were analyzed.

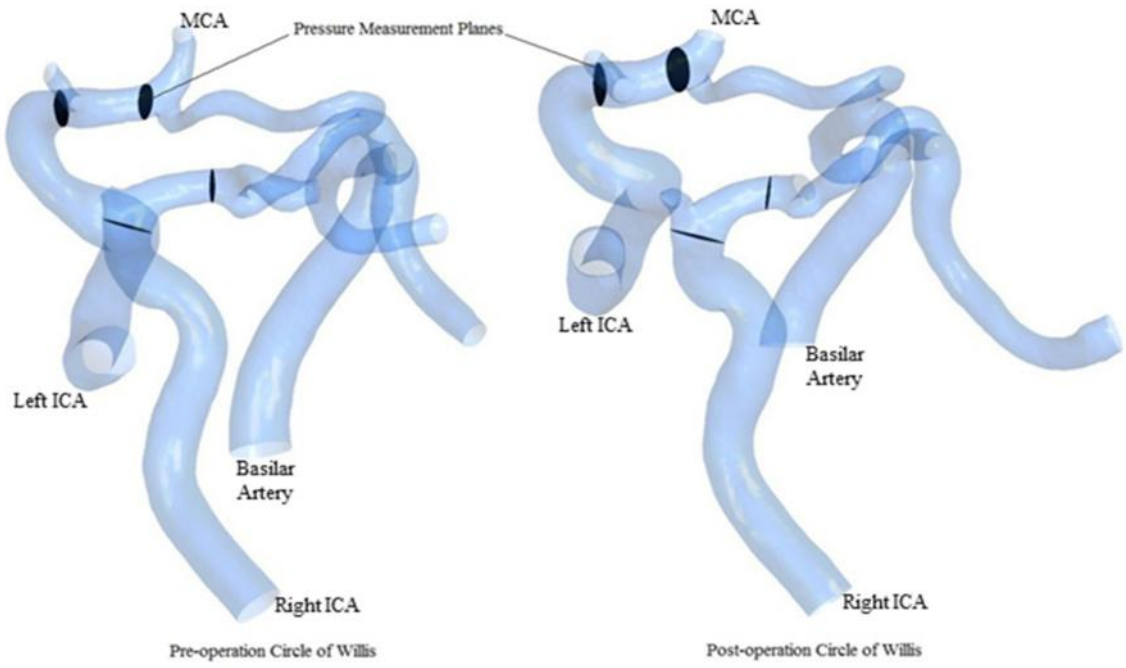


Figure 6-1 Pressure measurement planes at the Circle of Willis for PDI calculation

## 6.4 Results

### 6.4.1 Percentage Flow Change Analysis

Patients' demographic is listed in Table 9. Flow measurements were done both at pre- and post-operation in all patients using TCD. The flow rate changes were documented and percentage decrease in flow rate was calculated. The results for the surgical and contralateral ICA are tabulated below. As observed from TCD and CFD results; the flow rate of the surgical ICA decreased by an average of 21% ± 9.4% for all patients classified clinically A-Significant Improvement at post-operation. In contrast, the patients termed B-Limited Improvement had an average increase of 10% ± 13% in flow rate at post-operation ($P<0.05$). This trend is in accordance with the objectives of combined STA-MCA bypass and EDMS approach, as blood flow through the ICA needs to be reduced to lower the hemodynamic load through the peripheral Moyamoya vessels. This is shown to successfully reduce the risk of rebleeding in adult hemorrhagic MMD patients. An intriguing aspect noted here is an insignificant albeit complementary increase in flow through contralateral ICA in A

(approximately 7% ± 13% increase) and vice versa: a 3 % ± 3.7% decrease in flow through contralateral ICA for limited improvement patients (Figure 6.2).

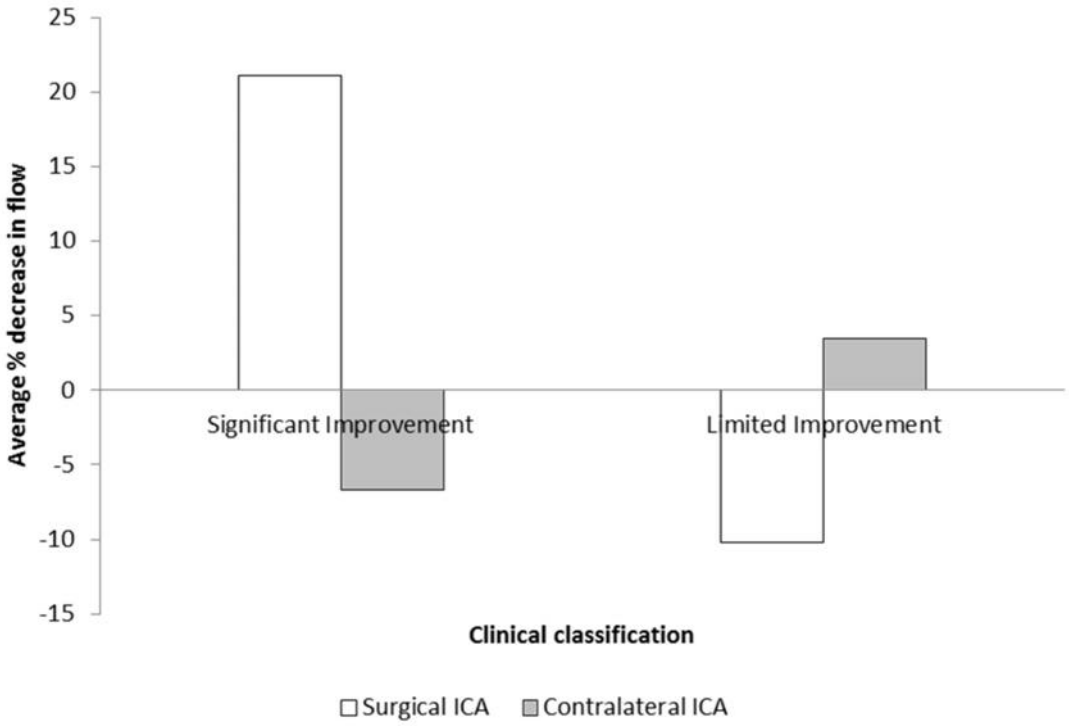


Figure 6-2 Average % decrease in flow rate in Surgical and Contralateral ICA of 8 patients (n=4 each)

### 6.4.2 Pressure Drop Index-PDI

Preceding research into PDI has established it as an indicator of treatment outcome of MMD patients bilaterally treated with indirect EDAS method. Pressure drop index is calculated as the difference between pressure reduction or head loss of the ICA between pre-operation and post-operation. Table 10 gives us the PDI values for surgical and contralateral ICA for eight patients.

Table 10 Calculated PDI values for all patients

| Case | Surgical Side | Status | Surgical ICA PDI (Pa) | Contralateral ICA PDI (Pa) |
|---|---|---|---|---|
| **1** | Right | A | -548.2 | 296.1 |
| **2** | Left | A | -141.9 | 71.4 |
| **3** | Left | A | -189.7 | 8.6 |
| **4** | Right | A | -526.3 | 42.4 |
| **5** | Left | B | -99.2 | 378.4 |
| **6** | Right | B | -82.6 | -356.6 |
| **7** | Left | B | 252.18 | 198.41 |
| **8** | Left | B | -17.179 | -546.04 |

The average PDI for A-Significant improvement cases was -352 Pa ± 107.8 for the surgical side, average PDI for B-Limited Improvement cases was computed as 13 Pa ±81.6 ($P<0.05$). The contralateral ICA had a reversed display of PDI values; the average PDI for A and B category cases were 105 ± 65.1 and -81 Pa ± 220.1 respectively (Figure 6.3).

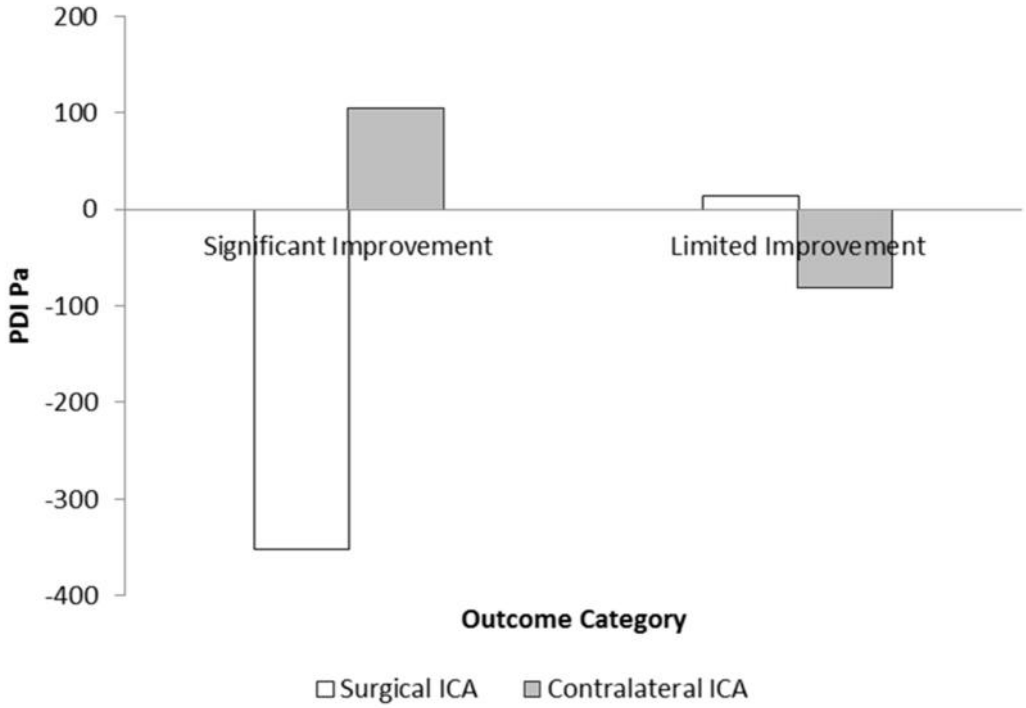


Figure 6-3 Average PDI values for Surgical and Contralateral ICA in 8 patients (n=4 each)

As the surgery is unilateral, a negative PDI for the surgical ICA of patients in category A is expected due to a higher percentage decrease in flow at post-operation than before surgery. The contralateral ICA shows a counteractive increase in PDI to balance the pressure loop, as the Circle of Willis was complete in all 8 patients selected according to the inclusion criteria from the database. The converse of this theory is evident for the category B cases in which an increase at the flow rate at post-op lead to an increase PDI across the surgical ICA; the contralateral hemisphere in this case has an offset reduction in PDI.

The calculated trend in PDI is further verified by the pressure contours captured from CFD results. Illustrated below are the pressure contours of the Circle of Willis of two patients (category A and B). The pressure contour of the surgical hemisphere for the patient A has a sharp reduction at post-operation in comparison to pre-operation due to successful vessel remodeling. The surgical ICA of patient B has increased pressure values at post-operation

(Figure 6.4). An overall increase in pressure is present in the contralateral hemisphere of both A and B patients treated with combined revascularization technique.

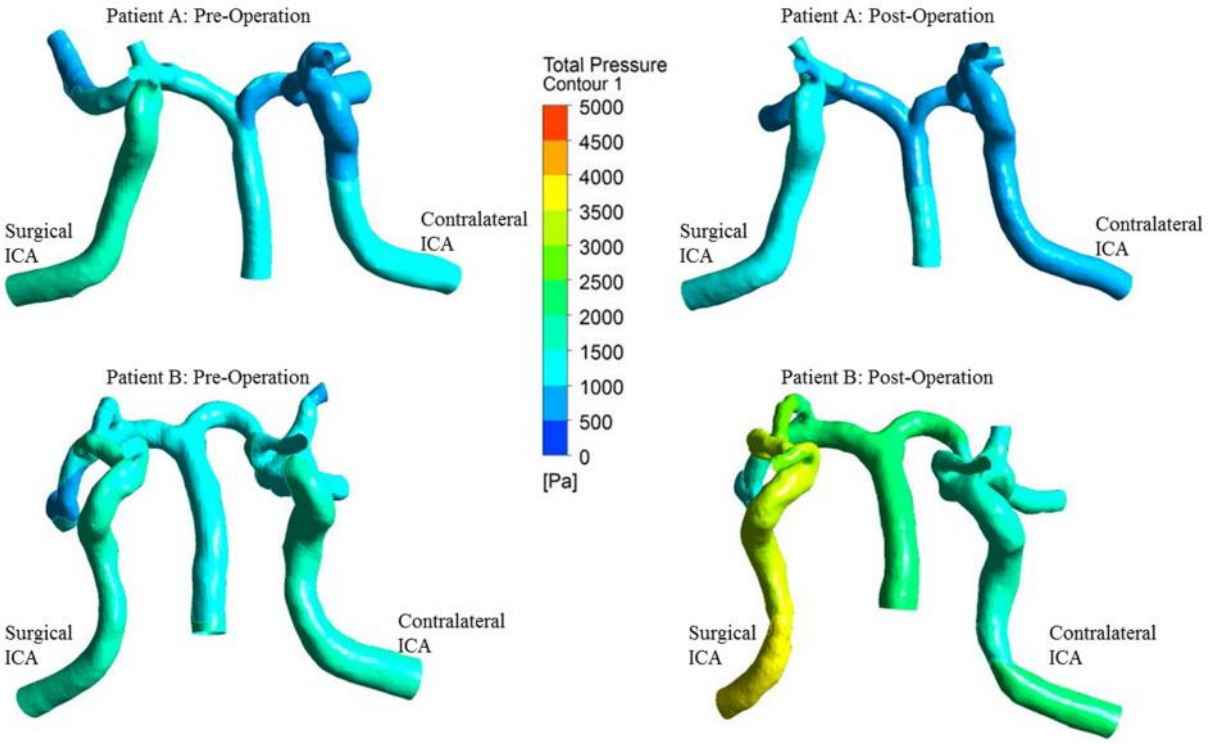


Figure 6-4 Pressure Contour of Patient A-Significant Improvement and Patient B-Limited Improvement.

## 6.5 Discussion

Asymptomatic MMD patients with no traces of ischemia or hemorrhage are recommended conservative treatment as there is inherent risk in revascularization surgery(250). Yet, Kuroda et al. reported that in 34 asymptomatic MMD patients treated conservatively, 4 patients suffered of hemorrhage and 3 patients had cerebral infarction.(259) This emphasizes the chronic nature of MMD with minimal or no response to treatments. Hence, surgical management to best control the momentum of the disorder is the only option for patients diagnosed with MMD. (104)Revascularization surgery has its own inherent risk of rebleeding and ischemic attacks. Guzman et al. reported a 5 year cumulative risk of perioperative or

subsequent stroke or death to be 5.5% in 450 adult and pediatric cases treated with revascularization surgery (both direct and indirect revascularization).(202)

Understanding the hemodynamics of MMD will enable us to gain insight into the intra- and perioperative complications that are associated with direct and indirect revascularization surgery. Quantitative MRI and MRA along with other imaging methods such as SPECT and PET have been indispensible in acquiring quantitative CBF data in MMD geometry with reasonable spatial resolution (109, 260).

In addition to diagnostic imaging techniques, CFD Technology has been used to hemodynamically quantify various cerebrovascular disorders such as aneurysms in the past.(138, 225) CFD technology can aid in calculating hemodynamic parameters besides just flow velocity such as total and relative pressure, wall shear, volume flow etc. Deployment of CFD technology in MMD has been attempted recently as these hemodynamic parameters have been proven to help clinicians in unraveling the disease pathogenesis and to plan surgical intervention in MMD patients. A study done by Duk Shul Shin in 2007 showed that shear stress distribution (Wall Shear Stress) in the distal ICA region; a site for MMD genesis, was relatively low in comparison to the other portions of ICA.(261) Low WSS is believed to augment constriction of the lumen/narrowing of blood vessels which contributes to hemorrhagic episodes.(220) Zhu et al. investigated the patency of bypass in STA-MCA surgery using CFD; the results proved that factors such as initial morphology of the bypass influenced the characteristic remodeling of the vessel by lowering the flow resistance.(174) In our previous work, we identified a novel hemodynamic parameter; PDI for assessing EDAS (indirect revascularization) treatment outcome. We showed for clinically successful patients the calculated PDI was negative. This implies greater pressure reduction across the vessel at post-operation than the follow up. The aim of this paper is to validate PDI as a reliable hemodynamic parameter for assessing MMD patients treated unilaterally with combined

direct STA-MCA bypass and indirect EDMS method. Of the eight patients (4-Male, 4-Female) we analyzed PDI was found to be negative in the surgical ICA for all four cases classified clinically as having significant improvement (A). The results were in agreement with our previous research with positive or near negative PDI values calculated in the surgical ICA of the four patients classified having limited improvement (B). However, being unilaterally treated, the contralateral PDIs were found to be complementary to that of the surgical hemispheres. The PDI values of contralateral ICA in group A were in the positive bands, the vice versa was found for the category B. This compensatory loop is also found in percentage decrease of blood flow through the surgical and contralateral ICA. The percentage decrease in blood flow was higher in category A than the B group cases for the treated hemispheres. It is of prime importance to emphasize that our study included patients with complete Circle of Willis. The right and left ICA along with Basilar Artery (BA) and Anterior Communicating artery have been known to play an important role in maintaining the CBF output through the Circle of Willis.(214) Nevertheless, this counterbalance in flow and pressure reduction across the Circle of Willis warrantees further research. Decrease in CBF and its associated negative PDI, post-operation, points to physiologically stable blood flow through the ICA denoting lower hemodynamic stress on the Moyamoya vessels.(227) Lower hemodynamic stress through the vessel is proven to significantly reduce the risk of rupture and thereby advent of peri-operative complications.(226)

Our results substantiate our claims that PDI can be used as a reliable parameter in assessing treatment outcomes for prediction of peri-operative complications. Characterization of MMD cases was done solely on the basis of computational hemodynamics and any clinical factors that arise from vessel remodeling were not discernable in our results. Despite the modest patient size, PDI has proved to be consistent in evaluating the treatment outcomes for both stand-alone EDAS and combined bypass surgery. A scaled up study design, consisting of comprehensive hemodynamic profiling of a larger cohort of patients, with long-term follow

up is currently underway. If established as an industry standard, PDI can assist clinicians in surgical planning and long-term prognosis of MMD patients in addition to image-based classification.

## 6.6 Conclusion

This study is a follow-up endeavor to our maiden research wherein PDI showed promising results as an indicator of treatment success in MMD patients. Our findings suggest that there is an unambiguous relationship between treatment outcome and PDI. An analysis of PDI in two groups of eight patients each treated with EDAS and combined STA-MCA bypass and EDMS respectively, confirmed that negative PDI is associated with improved clinical outcomes and positive/near negative PDI represents a risk of rebleeding. A follow-up study incorporating larger patient cohorts with sample sizes from other indirect surgical techniques is underway to establish PDI as an unfailing hemodynamic tool to assist surgeons in clinical decision-making.

# Chapter 7

## *Discussion and Conclusion*

## 7.1 CFD in cerebrovascular disease research

Computational Fluid Dynamics is a branch of mechanical engineering wherein complex problems relating to fluid flow, heat transfer and associated phenomenon are solved using computer-based simulation. Application of CFD to biomedical problems is an evolving field of research. The main limitation of CFD application in medical sciences is the complexity of living processes. But due to the recent advent of robust hardware and software it is now an accepted tool in understanding complex biological problems. CFD has been applied widely in vascular research to study diseases such as congestive heart failure, ventricular function and aortic disease, intracranial aneurysms, vascular stenosis etc. since the 1970s.(262, 263).

Cerebrovascular CFD research, in particular the application of CFD technology to understand the origin and rupture of intracranial aneurysms is an established field of research. It is now known that the hemodynamic environment in combination with biochemical and mechanobiological properties contribute to the origin, development and rupture of intracranial aneurysms. With advancement in diagnostic imaging and computational techniques it is now feasible to three-dimensionally analyze the morphology and flow characteristics of blood flow of a patient-specific aneurysm. The earliest research employing CFD principles to study aneurysms was published in 1992 by Gonsalvez et al(264). Despite application of CFD to study aneurysm hemodynamics existing since 1992, substantial hemodynamic findings have been around only since the advent of the millennium. There has been numerous CFD studies looking into hemodynamic and morphological parameters such as aspect ratio, size ratio, wall shear stress and pressure, which play a key role in evolution and rupture of intracranial aneurysms (155, 265, 266) SAH due to aneurysm rupture results in severe morbidity and mortality.(267) Treatment options include microvascular clipping and recently minimally invasive endovascular treatments such as coil embolization and flow diversion treatment are also engaged. Flow diverters are low porosity, high pore-density stents used in vascular

remodeling. There has been handful of CFD studies looking at the FD design and how it promotes vascular reconstruction. This thesis aims to understand how the metal coverage rate and porosity of flow diverters changes according to the deployment angle at aneurysm neck and how it thereby influences flow reduction inside the aneurysm thus promoting aneurysm occlusion and vascular remodeling.

Use of CFD technique to develop a patient specific simulation method that aids treatment planning and management of intracranial aneurysms has been a topic of interest to various research groups around the world due to the limitations posed by the available imaging modalities. Minimally invasive flow diversion treatment has been viewed favorable as it has been proven, in animal studies, to successfully divert blood flow at the aneurysm neck back into the parent vessel and thereby accelerating thrombosis. One prime concern of the treatment has been the occlusion of side branches of the parent arteries along with the aneurysm. Studies have found that porosity and metal coverage rate plays a major role in determining not only the percentage flow reduction inside the aneurysm but also the occlusion of side branch perforated arteries.(268) CFD researchers are starting to investigate the effect of flow diverter porosity and MCR to increase the efficiency of flow diversion and to eliminate secondary ischemic complications associated with side branch occlusion.(181, 269) Based on the radial force during deployment, the angle of the free stent segment may differ which influences the MCR across aneurysm neck. In our study, we looked at the hemodynamic of two patient-specific aneurysms with aspect ratios; 3.1 and 2.9 that were treated with varying angle of flow diverters. Percentage Energy Loss reduction post flow diversion and Mass flow reduction were analyzed in order to obtain information regarding aneurysm occlusion and rupture risk respectively. MFR has been proven to be a key factor in aneurysm occlusion wherein, Lower % Energy Loss reduction, post flow diversion, has been associated with unstable aneurysms with a greater risk of rupture.(193, 194)

In addition to our research in intracranial aneurysms, we sought to apply CFD technology in understanding the hemodynamics of another associated vascular disorder known as Moyamoya disease. As stated earlier in the dissertation, the etiology of Moyamoya disease remains largely unknown. The relationship between the complex hemodynamics and clinical disease progression of the disease has not been comprehensively evaluated. A handful of studies exist which investigate the relationship between cerebral Perfusion pressure, cerebrovascular reserve flow rate and angiographic findings. But there has been no significant improvement in our understanding of the disease prognosis.(270) Computational Fluid Dynamic studies of MMD are being favored as they are non-invasive diagnostic tools with better visualization capabilities. Few two-dimensional studies have been conducted prior to 2010 to understand how parameters such as WSS, Blood flow velocity and vascular tortuosity of ICA might lead to the genesis of MMD.(175, 261) However, we have identified key hemodynamic parameters that might be indicative of treatment outcome in a total of 34 three-dimensional patient specific MMD models, treated with both indirect and combined revascularization surgery.

Application of CFD technology in medical research has not been tapped to its full potential. There still exist several avenues of cerebrovascular disease research to which CFD technology has not been applied. For example: With the exception of few two-dimensional CFD studies studying MMD disease progression, this thesis is the first to employ CFD techniques in analysis of three-dimensional MMD hemodynamics. Even in the established field of Intracranial aneurysm research, finite element analytic studies have conducted to examine the FD design parameters such as radial stiffness, longitudinal flexibility and maximum strain(271), but a recent search of the PubMed database using words such as “flow diverter angle”, “metal coverage rate”, “hemodynamics”, “CFD” and “aneurysm” has led us to state with reasonable certainty that ours is the first computational fluid dynamics study to

investigate the effect of metal coverage rate and the angle of the free stent segment (across aneurysm neck) on aneurysmal hemodynamics.

The central findings of this thesis have been listed below

I. Our study on the influence of the angle of the free stent segment (0°, 10° and 25°) at aneurysm neck of two patients A and B have established that as a result of deployment, the flow diverter's original metal coverage rate changes. This change in MCR is attributed to the compression and stretching involved upon its delivery. The three angles were inversely proportional to the metal coverage rate as the MCR decreased from 71% to 35% with increase in the flow diverter angle from 0° to 25° at the aneurysm neck.
    a. The best treatment outcome with highest MFR and EL reduction was found in the 10° FD configuration. This implied better occlusion process along with the lowest risk of rupture. In a straight stent (0°) configuration, the flow pattern, although stable had an increased jet flow impingement velocity on the aneurysm dome. The 25° stent had a modest to low flow reduction post treatment.
    b. The study showed that the deployment angle of the free stent segment played an important role in determining the Metal Coverage rate across the neck. A MCR >35% has been identified via PIV experiments to be ideal in maximizing aneurysm flow reduction.(181) We have identified an ideal MCR % of 50-60 in reducing approximately 90.4% ±3.8 of the original flow entering the aneurysm.
II. For the next part of the thesis, a total of 34 MMD patients (8-indirect revascularization surgery EDAS, 26-combined direct STA-MCA bypass + EDMS surgery) had been analyzed computational to identify novel hemodynamic parameters which correlate

with prediction of treatment outcome. In our pilot study we examined eight adult MMD patients who have been treated bilaterally with indirect revascularization surgery (EDAS).The patients had undergone angiographic follow-up examination (~6 months) and were classified as I-improved, II-no change and III-retrogressed as per Matsushima's method. From our calculations, for all patients classified as I-improved, the pressure drop across stenotic ICA at post-operation was greater than at follow-up. At follow-up, the pressure difference between the blood flow inlets and outlets of ICA, fall within the physiologically accepted range for those patients deemed improved. Patients classified as II-no change or III-retrogressed had a higher pressure difference between ICA inlet and outlet at follow-up, as negligible revascularization leads to increased flow velocities through the stenotic ICA.

a. In our follow-up studies we calculated PDI for twenty-six adult MMD patients (18-incomplete CoW and 8-complete CoW) treated unilaterally with combined direct STA-MCA bypass and EDMS. The patients with incomplete CoW were graded as A-Significant Improvement, B-Limited Improvement and C-No Improvement based on the angiographic outcome (Matsushima). Patients with complete CoW were graded as A-Significant improvement and B-Limited Improvement based on MRA measurements at follow-up. Characteristic pattern in PDI was observed in the surgical ICA in all patient groups. The pressure difference across surgical ICA was found to be consistently lower at follow-up than pre-surgery for patients showing significant improvement. This trend in PDI was analogous to our pilot study wherein PDI was steadily increasing for patients belonging to groups B and C.
b. We also attempted to study the characteristic remodeling of STA at follow-up in the eighteen patients lacking a complete CoW. Vascular tortuosity and WSS was studied in the surgical ICA of all 18 patients. There was an increase in WSS of the surgical ICA for patients in category B and C. This was

accompanied with severe ICA stenosis in many cases with no significant changes in vascular tortuosity. In contrast, the vascular tortuosity and vessel diameter of the surgical ICA decreased in patients of group A- significant improvement. Higher vessel tortuosity index (VTI) has been linked to the etiology of several vascular disorders.(272, 273) Our results suggest that there exists a link between tortuosity index and treatment outcome of MMD patients.

There has been monumental progress in application of CFD to study vascular diseases over the past few decades. Various groups have reported significant hemodynamic and morphological mechanisms responsible for disease initiation and progression. Despite these improvements, there is hesitation among clinicians to adopt CFD as a complementary decision making tool in disease prognosis.(136, 143, 197). This is primarily due to lack of documented protocols for validation of CFD findings. In addition to this, large-scale multi center studies are essential to verify statistical significance of CFD results. This requires access to consolidated patient data across various locations. There is a critical need for clinicians to work hand in hand with CFD researchers to overcome the hurdle and utilize the untapped potential of CFD in future.

### 7.1.1 Future Directions

An apparent limitation to our study is the small sample size of patients. In order to propose a quantifiable correlation between; a. MCR of the free stent segment and flow diversion treatment outcome in intracranial aneurysms, and b. PDI and revascularization treatment outcome in MMD, a larger sample of patient cohort with need to be researched.

In flow diverter treatment, the relationship between MCR and angle of free stent segment has been exhibited to be inversely proportional. A larger aneurysm patient sample size consisting of varying parent vessel morphology and exhaustive FB configurations is proposed to

determine the effect of parent vessel tortuosity and free stent segment angle on aneurysm occlusion post flow diversion treatment. This study holds the potential to help clinicians virtually plan endovascular FD deployment prior to surgery to maximize treatment success.

The current study on MMD revealed a few notable hemodynamic trends. While the pressure drop of the surgical ICA decreased at follow-up, the reverse was observed in the contralateral ICA in unilaterally treated MMD patients. The pressure difference of contralateral ICA at follow-up showed a marked increase when compared to pre-operative measurements. This was seen in our PDI calculations of all 26 patients treated unilaterally irrespective of CoW anomalies. Additionally, structural irregularities of CoW have been previously stated as a risk factor for various cerebrovascular disorders. In our study all patients graded as C-No Improvement possessed an incomplete CoW. Angiographic and computational assessment of a larger cohort of patients possessing an incomplete CoW will throw light into the relationship between an incomplete CoW and the regressive nature of treatment outcome. We also intend to further comprehend the relationship between vascular tortuosity and treatment outcome in our future studies. We are working on a large-scale, multi-center computational analysis of MMD patients to statistically quantify the significance of PDI and vascular tortuosity index as non-invasive hemodynamic tools in assessing the treatment outcome of revascularization surgery.

## 7.2 Conclusion

CFD has been widely applied to understand the hemodynamic mechanism underlying the origin and development of several cerebrovascular diseases. This dissertation aimed to hemodynamically assess the treatment outcome of cerebrovascular disorders namely intracranial aneurysms and MMD. We have succeeded in identifying parameters such as Metal coverage Rate (MCR) and free stent angle of flow diverter in aneurysms and PDI of ICA in MMD patients, which play a crucial role in determining the success or failure of the flow-diversion and revascularization treatment respectively. Further research into these parameters with a larger cohort of patients will help us establish statistical significance that will lead to these parameters to be accepted clinically as assistive tools in surgical planning and management of intracranial aneurysms and Moyamoya disease.

# *References*

Reference list

1. Paulson OB, Strandgaard S, Edvinsson L. Cerebral autoregulation. Cerebrovasc Brain Metab Rev. 1990;2(2):161-92.

2. Phillips SJ, Whisnant JP. Hypertension and the brain. The National High Blood Pressure Education Program. Arch Intern Med. 1992;152(5):938-45.

3. Kontos HA, Wei EP, Raper AJ, Rosenblum WI, Navari RM, Patterson JL, Jr. Role of tissue hypoxia in local regulation of cerebral microcirculation. Am J Physiol. 1978;234(5):H582-91.

4. Faraci FM, Heistad DD. Regulation of large cerebral arteries and cerebral microvascular pressure. Circ Res. 1990;66(1):8-17.

5. Alpers BJ, Berry RG, Paddison RM. Anatomical studies of the circle of Willis in normal brain. AMA Arch Neurol Psychiatry. 1959;81(4):409-18.

6. Macchi C, Lova RM, Miniati B, Gulisano M, Pratesi C, Conti AA, et al. The circle of Willis in healthy older persons. J Cardiovasc Surg. 2002;43(6):887-90.

7. Kayembe KN, Sasahara M, Hazama F. Cerebral aneurysms and variations in the circle of Willis. Stroke. 1984;15(5):846-50.

8. Harnsberger HR OA, Ross J, Macdonals A. Diagnostic and Surgical Imaging Anatomy: Brain, Head and Neck, Spine: Lippincott Williams & Wilkins; 2006.

9. Meyers PM, Schumacher HC, Higashida RT, Derdeyn CP, Nesbit GM, Sacks D, et al. Reporting standards for endovascular repair of saccular intracranial cerebral aneurysms. Journal of NeuroInterventional Surgery. 2010;2(4):312-23.

10. Rinkel GJE, Djibuti M, Algra A, van Gijn J. Prevalence and Risk of Rupture of Intracranial Aneurysms: A Systematic Review. Stroke. 1998;29(1):251-6.

11. Gasparotti R, Liserre R. Intracranial aneurysms. Eur Radiol. 2005;15(3):441-7.

12. Vlak MHM, Algra A, Brandenburg R, Rinkel GJE. Prevalence of unruptured intracranial aneurysms, with emphasis on sex, age, comorbidity, country, and time period: A systematic review and meta-analysis. The Lancet Neurology. 2011;10(7):626-36.

13. Williams LN, Brown RD. Management of unruptured intracranial aneurysms. Neurology: Clinical Practice. 2013;3(2):99-108.

14. Kassell NF, Torner JC, Haley EC, Jane JA, Adams HP, Kongable GL. The International Cooperative Studyon the Timing of Aneurysm Surgery. Journal of Neurosurgery. 1990;73(1):18-36.

15. Unruptured Intracranial Aneurysms — Risk of Rupture and Risks of Surgical Intervention. New England Journal of Medicine. 1998;339(24):1725-33.

16. Meyer FB, Sundt Jr TM, Fode NC, Morgan MK, Forbes GS, Mellinger JF. Cerebral aneurysms in childhood and adolescence. Journal of Neurosurgery. 1989;70(3):420-5.

17. Kassell NF, Torner JC, Jane JA, Haley Jr EC, Adams HP. The International Cooperative Study on the Timing of Aneurysm Surgery. Part 2: Surgical results. Journal of Neurosurgery. 1990;73(1):37-47.

18. Rinne J, Hernesniemi J, Puranen M, Saari T, Solomon RA, Piepgras DG. Multiple intracranial aneurysms in a defined population: Prospective angiographic and clinical study. Neurosurgery. 1994;35(5):803-8.

19. Hashimoto N, Handa H, Nagata I, Hazama F. Experimentally induced cerebral aneurysms in rats: Part V. Relation of hemodynamics in the circle of Willis to formation of aneurysms. Surg Neurol. 1980;13(1):41-5.

20. Kilic T, Sohrabifar M, Kurtkaya O, Yildirim O, Elmaci I, Gunel M, et al. Expression of structural proteins and angiogenic factors in normal arterial and unruptured and ruptured aneurysm walls. Neurosurgery. 2005;57(5):997-1007.

21. Caranci F, Briganti F, Cirillo L, Leonardi M, Muto M. Epidemiology and genetics of intracranial aneurysms. Eur J Radiol. 2013;82(10):1598-605.

22. Schievink WI, Michels VV, Piepgras DG. Neurovascular manifestations of heritable connective tissue disorders. A review. Stroke. 1994;25(4):889-903.

23. Nakajima K, Ito Z, Hen R, Uemura K, Matsuoka S. [Congenital anomalies of cerebral artery and intracranial aneurysm]. No To Shinkei. 1976;28(2):197-201.

24. Chambers WR, Harper BF, Simpson JR. Familial Incidence Of Congenital Aneurysms Of Cerebral Arteries - Report Of Cases Of Ruptured Aneurysms In Father And Son. Jama-J Am Med Assoc. 1954;155(4):358-9.

25. Leblanc R, Worsley KJ, Melanson D, Tampieri D. Angiographic screening and elective surgery of familial cerebral aneurysms: a decision analysis. Neurosurgery. 1994;35(1):9-18.

26. Norrgard O, Angquist KA, Fodstad H, Forsell A, Lindberg M. Intracranial Aneurysms And Heredity. Neurosurgery. 1987;20(2):236-9.

27. Wang MC, Rubinstein D, Kindt GW, Breeze RE. Prevalence of intracranial aneurysms in first-degree relatives of patients with aneurysms. Neurosurg Focus. 2002;13(3).

28. Broderick JP, Brown RD, Jr., Sauerbeck L, Hornung R, Huston J, 3rd, Woo D, et al. Greater rupture risk for familial as compared to sporadic unruptured intracranial aneurysms. Stroke. 2009;40(6):1952-7.

29. Bromberg JEC, Rinkel GJE, Algra A, Greebe P, van Duyn CM, Hasan D, et al. Subarachnoid haemorrhage in first and second degree relatives of patients with subarachnoid haemorrhage. BMJ. 1995;311(7000):288-9.

30. Alg VS, Sofat R, Houlden H, Werring DJ. Genetic risk factors for intracranial aneurysms: a meta-analysis in more than 116,000 individuals. Neurology. 2013;80(23):2154-65.

31. Riggs HE, Rupp C. Variation in form of circle of Willis. The relation of the variations to collateral circulation: anatomic analysis. Arch Neurol. 1963;8:8-14.

32. Stehbens WE. Pathology of the Cerebral Blood Vessels: C. V. Mosby; 1972.

33. Broderick JP, Viscoli CM, Brott T, Kernan WN, Brass LM, Feldmann E, et al. Major risk factors for aneurysmal subarachnoid hemorrhage in the young are modifiable. Stroke; a journal of cerebral circulation. 2003;34(6):1375-81.

34. Longstreth WT, Nelson LM, Koepsell TD, van Belle G. Cigarette smoking, alcohol use, and subarachnoid hemorrhage. Stroke. 1992;23(9):1242-9.

35. Qureshi AI, Suarez JI, Parekh PD, Sung G, Geocadin R, Bhardwaj A, et al. Risk Factors for Multiple Intracranial Aneurysms. Neurosurgery. 1998;43(1):22-6.

36. Juvela S, Hillbom M, Numminen H, Koskinen P. Cigarette smoking and alcohol consumption as risk factors for aneurysmal subarachnoid hemorrhage. Stroke. 1993;24(5):639-46.

37. Conway JE, Tamargo RJ. Cocaine Use Is an Independent Risk Factor for Cerebral Vasospasm After Aneurysmal Subarachnoid Hemorrhage. Stroke. 2001;32(10):2338-43.

38. Nanda A, Vannemreddy PS, Polin RS, Willis BK. Intracranial aneurysms and cocaine abuse: analysis of prognostic indicators. Neurosurgery. 2000;46(5):1063-7.

39. de la Monte SM, Moore GW, Monk MA, Hutchins GM. Risk factors for the development and rupture of intracranial berry aneurysms. Am J Med. 1985;78(6 Pt 1):957-64.

40. Taylor CL, Yuan Z, Selman WR, Ratcheson RA, Rimm AA. Cerebral arterial aneurysm formation and rupture in 20,767 elderly patients: hypertension and other risk factors. J Neurosurg. 1995;83(5):812-9.

41. Forsting MM, Cognard CC. Intracranial Vascular Malformations and AneurysmsFrom Diagnostic Work-Up to Endovascular Therapy-From Diagnostic Work-Up to Endovascular Therapy. London: Springer Berlin Heidelberg; 2008. 254 p.

42. Dubey A, Sung W-S, Chen Y-Y, Amato D, Mujic A, Waites P, et al. Traumatic intracranial aneurysm: A brief review. Journal of Clinical Neuroscience. 2008;15(6):609-12.

43. Linn FHH, Rinkel GJE, Algra A, van Gijn J. Headache characteristics in subarachnoid haemorrhage and benign thunderclap headache. Journal of Neurology, Neurosurgery & Psychiatry. 1998;65(5):791-3.

44. van Gijn J, Rinkel GJE. Subarachnoid haemorrhage: diagnosis, causes and management. Brain. 2001;124(2):249-78.

45. Nishioka H. Report on the cooperative study of intracranial aneurysms and subarachnoid hemorrhage. Section VII. I. Evaluation of the conservative management of ruptured intracranial aneurysms. J Neurosurg. 1966;25(5):574-92.

46. Hijdra A, van Gijn J, Nagelkerke NJ, Vermeulen M, van Crevel H. Prediction of delayed cerebral ischemia, rebleeding, and outcome after aneurysmal subarachnoid hemorrhage. Stroke. 1988;19(10):1250-6.

47. Calviere L, Viguier A, Da Silva NA, Jr., Cognard C, Larrue V. Unruptured intracranial aneurysm as a cause of cerebral ischemia. Clin Neurol Neurosurg. 2011;113(1):28-33.

48. Bederson JB, Awad IA, Wiebers DO, Piepgras D, Haley EC, Brott T, et al. Recommendations for the Management of Patients With Unruptured Intracranial Aneurysms: A Statement for Healthcare Professionals From the Stroke Council of the American Heart Association. Circulation. 2000;102(18):2300-8.

49. Solomon RA, Fink ME, Pile-Spellman J. Surgical management of unruptured intracranial aneurysms. J Neurosurg. 1994;80(3):440-6.

50. Hong Y, Guo S, Chen S, Sun C, Zhang J, Sun X. Beneficial effect of hydrogen-rich saline on cerebral vasospasm after experimental subarachnoid hemorrhage in rats. Journal of Neuroscience Research. 2012;90(8):1670-80.

51. Hop JW, Rinkel GJ, Algra A, van Gijn J. Case-fatality rates and functional outcome after subarachnoid hemorrhage: a systematic review. Stroke. 1997;28(3):660-4.

52. McCormick WF, Nofzinger JD. Saccular Intracranial Aneurysms: An Autopsy Study. J Neurosurg. 1965;22:155-9.

53. Rosenørn J, Eskesen V, Schmidt K. Unruptured Intracranial Aneurysms: An Assessment of the Annual Risk of Rupture Based on Epidemiological and Clinical Data. British Journal of Neurosurgery. 1988;2(3):369-77.

54. Bederson JB, Awad IA, Wiebers DO, Piepgras D, Haley EC, Jr., Brott T, et al. Recommendations for the management of patients with unruptured intracranial aneurysms: A Statement for healthcare professionals from the Stroke Council of the American Heart Association. Stroke. 2000;31(11):2742-50.

55. Lysack JT, Coakley A. Asymptomatic unruptured intracranial aneurysms: Approach to screening and treatment. Canadian Family Physician. 2008;54(11):1535-8.

56. Andaluz N, Zuccarello M. Recent trends in the treatment of cerebral aneurysms: Analysis of a nationwide inpatient database. Journal of Neurosurgery. 2008;108(6):1163-9.

57. Broderick JP, Brott T, Tomsick T, Miller R, Huster G. Intracerebral hemorrhage more than twice as common as subarachnoid hemorrhage. Journal of Neurosurgery. 1993;78(2):188-91.

58. Cruickshank A, Auld P, Beetham R, Burrows G, Egner W, Holbrook I, et al. Revised national guidelines for analysis of cerebrospinal fluid for bilirubin in suspected subarachnoid haemorrhage. Annals of Clinical Biochemistry. 2008;45(3):238-44.

59. Edlow JA. Diagnosis of subarachnoid hemorrhage. Neurocritical Care. 2005;2(2):99-109.

60. van Gijn J, van Dongen KJ. The time course of aneurysmal haemorrhage on computed tomograms. Neuroradiology. 1982;23(3):153-6.

61. Van Der Wee N, Rinkel GJE, Hasan D, Van Gijn J. Detection of subarachnoid haemorrhage on early CT: Is lumbar puncture still needed after a negative scan? Journal of Neurology, Neurosurgery and Psychiatry. 1995;58(3):357-9.

62. Ogawa T, Inugami A, Fujita H, Hatazawa J, Shimosegawa E, Noguchi K, et al. MR diagnosis of subacute and chronic subarachnoid hemorrhage: comparison with CT. AJR Am J Roentgenol. 1995;165(5):1257-62.

63. Ausman JI. Handbook of Neurosurgery, 7(th) Edition. Surgical Neurology International. 2010;1:19.

64. van Rooij WJ, Sprengers ME, de Gast AN, Peluso JPP, Sluzewski M. 3D Rotational Angiography: The New Gold Standard in the Detection of Additional Intracranial Aneurysms. American Journal of Neuroradiology. 2008;29(5):976-9.

65. Cloft HJ, Joseph GJ, Dion JE. Risk of Cerebral Angiography in Patients With Subarachnoid Hemorrhage, Cerebral Aneurysm, and Arteriovenous Malformation: A Meta-Analysis. Stroke. 1999;30(2):317-20.

66. Ross JS, Masaryk TJ, Modic MT, Ruggieri PM, Haacke EM, Selman WR. Intracranial aneurysms: evaluation by MR angiography. American Journal of Neuroradiology. 1990;11(3):449-55.

67. Hacein-Bey L, Provenzale JM. Current imaging assessment and treatment of intracranial aneurysms. AJR Am J Roentgenol. 2011;196(1):32-44.

68. Yoon DY, Lim KJ, Choi CS, Cho BM, Oh SM, Chang SK. Detection and Characterization of Intracranial Aneurysms with 16-Channel Multidetector Row CT Angiography: A Prospective Comparison of Volume-Rendered Images and Digital Subtraction Angiography. American Journal of Neuroradiology. 2007;28(1):60-7.

69. van Gijn J, van Dongen KJ. Computed tomography in the diagnosis of subarachnoid haemorrhage and ruptured aneurysm. Clinical Neurology and Neurosurgery. 1980;82(1):11-24.

70. Lu L, Zhang LJ, Poon CS, Wu SY, Zhou CS, Luo S, et al. Digital subtraction CT angiography for detection of intracranial aneurysms: comparison with three-dimensional digital subtraction angiography. Radiology. 2012;262(2):605-12.

71. McKinney AM, Palmer CS, Truwit CL, Karagulle A, Teksam M. Detection of aneurysms by 64-section multidetector CT angiography in patients acutely suspected of having an intracranial aneurysm and comparison with digital subtraction and 3D rotational angiography. AJNR Am J Neuroradiol. 2008;29(3):594-602.

72. Smith-Bindman R, Lipson J, Marcus R, et al. RAdiation dose associated with common computed tomography examinations and the associated lifetime attributable risk of cancer. Archives of Internal Medicine. 2009;169(22):2078-86.

73. Jeong HW, Seo JH, Kim ST, Jung CK, Suh SI. Clinical practice guideline for the management of intracranial aneurysms. Neurointervention. 2014;9(2):63-71.

74. Tummala RP, Baskaya MK, Heros RC. Contemporary management of incidental intracranial aneurysms. Neurosurg Focus. 2005;18(1).

75. Guglielmi G, Viñuela F, Dion J, Duckwiler G. Electrothrombosis of saccular aneurysms via endovascular approach. Journal of Neurosurgery. 1991;75(1):8-14.

76. Guglielmi G, Viñuela F, Sepetka I, Macellari V. Electrothrombosis of saccular aneurysms via endovascular approach. Journal of Neurosurgery. 1991;75(1):1-7.

77. Naggara ON, Lecler A, Oppenheim C, Meder JF, Raymond J. Endovascular treatment of intracranial unruptured aneurysms: A systematic review of the literature on safety with emphasis on subgroup analyses. Radiology. 2012;263(3):828-35.

78. Lanterna LA, Tredici G, Dimitrov BD, Biroli F. Treatment of unruptured cerebral aneurysms by embolization with guglielmi detachable coils: case-fatality, morbidity, and effectiveness in preventing bleeding--a systematic review of the literature. Neurosurgery. 2004;55(4):767-75.

79. Kallmes DF, Hanel R, Lopes D, Boccardi E, Bonafé A, Cekirge S, et al. International Retrospective Study of the Pipeline Embolization Device: A Multicenter Aneurysm Treatment Study. American Journal of Neuroradiology. 2015;36(1):108-15.

80. Smith ER, Scott RM. Moyamoya: Epidemiology, Presentation, and Diagnosis. Neurosurgery Clinics of North America. 2010;21(3):543-51.

81. Kamada F, Aoki Y, Narisawa A, Abe Y, Komatsuzaki S, Kikuchi A, et al. A genome-wide association study identifies RNF213 as the first Moyamoya disease gene. J Hum Genet. 2011;56(1):34-40.

82. Ikeda H, Sasaki T, Yoshimoto T, Fukui M, Arinami T. Mapping of a Familial Moyamoya Disease Gene to Chromosome 3p24.2-p26. The American Journal of Human Genetics. 1999;64(2):533-7.

83. Nanba R, Tada M, Kuroda S, Houkin K, Iwasaki Y. Sequence analysis and bioinformatics analysis of chromosome 17q25 in familial moyamoya disease. Childs Nerv Syst. 2005;21(1):62-8.

84. Scott RM, Smith JL, Robertson RL, Madsen JR, Soriano SG, Rockoff MA. Long-term outcome in children with moyamoya syndrome after cranial revascularization by pial synangiosis. Journal of Neurosurgery: Pediatrics. 2004;100(2):142-9.

85. Tanghetti B, Capra R, Giunta F, Marini G, Orlandini A. Moyamoya syndrome in only one of two identical twins. Journal of Neurosurgery. 1983;59(6):1092-4.

86. Lim M, Cheshier S, Steinberg GK. New vessel formation in the central nervous system during tumor growth, vascular malformations, and Moyamoya. Curr Neurovasc Res. 2006;3(3):237-45.

87. Soriano SG, Cowan DB, Proctor MR, Scott RM. Levels of soluble adhesion molecules are elevated in the cerebrospinal fluid of children with moyamoya syndrome. Neurosurgery. 2002;50(3):544-9.

88. Takagi Y, Kikuta K, Nozaki K, Fujimoto M, Hayashi J, Imamura H, et al. Expression of hypoxia-inducinc factor-1 alpha and endoglin in intimal hyperplasia of the middle cerebral artery of patients with Moyamoya disease. Neurosurgery. 2007;60(2):338-45.

89. Liu XM, Ruan XZ, Cai Z, Yu BR, He SP, Gong YH. Moyamoya disease caused by leptospiral cerebral arteritis. Chin Med J. 1980;93(9):599-604.

90. Mathew NT, Abraham J, Chandy J. Cerebral angiographic features in tuberculous meningitis. Neurology. 1970;20(10):1015-23.

91. Yamada H, Deguchi K, Tanigawara T, Takenaka K, Nishimura Y, Shinoda J, et al. The relationship between Moyamoya disease and bacterial infection. Clinical Neurology and Neurosurgery. 1997;99(SUPPL. 2):S221-S4.

92. Desai SS, Paulino AC, Mai WY, Teh BS. Radiation-induced moyamoya syndrome. Int J Radiat Oncol Biol Phys. 2006;65(4):1222-7.

93. Ullrich NJ, Robertson R, Kinnamon DD, Scott RM, Kieran MW, Turner CD, et al. Moyamoya following cranial irradiation for primary brain tumors in children. Neurology. 2007;68(12):932-8.

94. Im SH, Oh CW, Kwon OK, Kim JE, Han DH. Moyamoya disease associated with Graves disease: special considerations regarding clinical significance and management. J Neurosurg. 2005;102(6):1013-7.

95. Jea A, Smith ER, Robertson R, Scott RM. Moyamoya syndrome associated with down syndrome: Outcome after surgical revascularization. Pediatrics. 2005;116(5):e694-e701.

96. Hosoda Y, Ikeda E, Hirose S. Histopathological studies on spontaneous occlusion of the circle of Willis (cerebrovascular Moyamoya disease). Clinical Neurology and Neurosurgery. 1997;99, Supplement 2:S203-S8.

97. Fukui M, Members of the Research Committee on Spontaneous Occlusion of the Circle of Willis of the Ministry of H, Welfare J. Guidelines for the diagnosis and treatment of spontaneous occlusion of the circle of Willis (`Moyamoya' disease)1. Clinical Neurology and Neurosurgery. 1997;99, Supplement 2:S238-S40.

98. Fukui M, Kono S, Sueishi K, Ikezaki K. Moyamoya disease. Neuropathology. 2000;20:61-4.

99. Hallemeier CL, Rich KM, Grubb Jr RL, Chicoine MR, Moran CJ, Cross Iii DT, et al. Clinical features and outcome in North American adults with moyamoya phenomenon. Stroke. 2006;37(6):1490-6.

100. Oka K, Yamashita M, Sadoshima S, Tanaka K. Cerebral haemorrhage in Moyamoya disease at autopsy. Virchows Arch A Path Anat and Histol. 1981;392(3):247-61.

101. Scott RM, Smith JL, Robertson RL, Madsen JR, Soriano SG, Rockoff MA. Long-term outcome in children with moyamoya syndrome after cranial revascularization by pial synangiosis. Journal of Neurosurgery. 2004;100(2):142-9.

102. Scott RM, Smith ER. Moyamoya Disease and Moyamoya Syndrome. New England Journal of Medicine. 2009;360(12):1226-37.

103. Suzuki J, Kodama N. Moyamoya disease--a review. Stroke. 1983;14(1):104-9.

104. Kuroda S, Houkin K. Moyamoya disease: current concepts and future perspectives. The Lancet Neurology. 2008;7(11):1056-66.

105. Hung SC, Liang ML, Lin CF, Lin CJ, Guo WY, Chang FC, et al. New grading of moyamoya disease using color-coded parametric quantitative digital subtraction angiography. J Chin Med Assoc. 2014;77(8):437-42.

106. Czabanka M, Pena-Tapia P, Schubert GA, Heppner FL, Martus P, Horn P, et al. Proposal for a new grading of Moyamoya disease in adult patients. Cerebrovasc Dis. 2011;32(1):41-50.

107. Houkin K, Nakayama N, Kuroda S, Nonaka T, Shonai T, Yoshimoto T. Novel magnetic resonance angiography stage grading for moyamoya disease. Cerebrovascular Diseases. 2005;20(5):347-54.

108. Yamada I, Suzuki S, Matsushima Y. Moyamoya disease: diagnostic accuracy of MRI. Neuroradiology. 1995;37(5):356-61.

109. Houkin K, Aoki T, Takahashi A, Abe H. Diagnosis of moyamoya disease with magnetic resonance angiography. Stroke. 1994;25(11):2159-64.

110. Kodama N, Aoki Y, Hiraga H, Wada T, Suzuki J. ELectroencephalographic findings in children with moyamoya disease. Archives of Neurology. 1979;36(1):16-9.

111. Ikezaki K. Rational approach to treatment of moyamoya disease in childhood. J Child Neurol. 2000;15(5):350-6.

112. Gross BA, Thomas AJ, Frerichs KU. Endovascular treatment of symptomatic moyamoya. Neurosurg Rev. 2014;37(4):579-83.

113. Yu JL, Wang HL, Xu K, Li Y, Luo Q. Endovascular Treatment of Intracranial Aneurysms Associated with Moyamoya Disease or Moyamoya Syndrome. Interventional Neuroradiology. 2010;16(3):240-8.

114. Suzuki J, Takaku A, Kodama N, Sato S. An attempt to treat cerebrovascular 'Moyamoya' disease in children. Childs Brain. 1975;1(4):193-206.

115. Karasawa J, Kikuchi H, Furuse S, Kawamura J, Sakaki T. Treatment of moyamoya disease with STA-MCA anastomosis. J Neurosurg. 1978;49(5):679-88.

116. Kinugasa K, Mandai S, Kamata I, Sugiu K, Ohmoto T. Surgical treatment of moyamoya disease: operative technique for encephalo-duro-arterio-myo-synangiosis, its follow-up, clinical results, and angiograms. Neurosurgery. 1993;32(4):527-31.

117. Yasargil MG. A legacy of microneurosurgery: memoirs, lessons, and axioms. Neurosurgery. 1999;45(5):1025-92.

118. Jun Karasawa, Haruhiko Kikuchi, Seiji Furuse, Junichiro Kawamura, Toshisuke Sakaki. Treatment of moyamoya disease with STA-MCA anastomosis. Journal of Neurosurgery. 1978;49(5):679-88.

119. Miyamoto S, Akiyama Y, Nagata I, Karasawa J, Nozaki K, Hashimoto N, et al. Long-term outcome after STA-MCA anastomosis for moyamoya disease. Neurosurg Focus. 1998;5(5).

120. Langer DJ, Vajkoczy P. ELANA: Excimer Laser-Assisted Nonocclusive Anastomosis for Extracranial-to-Intracranial and Intracranial-to-Intracranial Bypass: A Review. Skull Base. 2005;15(3):191-205.

121. Langer DJ VP, Chakraborty S, Tymianski M, Amin-Hanjani S, Charbel FT, et al. Final Results of the ELANA FDA-IDE Study on High Flow Cerebral Bypasses for Surgical Treatment of Anterior Circulation Aneurysms. Neurosurgery. 2012;71(2):E551-4.

122. Mesiwala AH, Sviri G, Fatemi N, Britz GW, Newell DW. Long-term outcome of superficial temporal artery-middle cerebral artery bypass for patients with moyamoya disease in the US. Neurosurg Focus. 2008;24(2).

123. Kim DS, Kang SG, Yoo DS, Huh PW, Cho KS, Park CK. Surgical results in pediatric moyamoya disease: angiographic revascularization and the clinical results. Clin Neurol Neurosurg. 2007;109(2):125-31.

124. Patel NN, Mangano FT, Klimo Jr P. Indirect Revascularization Techniques for Treating Moyamoya Disease. Neurosurgery Clinics of North America. 2010;21(3):553-63.

125. Touho H, Karasawa J, Tenjin H, Ueda S. Omental transplantation using a superficial temporal artery previously used for encephaloduroarteriosynangiosis. Surg Neurol. 1996;45(6):550-8.

126. Takeuchi S, Tsuchida T, Kobayashi K, Fukuda M, Ishii R, Tanaka R, et al. Treatment of moyamoya disease by temporal muscle graft 'encephalo-myo-synangiosis'. Childs Brain. 1983;10(1):1-15.

127. Matsushima T, Inoue T, Katsuta T, Natori Y, Suzuki S, Ikezaki K, et al. An Indirect Revascularization Method in the Surgical Treatment of Moyamoya DiseaseVarious Kinds of Indirect Procedures and a Multiple Combined Indirect Procedure. Neurologia medico-chirurgica. 1998;38(suppl):297-302.

128. Matsushima T, Inoue TK, Suzuki SO, Inoue T, Ikezaki K, Fukui M, et al. Surgical techniques and the results of a fronto-temporo-parietal combined indirect bypass procedure for children with Moyamoya disease: A comparison with the results of encephalo-duro-arterio-synangiosis alone. Clinical Neurology and Neurosurgery. 1997;99(SUPPL. 2):S123-S7.

129. Houkin K, Kamiyama H, Abe H, Takahashi A, Kuroda S. Surgical Therapy for Adult Moyamoya Disease: Can Surgical Revascularization Prevent the Recurrence of Intracerebral Hemorrhage? Stroke. 1996;27(8):1342-6.

130. Golby AJ, Marks MP, Thompson RC, Steinberg GK. Direct and combined revascularization in pediatric moyamoya disease. Neurosurgery. 1999;45(1):50-8.

131. Houkin K, Kuroda S, Nakayama N. Cerebral revascularization for moyamoya disease in children. Neurosurgery Clinics of North America. 2001;12(3):575-84.

132. Hayashi T, Shirane R, Tominaga T. Additional surgery for postoperative ischemic symptoms in patients with moyamoya disease: the effectiveness of occipital artery-posterior

cerebral artery bypass with an indirect procedure: technical case report. Neurosurgery. 2009;64(1):26.

133. Esposito G, Kronenburg A, Fierstra J, Braun KP, Klijn CJ, van der Zwan A, et al. "STA-MCA bypass with encephalo-duro-myo-synangiosis combined with bifrontal encephalo-duro-periosteal-synangiosis" as a one-staged revascularization strategy for pediatric moyamoya vasculopathy. Childs Nerv Syst. 2015;31(5):765-72.

134. Castro MA, Putman CM, Cebral JR. Computational fluid dynamics modeling of intracranial aneurysms: Effects of parent artery segmentation on intra-aneurysmal hemodynamics. American Journal of Neuroradiology. 2006;27(8):1703-9.

135. Humphrey JD. Coupling hemodynamics with vascular wall mechanics and mechanobiology to understand intracranial aneurysms. International journal of computational fluid dynamics. 2009;23(8):569-81.

136. Bisbal J, Engelbrecht G, Villa-Uriol MC, Frangi AF. Prediction of cerebral aneurysm rupture using hemodynamic, morphologic and clinical features: A data mining approach. 2011. p. 59-73.

137. Nikolic I, Tasic G, Bogosavljevic V, Nestorovic B, Jovanovic V, Kojic Z, et al. Predictable morphometric parameters for rupture of intracranial aneurysms - a series of 142 operated aneurysms. Turk Neurosurg. 2012;22(4):420-6.

138. Dhar S, Tremmel M, Mocco J, Kim M, Yamamoto J, Siddiqui AH, et al. Morphology parameters for intracranial aneurysm rupture risk assessment. Neurosurgery. 2008;63(2):185-96; discussion 96-7. Epub 2008/09/18.

139. Raghavan ML, Ma B, Harbaugh RE. Quantified aneurysm shape and rupture risk. J Neurosurg. 2005;102(2):355-62.

140. Ujiie H, Tamano Y, Sasaki K, Hori T. Is the aspect ratio a reliable index for predicting the rupture of a saccular aneurysm? Neurosurgery. 2001;48(3):495-502.

141. Nader-Sepahi A, Casimiro M, Sen J, Kitchen ND. Is aspect ratio a reliable predictor of intracranial aneurysm rupture? Neurosurgery. 2004;54(6):1343-7.

142. Weir B, Amidei C, Kongable G, Findlay JM, Kassell NF, Kelly J, et al. The aspect ratio (dome/neck) of ruptured and unruptured aneurysms. J Neurosurg. 2003;99(3):447-51.

143. Baharoglu MI, Schirmer CM, Hoit DA, Gao BL, Malek AM. Aneurysm inflow-angle as a discriminant for rupture in sidewall cerebral aneurysms: morphometric and computational fluid dynamic analysis. Stroke. 2010;41(7):1423-30.

144. Wong GKC, Poon WS. Current status of computational fluid dynamics for cerebral aneurysms: The clinician's perspective. Journal of Clinical Neuroscience. 2011;18(10):1285-8.

145. Tremmel M, Dhar S, Levy EI, Mocco J, Meng H. Influence of intracranial aneurysm-to-parent vessel size ratio on hemodynamics and implication for rupture: Results from a virtual experimental study. Neurosurgery. 2009;64(4):622-30.

146. Rahman M, Smietana J, Hauck E, Hoh B, Hopkins N, Siddiqui A, et al. Size ratio correlates with intracranial aneurysm rupture status: a prospective study. Stroke. 2010;41(5):916-20.

147. Lauric A, Baharoglu MI, Gao BL, Malek AM. Incremental contribution of size ratio as a discriminant for rupture status in cerebral aneurysms: Comparison with size, height, and vessel diameter. Neurosurgery. 2012;70(4):944-51.

148. Cebral JR, Mut F, Raschi M, Scrivano E, Ceratto R, Lylyk P, et al. Aneurysm Rupture Following Treatment with Flow-Diverting Stents: Computational Hemodynamics Analysis of Treatment. American Journal of Neuroradiology. 2011;32(1):27-33.

149. Shojima M, Oshima M, Takagi K, Torii R, Nagata K, Shirouzu I, et al. Role of the Bloodstream Impacting Force and the Local Pressure Elevation in the Rupture of Cerebral Aneurysms. Stroke. 2005;36(9):1933-8.

150. Burleson AC, Strother CM, Turitto VT. Computer modeling of intracranial saccular and lateral aneurysms for the study of their hemodynamics. Neurosurgery. 1995;37(4):774-82.

151. Shojima M, Oshima M, Takagi K, Torii R, Hayakawa M, Katada K, et al. Magnitude and role of wall shear stress on cerebral aneurysm: Computational fluid dynamic study of 20 middle cerebral artery aneurysms. Stroke. 2004;35(11):2500-5.

152. Jou LD, Morsi H, Shaltoni HM, Mawad ME. Hemodynamics of small aneurysm pairs at the internal carotid artery. Medical Engineering and Physics. 2012.

153. Cebral JR, Mut F, Weir J, Putman CM. Association of Hemodynamic Characteristics and Cerebral Aneurysm Rupture. American Journal of Neuroradiology. 2011;32(2):264-70.

154. Lu G, Huang L, Zhang XL, Wang SZ, Hong Y, Hu Z, et al. Influence of hemodynamic factors on rupture of intracranial aneurysms: patient-specific 3D mirror aneurysms model computational fluid dynamics simulation. AJNR Am J Neuroradiol. 2011;32(7):1255-61.

155. Xiang J, Natarajan SK, Tremmel M, Ma D, Mocco J, Hopkins LN, et al. Hemodynamic-morphologic discriminants for intracranial aneurysm rupture. Stroke. 2011;42(1):144-52.

156. Finol EA, Amon CH. Flow-induced wall shear stress in abdominal aortic aneurysms: Part II--pulsatile flow hemodynamics. Comput Methods Biomech Biomed Engin. 2002;5(4):319-28.

157. Goubergrits L, Schaller J, Kertzscher U, van den Bruck N, Poethkow K, Petz C, et al. Statistical wall shear stress maps of ruptured and unruptured middle cerebral artery aneurysms. Journal of The Royal Society Interface. 2012;9(69):677-88.

158. Kawaguchi T, Nishimura S, Kanamori M, Takazawa H, Omodaka S, Sato K, et al. Distinctive flow pattern of wall shear stress and oscillatory shear index: similarity and dissimilarity in ruptured and unruptured cerebral aneurysm blebs. J Neurosurg. 2012;117(4):774-80.

159. Jing L, Fan J, Wang Y, Li H, Wang S, Yang X, et al. Morphologic and Hemodynamic Analysis in the Patients with Multiple Intracranial Aneurysms: Ruptured versus Unruptured. PLoS ONE. 2015;10(7):e0132494.

160. Takao H, Murayama Y, Otsuka S, Qian Y, Mohamed A, Masuda S, et al. Hemodynamic differences between unruptured and ruptured intracranial aneurysms during observation. Stroke. 2012;43(5):1436-9.

161. Hu P, Qian Y, Lee C-J, Zhang H-Q, Ling F. The energy loss may predict rupture risks of anterior communicating aneurysms: a preliminary result. International Journal of Clinical and Experimental Medicine. 2015;8(3):4128-33.

162. Byun HS, Rhee K. CFD modeling of blood flow following coil embolization of aneurysms. Med Eng Phys. 2004;26(9):755-61.

163. Wei Y, Cotin S, Allard J, Fang L, Pan C, Ma S. Interactive blood-coil simulation in real-time during aneurysm embolization. Computers & Graphics. 2011;35(2):422-30.

164. Ma D, Dumont TM, Kosukegawa H, Ohta M, Yang X, Siddiqui AH, et al. High Fidelity Virtual Stenting (HiFiVS) for Intracranial Aneurysm Flow Diversion: In Vitro and In Silico. Annals of biomedical engineering. 2013;41(10):2143-56.

165. Augsburger L, Reymond P, Rufenacht DA, Stergiopulos N. Intracranial Stents Being Modeled as a Porous Medium: Flow Simulation in Stented Cerebral Aneurysms. Annals of biomedical engineering. 2011;39(2):850-63.

166. Raschi M, Mut F, Löhner R, Cebral JR. Strategy for modeling flow diverters in cerebral aneurysms as a porous medium. International Journal for Numerical Methods in Biomedical Engineering. 2014;30(9):909-25.

167. Tremmel M, Xiang J, Natarajan SK, Hopkins LN, Siddiqui AH, Levy EI, et al. Alteration of intra-aneurysmal hemodynamics for flow diversion using enterprise and vision stents. World Neurosurg. 2010;74(2-3):306-15.

168. Xu J, Deng B, Fang Y, Yu Y, Cheng J, Wang S, et al. Hemodynamic Changes Caused by Flow Diverters in Rabbit Aneurysm Models: Comparison of Virtual and Realistic FD Deployments Based on Micro-CT Reconstruction. PLoS ONE. 2013;8(6):e66072.

169. Irie K, Anzai H, Kojima M, Honjo N, Ohta M, Hirose Y, et al. Computational fluid dynamic analysis following recurrence of cerebral aneurysm after coil embolization. Asian Journal of Neurosurgery. 2012;7(3):109-15.

170. Takahashi S, Tanizaki Y, Kimura H, Akaji K, Nakazawa M, Yoshida K, et al. Hemodynamic stress distribution reflects ischemic clinical symptoms of patients with moyamoya disease. Clinical Neurology and Neurosurgery. 2015;138:104-10.

171. Togao O, Mihara F, Yoshiura T, Tanaka A, Noguchi T, Kuwabara Y, et al. Cerebral Hemodynamics in Moyamoya Disease: Correlation between Perfusion-Weighted MR Imaging and Cerebral Angiography. American Journal of Neuroradiology. 2006;27(2):391-7.

172. Kawabori M, Kuroda S, Nakayama N, Hirata K, Shiga T, Houkin K, et al. Effective Surgical Revascularization Improves Cerebral Hemodynamics and Resolves Headache in Pediatric Moyamoya Disease. World Neurosurgery. 2013;80(5):612-9.

173. Seol HJ, Shin DC, Kim YS, Shim EB, Kim SK, Cho BK, et al. Computational analysis of hemodynamics using a two-dimensional model in moyamoya disease. J Neurosurg Pediatr. 2010;5(3):297-301.

174. Zhu FP, Zhang Y, Higurashi M, Xu B, Gu YX, Mao Y, et al. Haemodynamic analysis of vessel remodelling in STA-MCA bypass for Moyamoya disease and its impact on bypass patency. J Biomech. 2014;47(8):1800-5.

175. Kim T, Bang J, Kwon OK, Hwang G, Kim J, Kang H-S, et al. Morphology and related hemodynamics of the internal carotid arteries of moyamoya patients. Acta Neurochirurgica. 2015;157(5):755-61.

176. Chong W, Zhang Y, Qian Y, Lai L, Parker G, Mitchell K. Computational Hemodynamics Analysis of Intracranial Aneurysms Treated with Flow Diverters: Correlation with Clinical Outcomes. American Journal of Neuroradiology. 2014;35(1):136-42.

177. Zhang Y, Chong W, Qian Y. Investigation of intracranial aneurysm hemodynamics following flow diverter stent treatment. Medical Engineering & Physics. 2013;35(5):608-15.

178. Adamson J, Humphries SE, Ostergaard JR, Voldby B, Richards P, Powell JT. Are cerebral aneurysms atherosclerotic? Stroke. 1994;25(5):963-6. Epub 1994/05/01.

179. Wagner A, Cortsen M, Hauerberg J, Romner B, Wagner MP. Treatment of intracranial aneurysms. Reconstruction of the parent artery with flow-diverting (Silk) stent. Neuroradiology. 2012;54(7):709-18.

180. Miyamoto S, Yoshimoto T, Hashimoto N, Okada Y, Tsuji I, Tominaga T, et al. Effects of Extracranial–Intracranial Bypass for Patients With Hemorrhagic Moyamoya Disease: Results of the Japan Adult Moyamoya Trial. Stroke. 2014;45(5):1415-21.

181. Wang K, Huang Q, Hong B, Li Z, Fang X, Liu J. Correlation of aneurysm occlusion with actual metal coverage at neck after implantation of flow-diverting stent in rabbit models. Neuroradiology. 2012;54(6):607-13.

182. Chung B, Cebral JR. CFD for evaluation and treatment planning of aneurysms: review of proposed clinical uses and their challenges. Ann Biomed Eng. 2015;43(1):122-38.

183. Chong W, Qian Y, Zhang Y, Mitchell K, Lai L. Computational fluid dynamics (CFD) modelling of virtual flow diverters (FD) to determine risk of delayed rupture of aneurysms after stenting with flow diverters.

184. Freeman JW, Snowhill PB, Nosher JL. A link between stent radial forces and vascular wall remodeling: the discovery of an optimal stent radial force for minimal vessel restenosis. Connect Tissue Res. 2010;51(4):314-26.

185. Peach T, Cornhill JF, Nguyen A, Riina H, Ventikos Y. The 'Sphere': A Dedicated Bifurcation Aneurysm Flow-Diverter Device. Cardiovasc Eng Technol. 2014;5(4):334-47.

186. Jamali AA, Deuel C, Perreira A, Salgado CJ, Hunter JC, Strong EB. Linear and angular measurements of computer-generated models: Are they accurate, valid, and reliable? Computer Aided Surgery. 2007;12(5):278-85.

187. Bernardini A, Larrabide I, Petrini L, Pennati G, Flore E, Kim M, et al. Deployment of self-expandable stents in aneurysmatic cerebral vessels: comparison of different

computational approaches for interventional planning. Computer Methods in Biomechanics and Biomedical Engineering. 2011;15(3):303-11.

188. Qian Y, Liu JL, Itatani K, Miyaji K, Umezu M. Computational hemodynamic analysis in congenital heart disease: simulation of the Norwood procedure. Ann Biomed Eng. 2010;38(7):2302-13.

189. Lindegaard KF, Lundar T, Wiberg J, Sjoberg D, Aaslid R, Nornes H. Variations in middle cerebral artery blood flow investigated with noninvasive transcranial blood velocity measurements. Stroke. 1987;18(6):1025-30.

190. Tang A, Chan, H. , Tsang, A. , Leung, G. , Leung, K. , Yu, A. and Chow, K. The effects of stent porosity on the endovascular treatment of intracranial aneurysms located near a bifurcation. Journal of Biomedical Science and Engineering. 2013;6:812-22.

191. Qian Y, Takao H, Umezu M, Murayama Y. Risk analysis of unruptured aneurysms using computational fluid dynamics technology: preliminary results. AJNR Am J Neuroradiol. 2011;32(10):1948-55.

192. Takao H, Murayama Y, Qian Y, Mohamed A, Matsuda W, Umezu M, et al. O-018 A new hemodynamic parameter: energy loss to anticipate aneurysm rupture. Journal of NeuroInterventional Surgery. 2010;2(Suppl 1):A8.

193. Cebral JR, Mut F, Raschi M, Hodis S, Ding YH, Erickson BJ, et al. Analysis of hemodynamics and aneurysm occlusion after flow-diverting treatment in rabbit models. AJNR Am J Neuroradiol. 2014;35(8):1567-73.

194. Kalani MY, Zabramski JM, Nakaji P, Spetzler RF. Bypass and flow reduction for complex basilar and vertebrobasilar junction aneurysms. Neurosurgery. 2013;72(5):763-75.

195. Farnoush A, Qian Y, Avolio AP. Effect of inflow on computational fluid dynamic simulation of cerebral bifurcation aneurysms.

196. Kulcsár Z, Houdart E, Bonafé A, Parker G, Millar J, Goddard AJP, et al. Intra-aneurysmal thrombosis as a possible cause of delayed aneurysm rupture after flow-diversion treatment. American Journal of Neuroradiology. 2011;32(1):20-5.

197. Cebral JR, Mut F, Weir J, Putman C. Quantitative characterization of the hemodynamic environment in ruptured and unruptured brain aneurysms. AJNR Am J Neuroradiol. 2011;32(1):145-51.

198. Kojima M, Irie K, Fukuda T, Arai F, Hirose Y, Negoro M. The study of flow diversion effects on aneurysm using multiple enterprise stents and two flow diverters. Asian J Neurosurg. 2012;7(4):159-65.

199. Zhang Y, Sia SF, Morgan MK, Qian Y. Flow resistance analysis of extracranial-to-intracranial (EC–IC) vein bypass. Journal of Biomechanics. 2012;45(8):1400-5.

200. Suzuki J, Takaku A. Cerebrovascular "moyamoya" disease: Disease showing abnormal net-like vessels in base of brain. Archives of Neurology. 1969;20(3):288-99.

201. Kuroda S, Ishikawa T, Houkin K, Nanba R, Hokari M, Iwasaki Y. Incidence and clinical features of disease progression in adult moyamoya disease. Stroke. 2005;36(10):2148-53.

202. Guzman R, Lee M, Achrol A, Bell-Stephens T, Kelly M, Do HM, et al. Clinical outcome after 450 revascularization procedures for moyamoya disease. Clinical article. J Neurosurg. 2009;111(5):927-35.

203. Imaizumi T, Hayashi K, Saito K, Osawa M, Fukuyama Y. Long-term outcomes of pediatric moyamoya disease monitored to adulthood. Pediatr Neurol. 1998;18(4):321-5.

204. Duan L, Bao XY, Yang WZ, Shi WC, Li DS, Zhang ZS, et al. Moyamoya disease in China: its clinical features and outcomes. Stroke. 2012;43(1):56-60.

205. Jo K-I, Kim J-S, Hong S-C, Lee J-I. Hemodynamic Changes in Arteriovenous Malformations After Radiosurgery: Transcranial Doppler Evaluation. World Neurosurgery. 2012;77(2):316-21.

206. Scott RM, Smith ER. Moyamoya disease and moyamoya syndrome. N Engl J Med. 2009;360(12):1226-37.

207. Benis Am, Usami S, Chien S. Effect of Hematocrit and Inertial Losses on Pressure-Flow Relations in the Isolated Hindpaw of the Dog. Circulation Research. 1970;27(6):1047-68.

208. Roth AC, Young DF, Cholvin NR. Effect of collateral and peripheral resistance on blood flow through arterial stenoses. Journal of Biomechanics. 1976;9(6):367-75.

209. Bao XY, Duan L, Li DS, Yang WZ, Sun WJ, Zhang ZS, et al. Clinical features, surgical treatment and long-term outcome in adult patients with Moyamoya disease in China. Cerebrovasc Dis. 2012;34(4):305-13.

210. Matsushima T, Inoue T, Suzuki SO, Fujii K, Fukui M, Hasuo K. Surgical treatment of moyamoya disease in pediatric patients--comparison between the results of indirect and direct revascularization procedures. Neurosurgery. 1992;31(3):401-5.

211. Kim M, Taulbee DB, Tremmel M, Meng H. Comparison of two stents in modifying cerebral aneurysm hemodynamics. Annals of Biomedical Engineering. 2008;36(5):726-41.

212. Kato M, Suzuki T, Ogino T, Kimura T. Compliance of the Peripheral Capacitance Vessels in Patients With Congestive Heart Failure. Angiology. 1976;27(12):698-706.

213. Qian Y, Liu JL, Itatani K, Miyaji K, Umezu M. Computational Hemodynamic Analysis in Congenital Heart Disease: Simulation of the Norwood Procedure. Annals of Biomedical Engineering. 2010;38(7):2302-13.

214. Zhang W, Qian Y, Lin J, Lv P, Karunanithi K, Zeng M. Hemodynamic analysis of renal artery stenosis using computational fluid dynamics technology based on unenhanced steady-state free precession magnetic resonance angiography: preliminary results. Int J Cardiovasc Imaging. 2014;30(2):367-75.

215. Young DF, Cholvin NR, Roth AC. Pressure drop across artificially induced stenoses in the femoral arteries of dogs. Circ Res. 1975;36(6):735-43.

216. Young DF, Tsai FY. Flow characteristics in models of arterial stenoses — I. Steady flow. Journal of Biomechanics. 1973;6(4):395-410.

217. Baba T, Houkin K, Kuroda S. Novel epidemiological features of moyamoya disease. J Neurol Neurosurg Psychiatry. 2008;79(8):900-4.

218. Fujii K, Ikezaki K, Irikura K, Miyasaka Y, Fukui M. The efficacy of bypass surgery for the patients with hemorrhagic Moyamoya disease. Clinical Neurology and Neurosurgery. 1997;99(SUPPL. 2):S194-S5.

219. Karasawa J, Touho H, Ohnishi H, Miyamoto S, Kikuchi H. Long-term follow-up study after extracranial-intracranial bypass surgery for anterior circulation ischemia in childhood moyamoya disease. Journal of Neurosurgery. 1992;77(1):84-9.

220. Iwama T, Hashimoto N, Murai BN, Tsukahara T, Yonekawa Y. Intracranial rebleeding in moyamoya disease. Journal of Clinical Neuroscience. 1997;4(2):169-72.

221. Obara K, Fukuuchi Y, Kobari M, Watanabe S, Dembo T. Cerebral hemodynamics in patients with Moyamoya disease and in patients with atherosclerotic occlusion of the major cerebral arterial trunks. Clinical Neurology and Neurosurgery. 1997;99, Supplement 2(0):S86-S9.

222. Yonekawa Y OT, Handa H. 'Moyamoya' disease: clinical review and surgical treatment. 1985;In: Fein JM, Flamm ES (eds): 557-80.

223. Gross B, Thomas A, Frerichs K. Endovascular treatment of symptomatic moyamoya. Neurosurgical Review. 2014:1-5.

224. Karunanithi K, Lee C-J, Zhang Y, Qian Y. Risk stratification of cerebrovascular aneurysms using CFD - a review.

225. Doenitz C, Schebesch KM, Zoephel R, Brawanski A. A mechanism for the rapid development of intracranial aneurysms: A case study. Neurosurgery. 2010;67(5):1213-21.

226. Hoshino T, Sakatani K, Kano T, Murata Y, Katayama Y. Cerebral blood oxygenation changes induced by bypass blood flow in moyamoya disease and non-moyamoya cerebral ischaemic disease. Acta Neurochir. 2006;148(5):551-7.

227. Sasoh M, Ogasawara K, Kuroda K, Okuguchi T, Terasaki K, Yamadate K, et al. Effects of EC-IC bypass surgery on cognitive impairment in patients with hemodynamic cerebral ischemia. Surgical Neurology. 2003;59(6):455-60.

228. Takagi Y, Hashimoto N, Iwama T, Hayashida K. Improvement of oxygen metabolic reserve after extracranial-intracranial bypass surgery in patients with severe haemodynamic insufficiency. Acta Neurochir. 1997;139(1):52-6.

229. Hanqiang Jiang, Wei Ni, Bin Xu, Yu Lei, Yanlong Tian, Feng Xu, et al. Outcome in adult patients with hemorrhagic moyamoya disease after combined extracranial-intracranial bypass. Journal of Neurosurgery. 2014;121(5):1048-55.

230. Lee CJ, Zhang Y, Takao H, Murayama Y, Qian Y. A fluid-structure interaction study using patient-specific ruptured and unruptured aneurysm: The effect of aneurysm morphology, hypertension and elasticity. Journal of Biomechanics. 2013;46(14):2402-10.

231. Zhang Y, Sia SF, Morgan MK, Qian Y. Flow resistance analysis of extracranial-to-intracranial (EC-IC) vein bypass. Journal of Biomechanics. 2012;45(8):1400-5.

232. Wong GKC, Poon WS. Current status of computational fluid dynamics for cerebral aneurysms: The clinician's perspective. Journal of Clinical Neuroscience. 2011;18(10):1285-8.

233. Sia SF, Qian Y, Zhang Y, Morgan MK. Mean arterial pressure required for maintaining patency of extracranial-to-intracranial bypass grafts: An investigation with computational hemodynamic models-case series. Neurosurgery. 2012;71(4):826-31.

234. Karunanithi K, Han C, Lee C-J, Shi W, Duan L, Qian Y. Identification of a hemodynamic parameter for assessing treatment outcome of EDAS in Moyamoya disease. Journal of Biomechanics. 2015;48(2):304-9.

235. Fawcett E, Blachford JV. The Circle of Willis: an Examination of 700 Specimens. J Anat Physiol. 1905;40(Pt 1):2-70.

236. van Kooij BJ, Hendrikse J, Benders MJ, de Vries LS, Groenendaal F. Anatomy of the circle of Willis and blood flow in the brain-feeding vasculature in prematurely born infants. Neonatology. 2010;97(3):235-41.

237. Iqbal S. A Comprehensive Study of the Anatomical Variations of the Circle of Willis in Adult Human Brains. Journal of Clinical and Diagnostic Research : JCDR. 2013;7(11):2423-7.

238. Xu B, Song DL, Mao Y, Gu YX, Xu H, Liao YJ, et al. Superficial temporal artery-middle cerebral artery bypass combined with encephalo-duro-myo-synangiosis in treating moyamoya disease: Surgical techniques, indications and midterm follow-up results. Chinese Medical Journal. 2012;125(24):4398-405.

239. Wang Y, Chen L, Pan H, Wang Y, Xu B, Liao Y. Hemodynamic study with duplex ultrasonography on combined (direct/indirect) revascularization in adult moyamoya disease. Journal of Stroke and Cerebrovascular Diseases. 2014;23(10):2573-9.

240. Matsushima Y, Inaba Y. Moyamoya Disease in Children and Its Surgical Treatment. Pediatric Neurosurgery. 1984;11(3):155-70.

241. Guey S, Tournier-Lasserve E, Hervé D, Kossorotoff M. Moyamoya disease and syndromes: From genetics to clinical management. Application of Clinical Genetics. 2015;8:49-68.

242. Vilela MD, Newell DW. Superficial temporal artery to middle cerebral artery bypass: past, present, and future. Neurosurg Focus. 2008;24(2).

243. Houkin K, Nakayama N, Kuroda S, Ishikawa T, Nonaka T. How does angiogenesis develop in pediatric moyamoya disease after surgery? A prospective study with MR angiography. Childs Nerv Syst. 2004;20(10):734-41.

244. Ho Jun Seol, Duk Chul Shin, Yoo Seok Kim, Eun Bo Shim, Seung-Ki Kim, Byung-Kyu Cho, et al. Computational analysis of hemodynamics using a two-dimensional model in moyamoya disease. Journal of Neurosurgery: Pediatrics. 2010;5(3):297-301.

245. Hertza J, Loughan A, Perna R, Davis AS, Segraves K, Tiberi NL. Moyamoya disease: a review of the literature. Appl Neuropsychol Adult. 2014;21(1):21-7.

246. Fung LW, Thompson D, Ganesan V. Revascularisation surgery for paediatric moyamoya: a review of the literature. Childs Nerv Syst. 2005;21(5):358-64.

247. Isono M, Ishii K, Kamida T, Inoue R, Fujiki M, Kobayashi H. Long-term outcomes of pediatric moyamoya disease treated by encephalo-duro-arterio-synangiosis. Pediatr Neurosurg. 2002;36(1):14-21.

248. Robertson RL, Burrows PE, Barnes PD, Robson CD, Poussaint TY, Scott RM. Angiographic changes after pial synangiosis in childhood moyamoya disease. AJNR Am J Neuroradiol. 1997;18(5):837-45.

249. Ross IB, Shevell MI, Montes JL, Rosenblatt B, Watters GV, Farmer JP, et al. Encephaloduroarteriosynangiosis (EDAS) for the treatment of childhood moyamoya disease. Pediatr Neurol. 1994;10(3):199-204.

250. Kobayashi E, Saeki N, Oishi H, Hirai S, Yamaura A. Long-term natural history of hemorrhagic moyamoya disease in 42 patients. J Neurosurg. 2000;93(6):976-80.

251. Uno M, Nakajima N, Nishi K, Shinno K, Nagahiro S. Hyperperfusion syndrome after extracranial-intracranial bypass in a patient with moyamoya disease--case report. Neurol Med Chir. 1998;38(7):420-4.

252. Phi JH, Wang KC, Lee JY, Kim SK. Moyamoya Syndrome: A Window of Moyamoya Disease. J Korean Neurosurg Soc. 2015;57(6):408-14.

253. Ishii K, Fujiki M, Kobayashi H. Invited article: surgical management of Moyamoya disease. Turk Neurosurg. 2008;18(2):107-13.

254. Miyamoto S. Study design for a prospective randomized trial of extracranial-intracranial bypass surgery for adults with moyamoya disease and hemorrhagic onset--the Japan Adult Moyamoya Trial Group. Neurol Med Chir. 2004;44(4):218-9.

255. Zhang C, Wang L, Li X, Li S, Pu F, Fan Y, et al. Modeling the circle of Willis to assess the effect of anatomical variations on the development of unilateral internal carotid artery stenosis. Biomed Mater Eng. 2014;24(1):491-9.

256. Tanaka H, Fujita N, Enoki T, Matsumoto K, Watanabe Y, Murase K, et al. Relationship between variations in the circle of Willis and flow rates in internal carotid and basilar arteries determined by means of magnetic resonance imaging with semiautomated lumen segmentation: reference data from 125 healthy volunteers. AJNR Am J Neuroradiol. 2006;27(8):1770-5.

257. Zhu G, Yuan Q, Yang J, Yeo J. Experimental study of hemodynamics in the circle of willis. BioMedical Engineering OnLine. 2015;14(Suppl 1):S10.

258. Zhang Y, Chong W, Qian Y. Investigation of intracranial aneurysm hemodynamics following flow diverter stent treatment. Med Eng Phys. 2013;35(5):608-15.

259. Kuroda S, Hashimoto N, Yoshimoto T, Iwasaki Y. Radiological findings, clinical course, and outcome in asymptomatic moyamoya disease: results of multicenter survey in Japan. Stroke. 2007;38(5):1430-5.

260. Wang D, Zhu F, Fung KM, Zhu W, Luo Y, Chu WC, et al. Predicting Cerebral Hyperperfusion Syndrome Following Superficial Temporal Artery to Middle Cerebral Artery Bypass based on Intraoperative Perfusion-Weighted Magnetic Resonance Imaging. Sci Rep. 2015;5(14140).

261. Shin D, Seol H, Kim S-K, Wang K-C, Cho B-K, Shim E. Computational analysis of the hemodynamics in cerebral arteries related to Moyamoya disease. In: Magjarevic R, Nagel JH, editors. World Congress on Medical Physics and Biomedical Engineering 2006: Springer Berlin Heidelberg; 2007. p. 155-8.

262. Lee BK. Computational fluid dynamics in cardiovascular disease. Korean Circ J. 2011;41(8):423-30.

263. Beneken JE. Some computer models in cardiovascular research. Cardiovascular fluid dynamics. 1972;1:173-223.

264. Gonzalez CF, Cho YI, Ortega HV, Moret J. Intracranial aneurysms: flow analysis of their origin and progression. American Journal of Neuroradiology. 1992;13(1):181-8.

265. Li H, Chen L, Huang C, Jiang Y, Wan W, Dong J, et al. RETRACTED: Hemodynamic Features of Unruptured Cerebral Aneurysms before Rupture: A CFD Study. Computational Molecular Bioscience. 2015;Vol.05No.01:6.

266. Cebral JR, Castro MA, Burgess JE, Pergolizzi RS, Sheridan MJ, Putman CM. Characterization of cerebral aneurysms for assessing risk of rupture by using patient-specific computational hemodynamics models. American Journal of Neuroradiology. 2005;26(10):2550-9.

267. Seifert V, Trost HA, Stolke D. Management morbidity and mortality in grade IV and V patients with aneurysmal subarachnoid haemorrhage. Acta Neurochirurgica. 1990;103(1-2):5-10.

268. Appanaboyina S, Mut F, Lohner R, Scrivano E, Miranda C, Lylyk P, et al. Computational modelling of blood flow in side arterial branches after stenting of cerebral aneurysms. Int J Comput Fluid Dyn. 2008;22(10):669-76.

269. Lieber B, Stancampiano A, Wakhloo A. Alteration of hemodynamics in aneurysm models by stenting: Influence of stent porosity. Annals of Biomedical Engineering. 1997;25(3):460-9.

270. Togao O, Mihara F, Yoshiura T, Tanaka A, Noguchi T, Kuwabara Y, et al. Cerebral hemodynamics in Moyamoya disease: correlation between perfusion-weighted MR imaging and cerebral angiography. AJNR Am J Neuroradiol. 2006;27(2):391-7.

271. Ma J, You Z, Byrne J, Rizkallah RR. Design and mechanical properties of a novel cerebral flow diverter stent. Annals of Biomedical Engineering. 2014;42(5):960-70.

272. Chmelova J, Kolar Z, Prochazka V, Curik R, Dvorackova J, Sirucek P, et al. Moyamoya disease is associated with endothelial activity detected by anti-nestin antibody. Biomed Pap Med Fac Univ Palacky Olomouc Czech Repub. 2010;154(2):159-62.

273. Han H-C. Twisted Blood Vessels: Symptoms, Etiology and Biomechanical Mechanisms. Journal of Vascular Research. 2012;49(3):185-97.

# *Appendix*